

**A New Photoremovable Protecting Group
Absorbing Above 500 nm:
(6-Hydroxy-3-oxo-3*H*-xanthen-9-yl)methyl
and its Derivatives**

Inauguraldissertation
zur Erlangung der Würde eines
Doktors der Philosophie
vorgelegt der
Philosophisch-Naturwissenschaftlichen Fakultät
der Universität Basel

von

Pavel Müller
aus Brno (Tschechische Republik)

Basel, 2007

Genehmigt von der Philosophisch-Naturwissenschaftlichen Fakultät auf Antrag der Herren

Prof. Dr. Hans-Jakob Wirz

Prof. Dr. Hanspeter Huber

Basel, den 11. Dezember 2007

Prof. Dr. Hans-Peter Hauri
(Dekan)

Dedicated to my family and to Eme

Acknowledgements

First of all, I would like to thank Prof. Hans-Jakob Wirz for giving me the opportunity to come to Basel for my Ph.D. studies and to learn a lot during my stay here.

I also thank Prof. Hanspeter Huber, who agreed to act as my co-referee.

My special thanks go to all my colleagues in the research group: to Jürgen Wintner, Dominik Heger, Yavor Kamdzhilov, Hassen Boudebous, Gaby Persy, Bogdan Tokarczyk and Anna Wisla for being always very friendly and helpful.

I am also grateful to the other colleagues from the institute, namely to Dr. Daniel Häussinger and Dr. Heinz Nadig for carrying out some of the NMR and MS measurements, and to my friends – Jaroslav Padevět, Ivan Shnitko, Mariusz Grzelakowski, Tomáš Samuely, Markéta Vlčková and many others.

Last but not least, I wish to thank my family and to Eme for their everlasting support and encouragement.

Table of Contents

| | |
|--|-----------|
| 1. Introduction | 1 |
| 1.1. Protecting Groups (PGs) | 1 |
| 1.2. Photoremovable Protecting Groups (PPGs) | 1 |
| 1.2.1. The <i>o</i> -Nitrobenzyl Group | 2 |
| 1.2.2. The Phenacyl Group | 5 |
| 1.2.3. The Benzoin Group | 9 |
| 1.2.4. The Coumarinyl Group | 11 |
| 1.2.5. Other Groups | 13 |
| 1.3. Applications of PPGs | 15 |
| 1.3.1. Caged Neurotransmitters and Second Messengers | 15 |
| 1.3.2. Two Photon Excitation (2PE) | 21 |
| 1.3.3. Photoactivatable Fluorophores | 22 |
| 1.3.4. Time-resolved X-ray | 23 |
| 1.3.5. Kinetics of protein folding | 24 |
| 1.3.6. Solid-phase Synthesis, Molecular Arrays | 24 |
| 2. Problem Statement | 26 |
| 3. Results and Discussion | 29 |
| 3.1. Fluorescence of 6-Hydroxy-9-methyl-3H-xanthen-3-one (1) | 29 |
| 3.2. Time-resolved Fluorescence Experiments | 33 |
| 3.3. Quantum Yield Measurements | 35 |
| 3.4. Laser Flash Photolysis (LFP) | 39 |
| 3.5. Photoproduct | 41 |
| 3.6. Stability Tests | 49 |
| 3.7. Calculations | 52 |
| 4. Summary | 55 |
| 5. Experimental | 57 |
| 5.1. Instruments | 57 |
| 5.2. Chemicals | 59 |
| 5.3. Data Analysis | 59 |
| 6. Index of Symbols and Abbreviations | 60 |

| | |
|---|-----------|
| 7. References | 63 |
| 8. Appendix | 72 |
| 8.1. Aqueous Oxidation of Phenylurea Herbicides by Triplet Aromatic Ketones | 73 |
| 8.2. Inverted Region Behavior in Proton Transfer to Carbanions | 79 |
| 9. Curriculum Vitae | 96 |

1. Introduction

1.1. Protecting Groups (PGs)

When a chemical reaction is to be carried out on a multifunctional compound in a selective way, other sites prone to chemical reaction under given conditions have to be temporarily blocked by a protecting (or protective) group (PG).

Chemistry of PGs dates back to the end of the 19th century¹ and it has been gaining in importance (not only for the organic synthesis) ever since.

PGs must fulfill a number of requirements. The introduction, as well as the cleavage of the selected PG must be compatible with other functionalities of the given molecule, i.e. the protection and the de-protection reactions must be well-defined, they must proceed under mild conditions, with high selectivity and high yields, and without the generation of new stereogenic centers. Furthermore, PGs should be inexpensive, easily (commercially) available, and preferably non-toxic. Last but not least, PGs should influence the reactivity of other functional groups of the molecule to the smallest possible extent².

1.2. Photoremovable Protecting Groups (PPGs)

Since harsh acidic or basic conditions are often needed for a chemical deprotection of molecules, a fast removal of the PG by irradiation, which can occur under mild (neutral) conditions, represents an appealing alternative to classical methods. Use of photoremovable protecting groups (PPGs) has also other no less important advantages. For instance, one avoids introducing new reagents and substrates which could interfere with the existing functionalities of the molecule. A reaction that is induced photochemically also allows control over spatial and temporal variables in the given system. Last but not least, photochemical reactions are sometimes more selective than the thermal ones³.

The development of the first PPGs goes back to the early 60's of the 20th century⁴ and since then, PPGs have been a subject of interest to many chemists and biochemists. Depending on the application they have been developed for, PPGs can be referred to as *photolabile groups*, *caging compounds*⁵, *phototriggers* or *photobiological switches*.

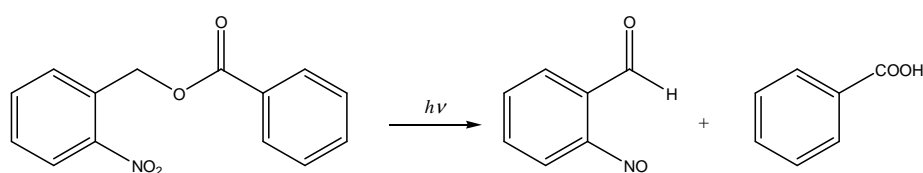
PPGs should meet several requirements, some of which are listed below:

- The deprotection reaction has to be clean, fast and efficient (quantum yields $\Phi \geq 0.1$).
- PPG should have high extinction coefficients ϵ at wavelengths above 320 nm in order to avoid damage of the biological material or other chromophores present in the system.
- A well-defined procedure for an efficient attachment of the PPG to the functionalities of interest has to be available.
- The products and by-products of photolysis should neither absorb at the wavelength of irradiation, nor should they react with other components of the system.
- When intended for use in medical, biological or biochemical applications, the PPG should not lower the solubility of the substrate in water or buffered water solutions (with pH around 7) and the released PG must not be toxic.
- No stereogenic centers should be generated upon photolysis.

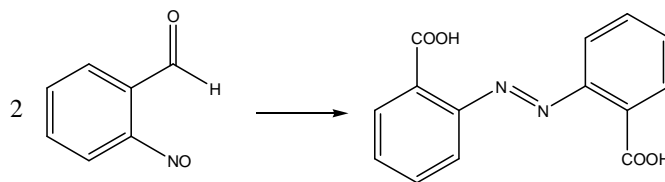
At present, the number of available (known and tested) PPGs is still relatively small² and there are no ideal PPGs that possess all the desired properties. Nonetheless, a suitable candidate for a PPG should not lack more than two of these features.

1.2.1. The *o*-Nitrobenzyl Group

The *o*-nitrobenzyl group (*o*-NB) was first used by Barltrop *et al.* in 1966 to mask benzoic acid⁶. The irradiation of 2-nitrobenzyl ester of benzoic acid yielded 2-nitrosobenzaldehyde and the free acid.

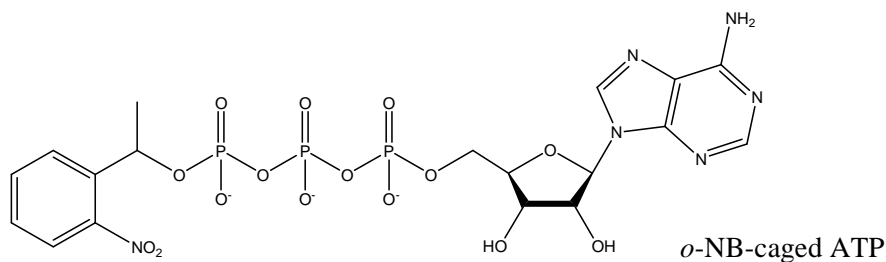


Two molecules of 2-nitrosobenzaldehyde reacted further to give the final product, 2,2'-(*E*)-diazene-1,2-diyl dibenzoic acid.



The *o*-nitrosobenzaldehyde formed is highly reactive and toxic and the final azobenzene derivative absorbs more than the primary caged compound. These are, however, not the only drawbacks the *o*-NB group has. Another disadvantage of the *o*-NB group is that the rate of its cleavage depends on many factors such as the quality of the leaving group (LG), solvents and pH (in water solutions, where the cleavage happens to be slowest at pH ~ 7). In spite of all these facts, the *o*-nitrobenzyl group is still the most used PPG for synthetic⁷, photolithographic (DNA arrays)⁸, as well as for biochemical applications⁹. This is most probably due to the ease of protection and deprotection, high quantum yields of deprotection, the possibility of irradiation with light above 320 nm and, last but not least, for historical reasons.

PPGs based on *o*-NB can be used e.g. for caging of carboxylic acids^{6, 10, 11}, carbonyls¹², alcohols¹³, thiols, sulfates, phosphates and nucleotides such as ATP⁵.

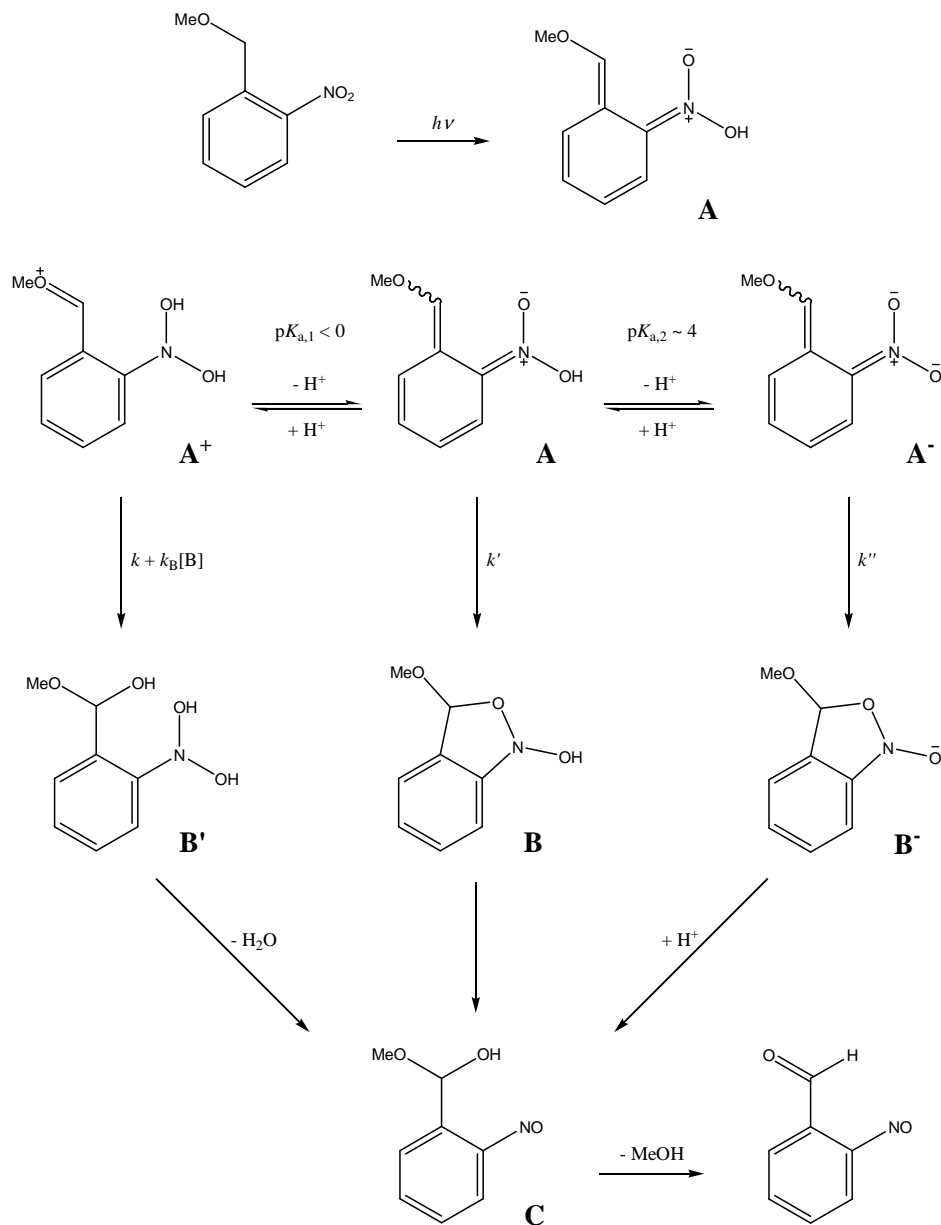


It has been known since the early 60's of the 20th century¹⁴ that *o*-nitroalkylbenzenes undergo a photoinduced intramolecular hydrogen transfer affording *aci*-nitro tautomers (**A**), which can be detected by flash photolysis ($\lambda_{\text{max}} \sim 420$ nm). However, the subsequent thermal reaction steps leading to the deprotection of *o*-NB cages have not been well understood until recently.

In 2004, Wirz *et al.*¹⁵ published a revised reaction mechanism of deprotection of *o*-NB methyl esters and caged ATP in water (Scheme 1). **A** formed from the singlet excited state of 2-nitrobenzyl methyl ether is in equilibrium with its protonated (**A**⁺) and deprotonated form

(\mathbf{A}^-). \mathbf{A}^+ can add a base (e.g. OH^-) to form a nitroso hydrate \mathbf{B}' . \mathbf{A} and \mathbf{A}^- cyclize to yield 3-methoxy-2,1-benzisoxazol-1(3*H*)-ol (\mathbf{B}) and its deprotonated form (\mathbf{B}^-), respectively.

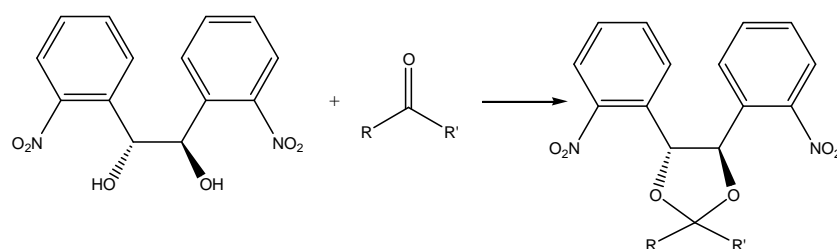
Scheme 1 Mechanism for the thermal reactions of the primary photochemical *aci*-nitro transient (\mathbf{A}) formed photochemically from 2-nitrobenzyl methyl ether in aqueous solutions¹⁵.



\mathbf{B}' , \mathbf{B} and \mathbf{B}^- then all give a hemiacetal (\mathbf{C}) of the final product, 2-nitrosobenzaldehyde. The rates of the process $\mathbf{A} \rightarrow \mathbf{B}$ rise steadily with increasing acid concentration for $\text{pH} < 10$. For $\text{pH} \geq 10$, this step is no longer acid-catalyzed and the rates remain constant. Rate constants k , k' and k'' determined with buffer solutions ($\text{pH} 3.5 - 10.5$) were found to increase linearly with buffer concentration indicating general acid catalysis.

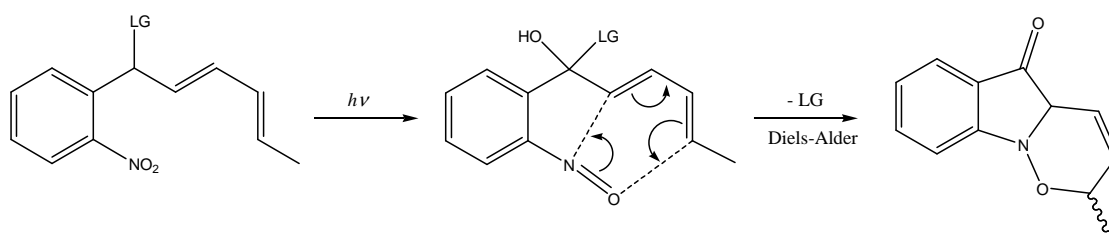
Several modifications of the *o*-NB group have been developed to improve its applicability. Adams and coworkers¹⁰ attached two methoxy groups to the positions 4 and 5 on the benzene ring to increase the extinction coefficient at $\lambda \geq 350$ nm. Blanc and Bochet¹² have prepared bis(*o*-nitrophenyl)ethanediol and used it as a PPG for aldehydes and ketones (Scheme 2).

Scheme 2 Protection of aldehydes and/or ketones by bis(*o*-nitrophenyl)ethanediol



Pirrung *et al.*¹⁶ designed another modification of *o*-NB with a pentadienyl chain, which traps the toxic nitroso species in an intramolecular hetero Diels–Alder reaction (Scheme 3).

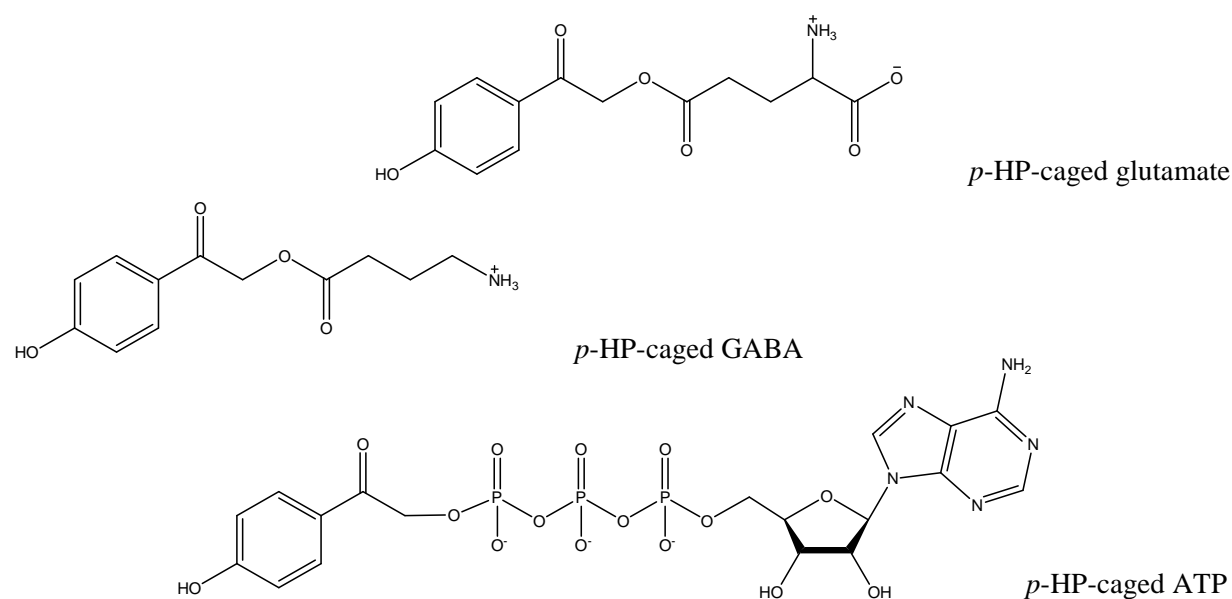
Scheme 3 *o*-NB protecting group modified by Pirrung and coworkers¹⁶



1.2.2. The Phenacyl Group

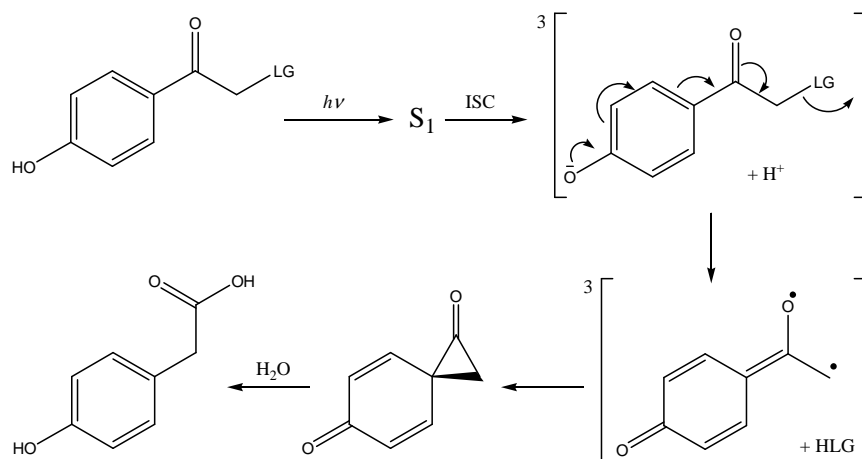
The *p*-hydroxyphenacyl group (*p*-HP) is at present one of the most promising alternatives to the *o*-NB group. *p*-HP cages can be readily prepared from commercially available *p*-hydroxyacetophenone. The derivatives are soluble and stable in aqueous solutions for a sufficiently long time. The photoproduct, *p*-hydroxyphenylacetic acid, is also water-soluble and non-toxic, contrary to the products formed by photolysis of *o*-NB compounds. The UV absorption of *p*-hydroxyphenylacetic acid is blue-shifted with respect to the starting material. Therefore, the photoproduct does not interfere with the absorption of the caged material and allows its quantitative photochemical conversion. Last but not least, the quantum yield of deprotection is generally high (e.g. 0.3 for carboxylates¹⁷ and up to 0.94 for phosphates¹⁸) and the release rates are remarkably fast⁹.

The usability of the *p*-methoxyphenacyl (*p*-MP) group as a PPG was first discovered by Sheehan and coworkers in 1973¹⁹, who have used it to protect carboxylic acids. They reported on the yields of deprotection of *p*-MP-caged benzoic acid and several amino acids in dioxane and/or ethanol after several hours of irradiation. Two decades later, Givens *et al.* used the *p*-HP as a new cage for a light-activated release of various bioactive molecules such as glutamate¹⁷, GABA¹⁷, cAMP, ATP²⁰, and oligopeptides²¹.



The mechanism of the photocleavage has not yet been positively established. Wirz *et al.*^{9, 18} showed that the reactive state is the triplet, which forms spiro[2.5]octa-4,7-diene-1,6-dione upon release of the LG and the spirocyclic species is then hydrolyzed to yield the final product, *p*-hydroxyphenylacetic acid (see Scheme 4).

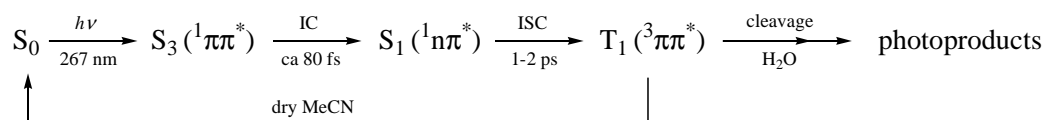
Scheme 4 Photocleavage of the *p*-HP cages



According to this mechanism, the release of the leaving group is synchronous with the decay of the excited triplet state ($10^8 - 10^9 \text{ s}^{-1}$). However, the attempts to identify the spirodienedione intermediate by means of time-resolved IR failed²².

Ma *et al.*^{23, 24} have recently carried out ultrafast time-resolved studies of the photophysical processes involved in the photochemical deprotection of *p*-HP-caged carboxylates and phosphates in $\text{H}_2\text{O}/\text{MeCN}$ solutions. Their results confirm the reactive state is the excited triplet and suggest that the photophysical and photochemical processes occur on well-separated time scales. The photophysical processes (excitation, IC, ISC) take femtoseconds to picoseconds and are not at all affected by the existence and/or the kind of the LG (Scheme 5). The photochemical process – the actual deprotection – is slower by two to three orders of magnitude (0.4 – 2.1 ns).

Scheme 5 Photophysical and photochemical processes associated with the deprotection of *p*-HP cages



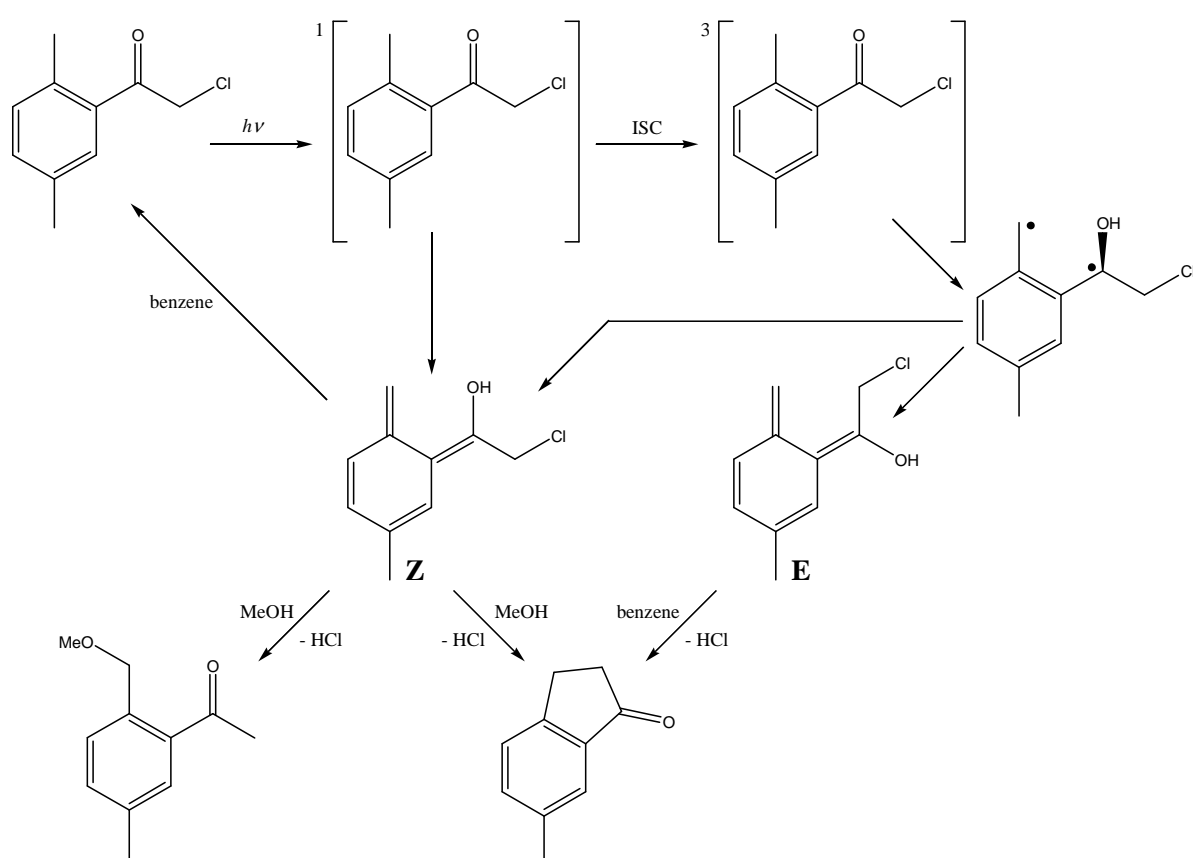
A photochemically induced enolization reaction of the *p*-HP chromophore was suggested to be a process competing with the triplet deactivation by cleavage and thus lowering the efficiency of the deprotection process.

The *p*-HP group has been successfully used for protection of carboxylic acids^{25, 26}, amino acids and peptides¹⁷, alcohols and phosphates²⁷. It has, however, one drawback, which is the low extinction coefficient at wavelengths above 320 nm. Conrad and coworkers²⁸ synthesized several 3,5-dimethoxy-4-hydroxyphenacyl esters, which absorbed light up to 400 nm. Unfortunately, the quantum yields of e.g. GABA and glutamate deprotection were significantly lower (0.03 – 0.04) than those of *p*-HP-caged GABA (0.35) and *p*-HP-caged glutamate (0.12)¹⁷ and the photocleavage followed a different reaction mechanism.

In 2000, Klán and coworkers introduced a new PPG for carboxylic compounds based on the phenacyl cage – 2,5-dimethylphenacyl (DMP)²⁹. Two years later, they also applied this cage to protect chlorides, phosphates and sulfates³⁰.

The first step of the proposed mechanism of the DMP chloride deprotection (Scheme 6) is an efficient enolization of the DMP moiety. In MeOH, the reaction proceeds from the major photoenol product – (*Z*)-xylylene (**Z**), which is formed predominantly from the singlet excited ketone ($\tau = 33 \mu\text{s}$). In benzene, however, both **Z** and **E** enols are formed but HCl is released only from the **E** isomer ($\tau = 10 \text{ ms}$), while the cage species cyclizes to 6-methylindan-1-one. This product is formed also in MeOH (from the **Z** isomer) but the main photoproduct in this solvent is 2-(methoxymethyl)-5-methylacetophenone.

Scheme 6 Mechanism of deprotection of DMP chloride³⁰



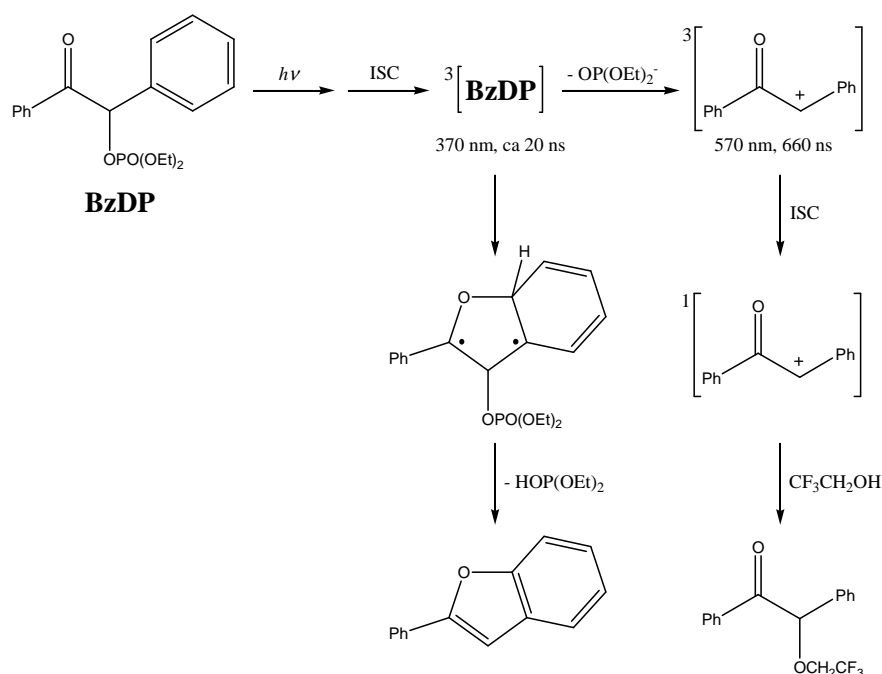
The quantum yields of deprotection of DMP chloride in MeOH and benzene were reported to be 76 % and 11 %, respectively^{31, 32}. The quantum yields for phosphates and sulfates are also fairly high ($\sim 70 \%$)³⁰, but the efficiency of the photoreaction of carboxylates is somewhat lower (18 – 25 % in non-polar solvents and ca 10 % in MeOH) since carboxylates are poorer leaving groups and their release was found to be too slow to compete with the intramolecular reketonisation of **Z**.

1.2.3. The Benzoin Group

The benzoin (Bz) group was first introduced as a PPG by Sheehan *et al.* in 1971³³, who used this group and its methoxy-substituted derivatives to cage acetic acid. All these cages cyclized upon fast and clean photolysis (at 366 nm) to yield the corresponding 2-phenylbenzofurans and the free acetate with high chemical (up to 99 %) and quantum yields (e.g. $\Phi \sim 0.64$ for 3',5'-dimethoxybenzoin, 3',5'-DMBz).

The resulting benzofuran products are biologically inert but red-shifted with respect to the starting cages. Their higher extinction coefficients at $\lambda > 261$ nm together with their strong fluorescence can be considered as the main drawbacks of this group. Another problem (especially for biological applications) is that the Bz-group lowers the solubility of the protected substrate in aqueous media and also of the major by-product of the reaction, 2-phenylbenzofuran. Irradiation of benzoin diethyl phosphate in fluorinated alcohols results in a formation of a different major photoproduct, alkoxy-substituted benzoin³⁴ (Scheme 7).

Scheme 7 Mechanism of photodissociation of benzoin diethyl phosphate (BzDP)³⁴



Several other substituted Bz-cages have been prepared in order to optimize the quantum yields and the product distribution, which also strongly depend on the leaving group and the reaction medium³⁴. Nevertheless, optimal results were obtained for 3',5'-DMBz, which is together with the parent benzoin the most widespread benzoin caging moiety⁹. So far, the Bz group has been successfully applied to cage carboxylic acids³³, phosphate esters³⁵, amines³⁶, carboxylic esters of oligopeptides³⁷, alcohols and nucleotides³⁸.

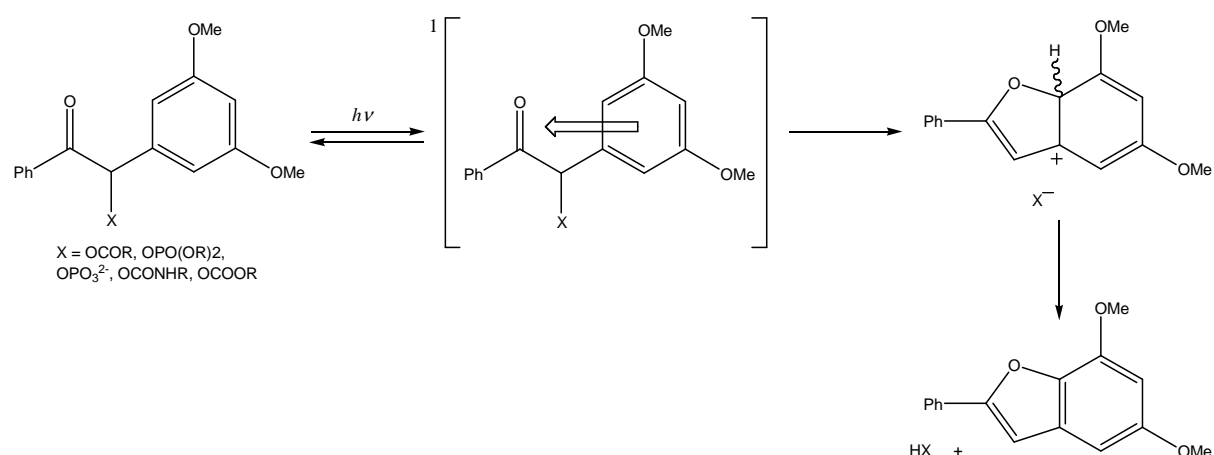
Quenching experiments described in the original work of Sheehan and coworkers³³ suggest that photorelease from unsubstituted benzoin and 3'-methoxybenzoin derivatives proceeds through the triplet excited state. A different mechanism was proposed for 3',5'-DMBz derivatives. The reaction was not affected by common triplet quenchers (neither naphthalene, nor piperylene), indicating that the triplet is very short-lived or that the reaction proceeds from the excited singlet state.

A study of benzoin diethyl phosphate by LFP by Rajesh and coworkers³⁴ has shown that 2-phenylbenzofuran is indeed formed from the triplet state within 20 ns (see Scheme 7). An additional transient ($\lambda_{\text{max}} = 570$ nm) was detected in $\text{CF}_3\text{CH}_2\text{OH}$, hexafluoropropan-2-ol and water. It was assigned to a triplet cation that is formed adiabatically by heterolytic dissociation of the triplet state. The cation is then attacked by nucleophilic $\text{CF}_3\text{CH}_2\text{OH}$ to form benzoin trifluoroethylether.

There are several proposed mechanisms for photocleavage of 3',5'-DMBz cages. Sheehan *et al.*³³ suggested an intramolecular Paterno–Büchi reaction of the excited singlet to form a strained tricyclic intermediate, followed by ring opening and loss of the protected species to give 2-benzofuran. Pirrung and Shuey³⁹ proposed heterolytic cleavage and formation of an ion pair directly from the singlet state, followed by ring closure and elimination.

Nanosecond LFP studies conducted by Shi and coworkers⁴⁰ on several 3',5'-DMBz esters indicated the initial process is a charge transfer from the electron-rich dimethoxybenzene ring to the electron-deficient oxygen of the n,π^* singlet-excited carbonyl. The intramolecular exciplex can then return to the ground state or undergo a cyclization reaction upon elimination of the protected moiety to give a cation, which is further stabilized by elimination of H^+ to form the final benzofuran (Scheme 8).

Scheme 8 Photoreaction of 3',5'-DMBz esters according to Shi *et al.*⁴⁰



Pirrung and Shuey³⁹ prepared 3',5'- and 2',3'-DMBz phosphate triesters (DMBz-protected ATP). The release was reported to be very efficient and much faster ($k > 10^5 \text{ s}^{-1}$) than that of nitrobenzyl-caged ATP. These authors have also developed a synthetic procedure to obtain an optically active benzoin. Givens *et al.* used the benzoin chromophore to prepare caged cAMP⁴¹. Free cAMP was generated with 34 % efficiency and a first-order rate constant as high as $3 \times 10^8 \text{ s}^{-1}$.

Only a few practical applications have been described as the development of this phototrigger is fairly recent but the high efficiency and rate of substrate release make the benzoin group a rather promising PPG. Boudebous *et al.*⁴² investigated 3',5'-DMBz acetate and fluoride by means of pump-probe spectroscopy. They identified a primary photoproduct – preoxetane biradical that decayed by different pathways depending on solvent polarity. In polar solvents such as acetonitrile or water, the biradical decayed by releasing acetate or fluoride with a lifetime about 2 ns. The authors therefore suggest DMBz derivatives are excellent PPGs for the investigation of fast processes such as protein folding (see also Chapter 1.3.).

1.2.4. The Coumarinyl Group

The first photochemical investigations of 7-methoxycoumarin-4-ylmethyl (MCM) esters date back to 1984, when Givens and Matuszewski⁴³ observed a photochemically-induced reaction of coumarinyl diethyl phosphate with a wide variety of nucleophilic functionalities, such as methanol, water, piperidine, cysteine, tyrosine, etc.). When irradiated by 360-nm light,

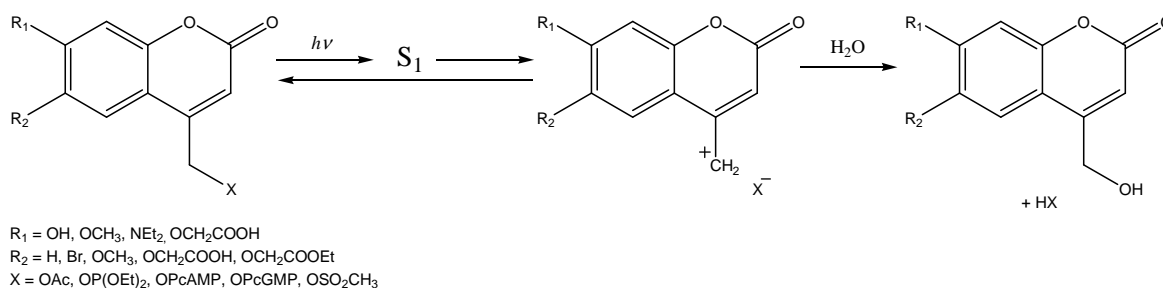
the diethyl phosphate group was replaced by the nucleophilic species. The authors proposed the use of the highly-fluorescent coumarinyl moiety for photochemical labeling of various organic substrates. Already one year earlier, this species had been used by Matuszewska and Borchardt⁴⁴ as a fluorescent tag for the enzymes α -chymotrypsin and histamine *N*-methyltransferase.

The coumarinyl group was rediscovered as a PPG by Furuta *et al.*⁴⁵ in 1995. The authors observed a moderately efficient photocleavage of MCM–cAMP ($\Phi = 0.12$) under physiological conditions (Ringer’s solution).

The moderate quantum yield of the coumarinyl photorelease ($\Phi = 0.26$ at the most) and the low stability of coumarinyl cages in neutral aqueous media are the two major drawbacks of this group. On the other hand, MCM and its derivatives exhibit very fast ($k \sim 10^9 \text{ s}^{-1}$) rates of deprotection⁴⁶ and high extinction coefficients even in the visible region (up to $\sim 435 \text{ nm}$ ⁴⁷). The absorption of the coumarinyl cage can be further red-shifted by addition of suitable substituents⁴⁸. Substituents can also be used to enhance the hydrophilicity and/or the quantum yields of the reaction⁴⁹.

The mechanism of photolysis of coumarinyl esters was investigated by Shade *et al.*⁴⁶ who observed a correlation between the quantum yield and the quality of the leaving group. The efficiency of the photoreaction also increased with the amount of polar protic solvent in the reaction mixture, which suggested an ionic mechanism (see Scheme 9).

Scheme 9 Mechanism of deprotection of coumarinyl esters in aqueous solutions⁴⁶



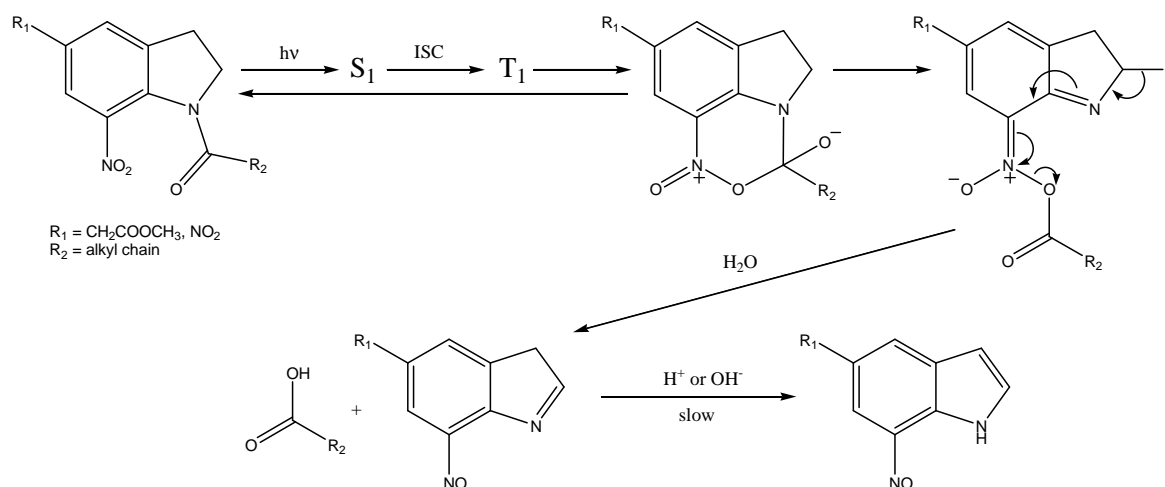
Photolysis of MCM–phosphate in a combined $\text{H}_2^{18}\text{O}/\text{CH}_3\text{CN}$ solution resulted in no incorporation of the labeled oxygen into the free phosphate, thus indicating an $\text{S}_{\text{N}}1$ mechanism.

Furuta and coworkers reported on a fairly high two-photon (740 nm) excitation cross section of coumarinyl derivatives, thus making these cages promising for 3D-resolved release of bioactive messengers⁴⁸ (more details will follow in the Chapter 1.3.).

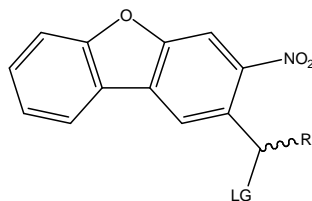
1.2.5. Other Groups

1-Acyl-7-nitroindolines have been used for a fast release of carboxylic acids in aqueous solutions⁵⁰ (Scheme 10). Under given conditions, acetic acid (acetate) was released with a rate constant of $5 \times 10^6 \text{ s}^{-1}$ and a relatively low quantum yield of 0.06 in water. The quantum yield can be slightly improved by introduction of suitable substituents (a 4-methoxy-7-nitroindoline derivative of glutamate was photolysed with an efficiency of 0.085).

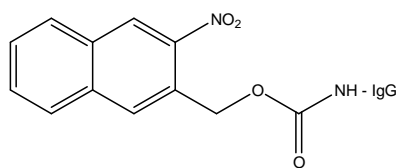
Scheme 10 Photolysis of 1-acyl-7-nitroindoline in water⁵⁰.



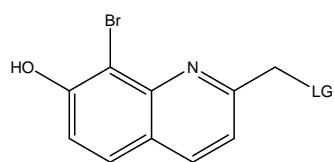
Nitrodibenzofuran has been introduced recently by Ellis-Davies⁵¹ as a very efficient caging agent for aminoacids or calcium ions ($\Phi \sim 0.6$). The mechanism of photodeprotection follows the same pattern as that of the well-known *o*-NB group, on which it is based. The cages are well-soluble and stable in water and the extinction coefficients at $\lambda_{\text{max}} = 330 \text{ nm}$ are as high as $1.84 \times 10^4 \text{ M}^{-1}\text{cm}^{-1}$. The compounds are also reported to have a reasonable cross-section for 2-photon absorption.



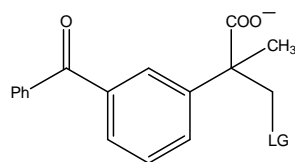
Another PPG based on the *o*-NB group was presented by Singh and coworkers⁵², who described the derivatives of **(3-nitro-2-naphthyl)methanol** as water-soluble caged compounds photocleavable with photons between 350 and 400 nm. On irradiation, the cages gave the expected nitroso-aldehyde photoproduct with high quantum yields (0.6 – 0.8). The PPG could be conveniently coupled to the amino residues of immunoglobulin (IgG) using diphenyl phosphorane. (3-nitro-2-naphthyl)methanol can be used as a photocaging agent under physiological conditions at wavelengths, which do not cause significant damage to biomolecules.



Fedoryak *et al.*⁵³ reported on a new photolabile protecting group for carboxylic acids based on **8-bromo-7-hydroxyquinoline**, which exhibited a greater single photon quantum efficiency than 4,5-dimethoxy-4-nitrobenzyl ester or 6-bromo-7-hydroxycoumarin-4-ylmethyl. It also had a sufficient sensitivity to multiphoton-induced photolysis. Its increased solubility in physiological buffers and low fluorescence make it a suitable caging group for biological messengers.



Lukeman and coworkers⁵⁴ have developed an efficient PPG for carboxylic acids, halides and alcohols derived from **ketoprofen**. The carboxylic functionality, which improves the solubility in water, is cleaved upon photolysis as CO₂ and the resulting carbanion gets stabilized by cleaving the caged substance (LG). The reported quantum yields of deprotection are very high (up to 0.7 for carboxylic acids and 0.2 for alcohols) and the resulting byproduct is biologically inert.



1.3. Applications of PPGs

The idea of using light to release biologically active substances is about 30 years old and it dates back to the first experiments with the photocleavage of *o*-NB-ATP and *o*-NB-cAMP cages^{5, 55}. The usefulness of PPGs became apparent to the neuroscience community a decade later, in 1986, when an NB-caged acetylcholine agonist, carbamoylcholine, was used to activate nicotinic acetylcholine receptors and to study their kinetics⁵⁶.

Animal and human cells contain ion channels that are directly activated by changes in factors such as transmembrane voltage, temperature, ligand binding, and mechanical forces, but none is known to be directly sensitive to light. A few specialized cell types such as rods and cones of the retina have naturally photoreceptive proteins (e.g. rhodopsin), but these receptors indirectly signal to ion channels through a cascade of complex biochemical processes. Hence, when experimenters want to rapidly elicit cellular responses mediated by ion channels (e.g. in nerve cells) they typically apply either an electrical or a chemical stimulus (see Fig. 1), which involves attaching or implanting electrodes or perfusion devices for chemical delivery⁵⁷.

For many reasons, remote stimulation by light is preferable to these types of invasive methods. A beam of light can be projected on tissue with both temporal and spatial precision and it may be focused on a single cell or even on a part of the cell. The light can be scanned across cells in a population, which is a feature that would be virtually impossible using electrodes⁵⁸.

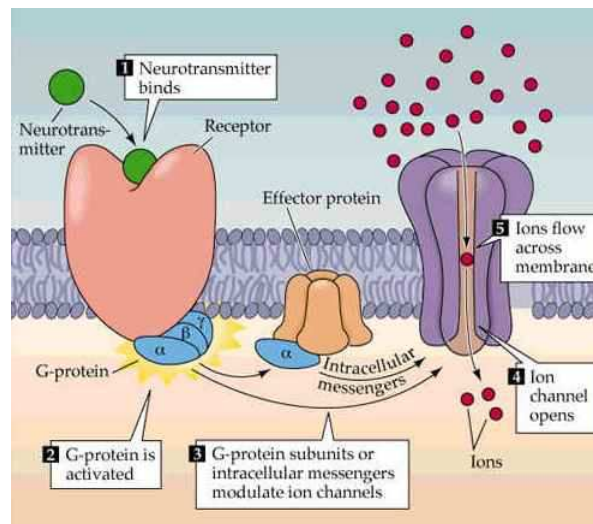
1.3.1. Caged Neurotransmitters and Second Messengers

Neurotransmitters are chemical substances that relay, amplify and modulate electrical signals between a neuron and another cell. They can be classified into three major groups:

- *amino acids* (glutamic acid, GABA, aspartic acid, glycine, etc.)
- *peptides* (endorphine, vasopressine, somatostatine, etc.)
- *biogenic amines* (acetylcholine, adrenalin, dopamine, serotonin, histamine, etc.).

Neurotransmitters and hormones (also called “first messengers”) activate the receptor in the cell membrane by binding to its external domain. The activation brings about a change in the level of a “second messenger” – an intracellular molecule that triggers cell responses (e.g. opening of an ion channel, see Fig. 1)⁹.

Fig. 1 The mechanism of action of neurotransmitters (here: activation of a G-protein-coupled receptor such as GABA_B receptor, which opens nearby potassium channels)⁵⁹



Since it is the receptor that dictates the actual effect of the neurotransmitter, the effects of an individual neurotransmitter can be manifold. Some examples of neurotransmitter actions are given below:

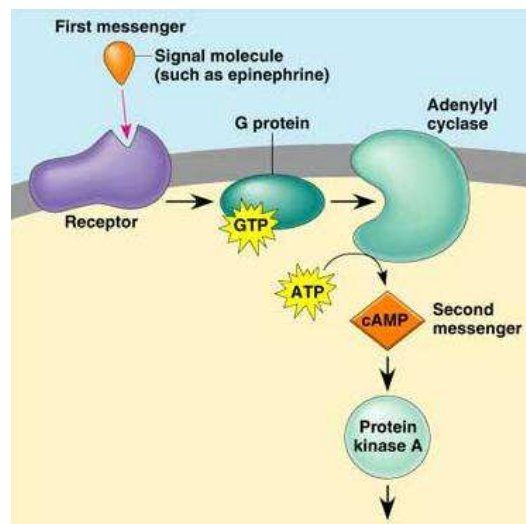
- acetylcholine – voluntary movement of the muscles,
- dopamine – voluntary movement and motivation, “wanting”,
- serotonin – memory, emotions, wakefulness, sleep and thermoregulation,
- GABA – inhibition of motoneurons,
- glycine – spinal reflexes and motor behavior,
- neuromodulators (e.g. endorphin, oligopeptide called “substance P”) – sensory transmission, pain, stress.

Second messengers are low-molecular-weight substances such as cyclic nucleotides (cAMP, cGMP), inositol triphosphate, diacylglycerol, nitric oxide or Ca²⁺ ions.

Cyclic adenosine monophosphate (cAMP) is synthesized from ATP by adenylyl cyclase, an enzyme located in the cell membranes. This enzyme is activated by the hormones glucagon

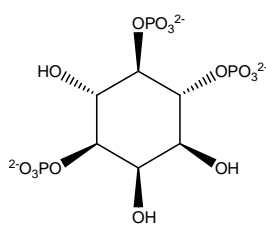
and adrenaline. The main purpose of cAMP is the activation of protein kinases – enzymes that phosphorylate other proteins (see Fig. 2). cAMP is also used to regulate the permeability of ion channels for Ca^{2+} ions, or to control glycogenolysis (glycogen decomposition into glucose) and lipolysis.

Fig. 2 Activation of protein kinase A by epinephrine (= adrenaline) through cAMP⁶⁰



Cyclic guanosine monophosphate (cGMP) is, analogously to cAMP, synthesized from GTP by guanylyl cyclase. Guanylyl cyclase is activated by peptide hormones or by nitric oxide. cGMP is responsible for ion channel conductance, glycogenolysis, cellular apoptosis (i.e. “cell suicide”), smooth muscle relaxation, and the response of the photoreceptors in the eye to light. Alike cAMP, sGMP is also involved in the regulation of protein kinases.

Inositol triphosphate (also referred to as triphosphoinositol, InsP_3) is released upon



hydrolysis of phosphatidylinositol-4,5-biphosphate (phospholipid located in the plasma membrane of a cell) by phospholipase C. It is used in signal transduction in cells, for mobilization of Ca^{2+} ions from storage organelles or for regulation of cell growth. InsP_3 is also responsible for contractions of smooth muscle cells: InsP_3 activates the

InsP_3 receptor on the membrane of the sarcoplasmic reticulum, resulting in the release of Ca^{2+} ions into the sarcoplasm. The increase in Ca^{2+} concentration activates a receptor-operated channel on the sarcoplasmic reticulum, leading to a further increase in the Ca^{2+} concentration in the muscle cell and resulting in its contraction⁶¹.

Diacylglycerol consists of two fatty acid chains covalently bonded to a glycerol molecule through ester linkages at the C-1 and C-2 positions. Synthesis of diacylglycerol begins with glycerol-3-phosphate, which is acylated twice by acyl-coenzyme A to form phosphatidic acid. Phosphatidic acid is then dephosphorylated to yield diacylglycerol. Mono- and diacylglycerols are common food additives and are to be found in animal or vegetable oil, bakery products, margarines, etc. Alike InsP_3 , diacylglycerol is also generated by phospholipase C. Once formed, it stays close to the plasma membrane and activates protein kinase C (higher concentration of Ca^{2+} primarily induced by InsP_3 is needed for diacylglycerol to activate the enzyme).

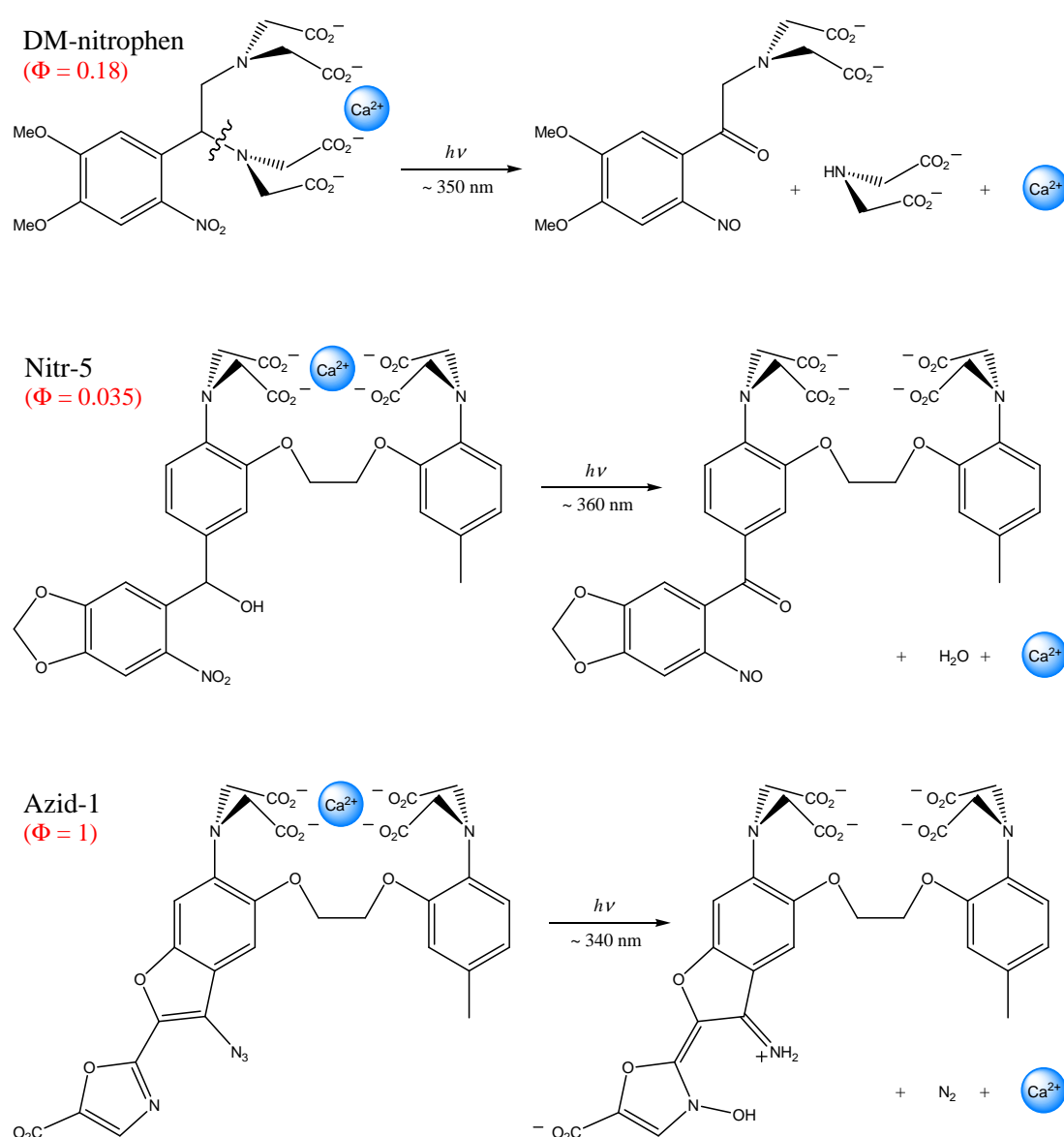
Calcium is the most abundant mineral in the human body. As indicated, calcium Ca^{2+} plays an important role in many biochemical processes – it is one of the most widespread second messengers used in signal transduction in eukaryotes. Increase in Ca^{2+} concentration can result e.g. in a contraction of muscle tissue, release of synaptic vesicles (vesicles containing neurotransmitters), secretion of hormones (insulin) and enzymes, adhesion of cells to an extracellular matrix, etc. Ca^{2+} is stored in sarcoplasmic reticula of the cells and in the extracellular fluid. Calcium ions can damage cells if their concentration exceeds the standard value (e.g. by overexcitation of neural circuits, which can occur after a brain trauma or a stroke). Ca^{2+} in excessive amounts may also cause apoptosis of the cell or its death by necrosis.

Caging of Ca^{2+} ions is based on the common ion chelators used in analytical chemistry such as EDTA (ethylenediamine tetraacetic acid)⁶² or BAPTA (1,2-bis(2-aminophenoxy)ethane-*N,N,N',N'*-tetraacetic acid), which are attached e.g. to an *o*-NB derivative⁶³. The mechanisms of action of these two classes of photolabile cages differ significantly. Lowering the ability of the EDTA-based cages (e.g. DM-nitrophen) to complex Ca^{2+} is achieved by photocleavage of one of the chelae. In the case of BAPTA cages (e.g. Nitr-5), the skeleton of the chelator is maintained, but the affinity for calcium is lowered (10 to 30 times) in consequence of a photo-induced change in its substituent (Scheme 11).

The main advantage of the nitr-5 cage over DM-nitrophen is its selectivity for calcium ions. On the other hand, DM-nitrophen exhibits a much greater affinity change towards Ca^{2+} upon photolysis, its photoreaction is faster and much more efficient⁹.

A decade ago, Adams *et al.*⁶⁴ developed a new PPG for calcium, which was also based on BAPTA. The photoactive moiety was no longer the *o*-NB group, but a derivative of fura-2, a fluorescent Ca^{2+} indicator with an azide substituent in the benzofuran 3-position. They named the cage Azid-1. Azid-1 does not fluoresce upon irradiation, but it undergoes an irreversible photoreaction (Scheme 11) yielding free Ca^{2+} with unity quantum yield. The high quantum yield of calcium release together with high absorption coefficients ($33\,000\text{ M}^{-1}\text{cm}^{-1}$ at 340 nm) make it a promising candidate for two-photon applications (two-photon absorption cross section $\sim 1.4\text{ GM}^*$ at 700 nm, see the next subchapter for more details)⁶⁵.

Scheme 11 Photolysis of caged calcium ions⁶²⁻⁶⁴



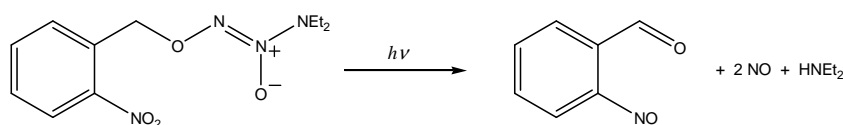
* 1 GM (Göppert-Mayer) = $10^{-50}\text{ cm}^4\text{ s photon}^{-1}$

The possibility to produce a fast jump in Ca^{2+} concentration in the cytoplasm is taken advantage of in the investigation of a number of cellular phenomena such as muscle contraction or neurotransmitter release⁶⁶.

Nitric oxide stimulates a formation cGMP and its effects include blood vessel dilatation, neurotransmission, modulation of the hair cycle, and penile erections. Sildenafil, popularly known by the trade name Viagra, works primarily by stimulating the release of NO within the vessels of the penis, inducing an erection⁶⁷. Nitric oxide is toxic to bacteria and other human pathogens, but many bacterial pathogens have evolved mechanisms for NO-resistance⁶⁸.

Caging of nitric oxide described by Makings and Tsien⁶⁹ is based on the known decomposition of diazeniumdiolates. The photosensitive derivatives are attached to the *o*-NB group and they release NO upon photolysis within 5 ms (Scheme 12).

Scheme 12 Photorelease of nitric oxide



Since the mid-80's, caged versions of numerous bioactive molecules have been synthesized and used on a variety of preparations. At present, neuroscientists and biochemists can choose out of several caging agents, which are more efficient than the NB-group, absorb at longer wavelengths, have biologically less-reactive byproducts and a higher efficiency of release. Some of the caged neurotransmitters are already commercially available.

Neurotransmitters, second messengers (except for nitric oxide, calcium and other ions) and other bioactive molecules such as proteins and peptides possess at least some of the following functionalities: carboxylate, amine, phosphate, hydroxyl or thiol. Their temporary deactivation by one of the PPGs introduced in Chapter 1.2. is therefore straightforward (several examples have been shown in the aforementioned chapter).

1.3.2. Two Photon Excitation (2PE)

The possibility of replacing UV-excitation by a simultaneous absorption of two IR-photons of equivalent total energy was first suggested by Göppert-Mayer in her doctoral thesis from the early 30's⁷⁰. However, it was not until the development of the first lasers in the early 60's that her prediction was corroborated⁷¹.

Two-photon excitation of photolabile compounds further improves the spatial and temporal resolution of the experiments investigating biological systems. By carefully focusing an IR-laser beam, one can selectively address volumes smaller than a femtolitre⁶⁵. Another advantage of this technique is that IR photons penetrate deeper in the tissue and are much less likely to damage it than the UV photons.

The probability of 2PE is proportional to I^2 and to δ , where I is the light intensity and δ the two-photon absorption cross section in GM. Hence, photolysis occurs only in the focal point of the laser beam and the surrounding area remains intact as long as the laser power is kept under ca 10 mW (higher powers may cause photodamage due to multiphoton absorption by the present biomolecules).

In principle, any chromophore can be excited by two long-wavelength photons and the subsequent "dark photochemistry" is usually the same as if it was excited by one UV photon. The only limitation of this technique is the photosensitivity of a molecule to 2PE. This photosensitivity is defined by the two-photon action cross section of the molecule δ_u ($\delta_u = \delta \times \Phi$). It was estimated that δ_u needed for practical applications at safe laser powers should be higher than 3 GM, which is a value higher than that of any known PPG (*o*-NB cages have δ_u values around 0.01 GM).

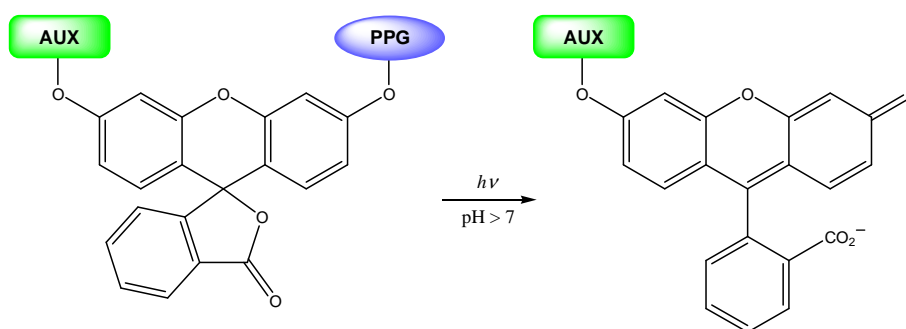
Nonetheless, successful two-photon release of calcium from azid-1 ($\delta_u \sim 1.4$ GM at 700 nm)⁶⁵ and of glutamate from its coumarinyl derivative ($\delta_u \sim 1.0$ GM at 740 nm)⁴⁸ have been reported. Brown *et al.*⁶⁵ calculated it would take a 10 μ s-long pulse of ca 7 mW power at 700 nm (Ti:sapphire laser) to photolyze all azid-1 within the focal volume of the given laser. Furuta and coworkers⁴⁸ applied the aforementioned caged glutamate to obtain the first 3D-resolved maps of the glutamate sensitivity of neurons in brain slices from rat cortex and hippocampus.

1.3.3. Photoactivatable Fluorophores

The active or diffusional movement of molecules in biological systems under steady-state conditions is conventionally measured using the FRAP (fluorescence recovery after photobleaching) technique. FRAP is based on the principal of observing the rate of recovery of fluorescence due to the movement of a fluorescent marker into an area of the membrane which contains this same marker but which has been rendered non-fluorescent via an intense photobleaching pulse of laser light. Photoactivation of fluorescence (PAF) achieved by photolysis of caged fluorophores attached to biomolecules and measurement of its dissipation is a complementary method with certain advantages over FRAP⁶⁶:

- PAF has a better signal to noise ratio since it generates positive signal against a negative background (the opposite of FRAP).
- Lower levels of fluorescent labeling are required (lesser perturbation of the properties of the biomolecule).
- With PAF, the light used for the photodeprotection (UV) and the light used for monitoring of the released fluorophore (VIS) are of different wavelengths, FRAP uses a one-wavelength setup, the bleaching and the monitoring light differ only in their relative intensities (additional bleaching by the probing light has to be taken into account).
- FRAP requires much higher light intensities than PAF, which might reduce side effects of irradiation on the biological system (even though more energetic light is used for PAF).
- Photoproducts of PAF – relatively stable fluorophores and nitrobenzaldehydes are not as destructive as the singlet oxygen released in the FRAP experiment.

Scheme 13 Photoactivation of fluorescein⁷²



AUX - auxiliary functional group that imparts particular solubility characteristics and/or covalent attachment capability
PPG - photoremovable protecting group

Besides fluorescein, *o*-NB-caged rhodamines, pyranines (NPE-HPTS), coumarins (NPE-HCC), resorufins and other fluorescent dyes have been prepared. The two-photon uncaging cross sections of some *o*-NB-caged coumarins at 740 nm were found to be fairly high (near 1 GM)⁷³.

Successful applications of photoactivatable fluorophores have been reported in various fields. They can function as photoactivatable fluorescent tracers when covalently attached to a macromolecule of interest. For example, Theriot *et al.* used resorufin coupled to G-actin to examine the motion of the pathogenic bacterium *Listeria monocytogenes* in the cytoplasm of infected epithelial cells. Moving bacteria generated "comet tails" of actin filaments in their trajectory that were marked by photoactivation of incorporated actin modified with caged resorufin. These marks stayed stationary relative to the substrate, rather than to the bacteria, and decayed within about half a minute⁷⁴. Reinsch *et al.* used caged fluorescein modified tubulin and PAF to examine microtubule assembly and transport during axonal growth⁷⁵.

1.3.4. Time-resolved X-ray

Co-crystallization of enzyme-substrate mixtures is virtually impossible since the two substances would react long before the crystals were ready for data collection. It is therefore desirable to find a way to protect one of the components and to trigger the reaction within the crystal. Mechanistic studies of enzymatic reactions may be studied e.g. by combining PPGs with Laue crystallography. The reaction can be initiated by a short laser pulse and then monitored by delayed synchrotron X-ray pulses. At present, the time resolution of such experiments is in the order of hundreds of picoseconds⁷⁶.

The time-resolved Laue crystallography has already been used for a number of studies of enzymatic reactions. In 1990, Schlichting and coworkers⁷⁷ used a time-resolved Laue study to investigate the conformational changes in Ha-ras p21 protein accompanying GTP hydrolysis. About a decade ago, Šrajcar *et al.*⁷⁸ published nanosecond crystallographic snapshots of CO photodissociation from the heme of myoglobin. Cohen *et al.*⁷⁹ synthesized caged NADP and NAD and used these compounds in a crystallographic study of isocitrate dehydrogenase.

1.3.5. Kinetics of protein folding

It was until recently that kinetic studies of protein folding were limited to stopped-flow experiments. A decade ago, Hochstrasser and coworkers^{80, 81} attempted to photoinitiate the formation of α -helical peptide by cleaving the disulfide bridge (by a 270 nm-light), which constrained the peptide in a non-helical conformation. The authors intended to monitor the folding process by means of IR and CD spectroscopy. However, they have experienced problems with a subsequent recombination of the thiyl radicals. A few years later, Hansen *et al.*⁸² used benzoin as a linker between the N-terminus of the peptide and the internal amino acid side chain (Scheme 14). The authors believe to have observed the formation of the α -helix based on the change in circular dichroism but more informative methods such as time-resolved IR would be required to confirm their point.

Scheme 14 Photoinduced protein folding⁸²



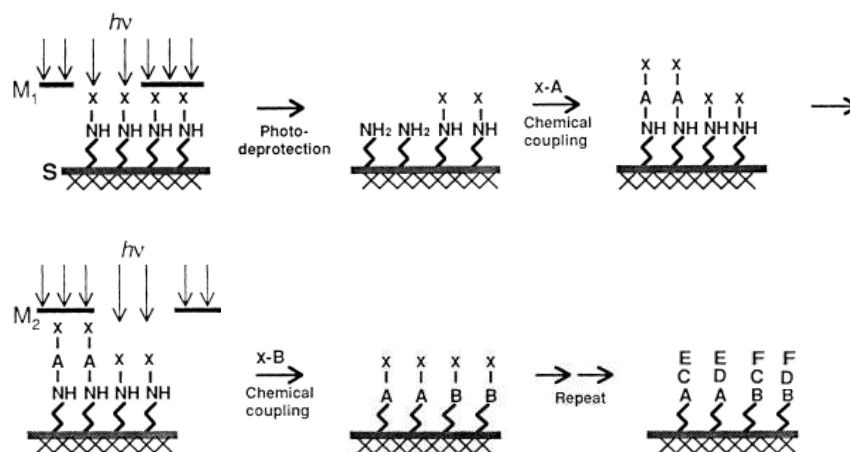
Abbruzzetti and coworkers used laser-induced pH jumps to study the kinetics of local helix formation in poly-L-glutamic acid by means of photoacoustics⁸³. pH jumps can be brought about by using caged protons, e.g. in a form of *o*-nitrobenzaldehyde, which rearranges to *o*-nitrosobenzoic acid and releases a proton upon irradiation (two-photon photolysis of *o*-nitrobenzaldehyde has been reported recently by Diaspro *et al.*⁸⁴). In addition to pH jumps, laser-induced temperature jumps as well as energy-transfer methods are increasingly applied to study these processes⁹.

1.3.6. Solid-phase Synthesis, Molecular Arrays

In 1991, Fodor and coworkers⁸⁵ published a revolutionary paper, in which they reported on a light-directed, spatially addressable parallel chemical synthesis to yield a highly diverse set of chemical products. They combined solid-phase chemistry, PPGs and photolithography to synthesize an array of 1024 ($= 2^{10}$) different peptides in ten steps. The authors attached protected building blocks to a solid support and irradiated them through a mask. Only the

molecules exposed to light were deprotected, the rest remained intact. The free functionalities were coupled with other caged molecules of a different kind and the rest washed away. Then, a different mask was used to deprotect another set of molecules, which became free to react. By repeating these irradiation and coupling steps n -times, they were able to synthesize up to 2^n different compounds (see Scheme 15).

Scheme 15 Concept of light-directed spatially addressable parallel chemical synthesis⁸⁵



Affymetrix, Inc. utilizes the ability to produce high-density oligonucleotide arrays, the so-called DNA chips (GenChip® probe arrays), for DNA sequencing. Vossmeier *et al.*⁸⁶ extended Fodor's technique to light-directed assembly of nanoparticles onto a solid substrate. A similar photolithographic technique has been also used for a synthesis of short (10 nucleotides) DNA-fragments⁸⁷.

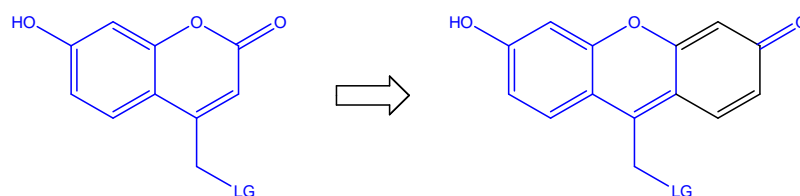
2. Problem Statement

The aim of this work was to investigate the photophysical and photochemical properties of the derivatives of a new photoremovable protecting group for acids and phosphates, (6-hydroxy-3-oxo-3*H*-xanthen-9-yl)methyl. Three derivatives of this PPG, namely diethylphosphate, acetate and bromide, have been synthesized by a former member of our group, Jürgen Wintner. The syntheses and the spectrophotometric titrations of the prototropic forms of the three compounds are described in his doctoral work⁸⁸. The bromide derivative was synthesized as a test compound to verify, whether the idea works, since bromide is a good leaving group.

The concept was based on the photochemistry of 7-hydroxycoumarin-4-yl-methyl (HCM) acetate described by Furuta and coworkers⁴⁸. The photolysis of HCM acetate is analogous to that of other coumarins and it has already been shown in Scheme 9. HCM shows a high two-photon action cross section. This cross section can be further increased by an introduction of a bromine atom to the 6-position. This substitution of hydrogen by bromine also results in lowering of the pK_a of the C7 hydroxyl, which becomes deprotonated under physiological conditions (pH 7). The anionic form of HCMs absorbs more strongly than the neutral one (and at longer wavelengths), which is also favorable for the two-photon excitation.

The structure of our novel PPG was derived from the structure of HCM cages by extending the chromophore by one more aromatic ring to form a derivative of 6-hydroxy-3*H*-xanthen-3-one (Scheme 16).

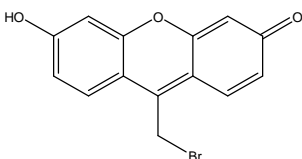
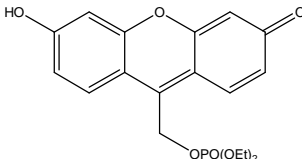
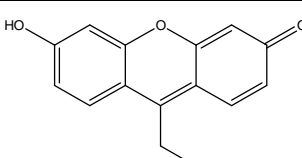
Scheme 16 Structural similarity between the hydroxycoumarin cages and the new caged compounds derived from 6-hydroxy-3*H*-xanthen-3-one.



Extending the chromophore by one more aromatic ring had two desirable effects: a decrease of pK_a of the hydroxyl group, which dropped from > 7 (HCM⁴⁸) to about 6.2 ± 0.1 ⁸⁸,

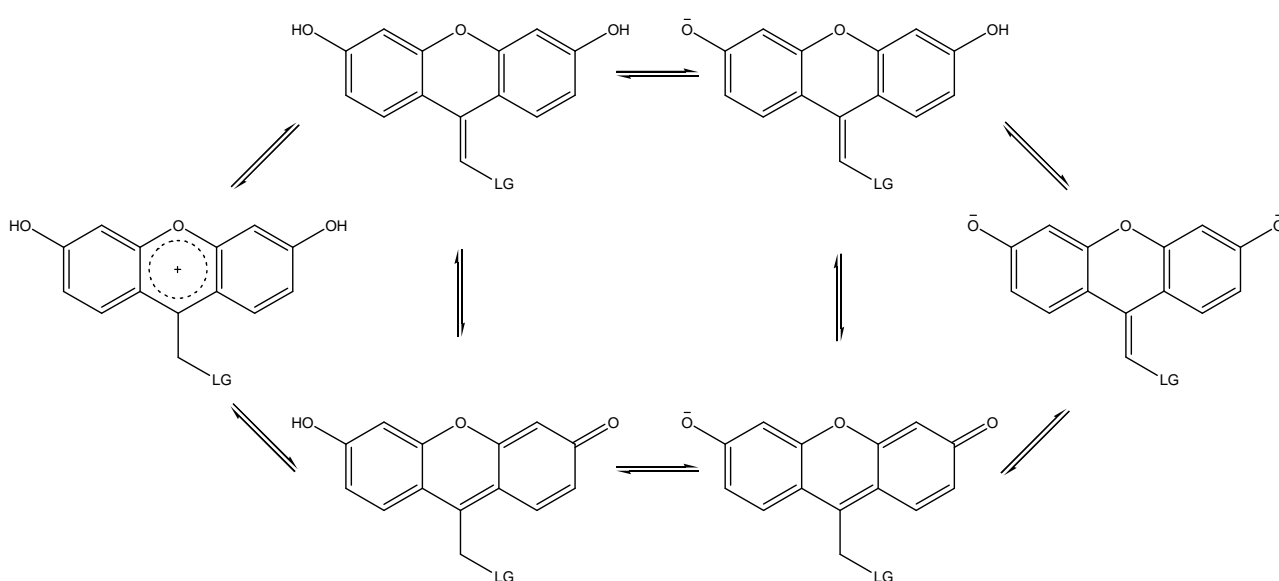
and a substantial red shift of the first absorption band of the prevailing form at pH 7, i.e. anionic xanthen chromophore ($\lambda_{\max} > 510$ nm for the three synthesized derivatives, see Table 1) and the neutral HCM chromophore ($\lambda_{\max} = 325$ nm).

Table 1 Absorption maxima and molar extinction coefficients of the three derivatives of (6-hydroxy-3-oxo-3*H*-xanthen-9-yl)methyl at pH 7 (phosphate buffer, $I = 0.1$ M)⁸⁸

| Compound | λ_{\max} / nm | $\epsilon_{\lambda_{\max}}$ / $\text{dm}^3 \text{mol}^{-1} \text{cm}^{-1}$ |
|--|-----------------------|--|
|  | 519 | 25 750 |
|  | 528 | 24 460 |
|  | 522 | 22 720 |

A somewhat undesirable effect of the chromophore extension is a complication of the system due to tautomerism that comes into play (see Scheme 17).

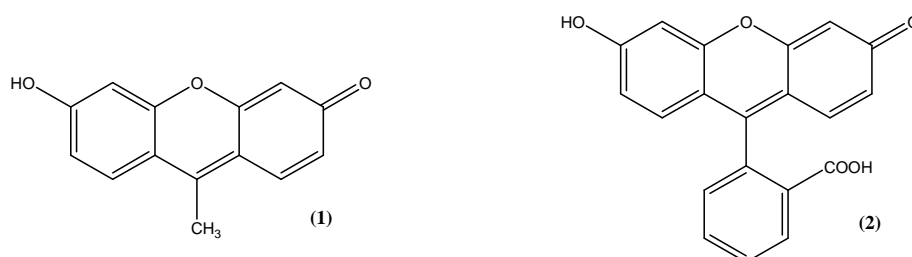
Scheme 17 Protolytic equilibria of the (6-hydroxy-3-oxo-3*H*-xanthen-9-yl)methyl cage (LG = leaving group)



Scheme 17 shows all the possible prototropic forms of the (6-hydroxy-3-oxo-3*H*-xanthene-9-yl)methyl cage. The neutral and the monoanionic species can exist in two tautomeric forms, keto (K) and enol (E) form. The experimental dissociation constants $pK_{a,1}$ and $pK_{a,2}$ are composites of the keto and the enol forms. The ratios K/E and K^-/E^- are constant regardless of the pH, provided the equilibration is fast enough (on the measurement time scale). The monoanionic and the neutral forms hence behave spectrally as if they were each a single species.

3. Results and Discussion

3.1. Fluorescence of 6-Hydroxy-9-methyl-3*H*-xanthen-3-one (**1**)



In 1996, Klonis and Sawyer reported on the spectral properties of prototropic forms of fluorescein (**2**) in aqueous solutions⁸⁹. Compared to 6-hydroxy-9-methyl-3*H*-xanthen-3-one (**1**), fluorescein has an additional –COOH group and the pK_a values for deprotonation of the cationic, neutral and monoanionic forms are 2.2, 4.3, and 6.4, respectively. The fluorescence spectra of the neutral and the anionic form of **1** correspond to the mono- and dianionic forms of **2**, respectively (see Fig. 3).

The fluorescence spectra of **1** and **1**[–] are very similar, both having maxima at 505 and 545 nm. The only difference is in the relative intensity of the two bands. The 545 nm band of **1**[–] is about 1/3 of the intensity of the band at 505 nm, whereas these two bands are approximately of the same intensity (10:9) in a spectrum of neutral **1**.

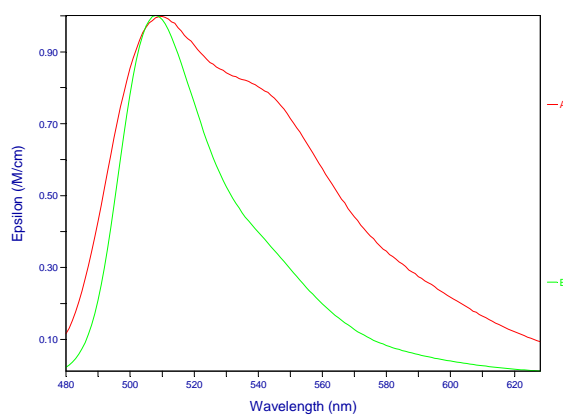
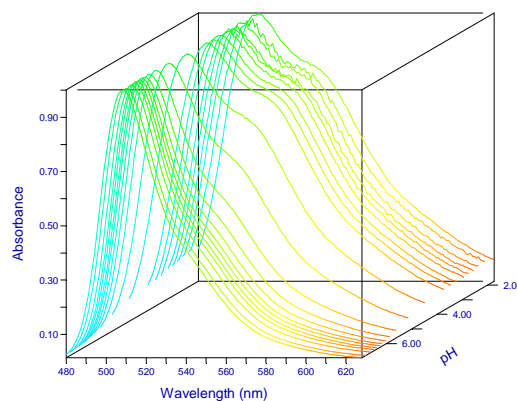
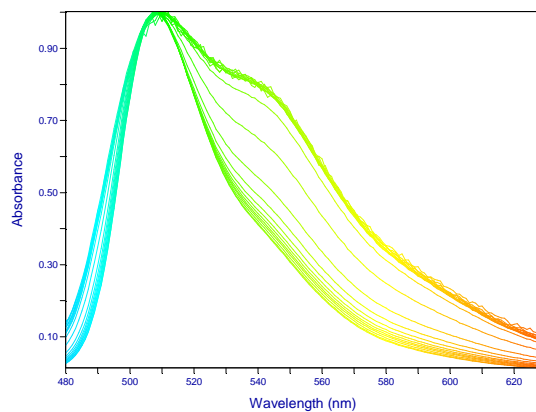
Table 2 pK_a values of **1** in the ground state and in the excited state

| | $pK_{a,1}$ | $pK_{a,2}$ | $pK_{a,3}$ |
|---|------------|------------|------------|
| Ground state (experimental values) ⁸⁸ | 3.44 | 6.31 | 13.6 |
| Excited state (estimate, see below) | -0.76 | 4.78 | – |

Due to the pK_a^* values (i.e. pK_a in the excited singlet state, see Table 2) and to a fast deprotonation of **1**⁺ in the excited state, the only species fluorescing in the pH range 1.5 – 4 is the neutral **1**. The apparent value of $pK_{a,2}^*$ obtained experimentally by means of a fluorometric titration (Fig. 3) of **1** starting with a phosphate buffer solution ($I = 0.1$ M) was 5.37. This experimental value would most probably approach the estimated one (4.78, see below)

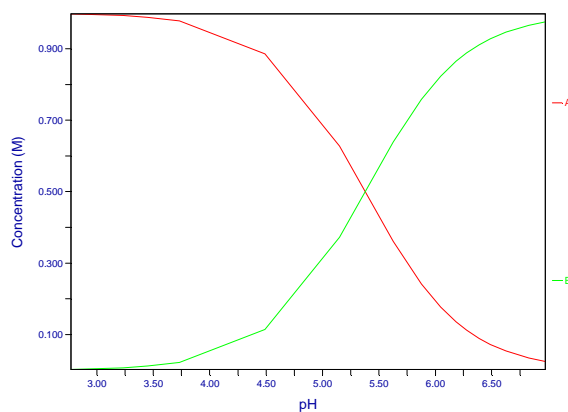
e.g. in a 1 M acetate buffer (higher concentration of a base, phosphate or acetate, is needed to achieve full equilibration within the lifetime of the excited species).

Fig. 3 Fluorometric Titration (SPEX)



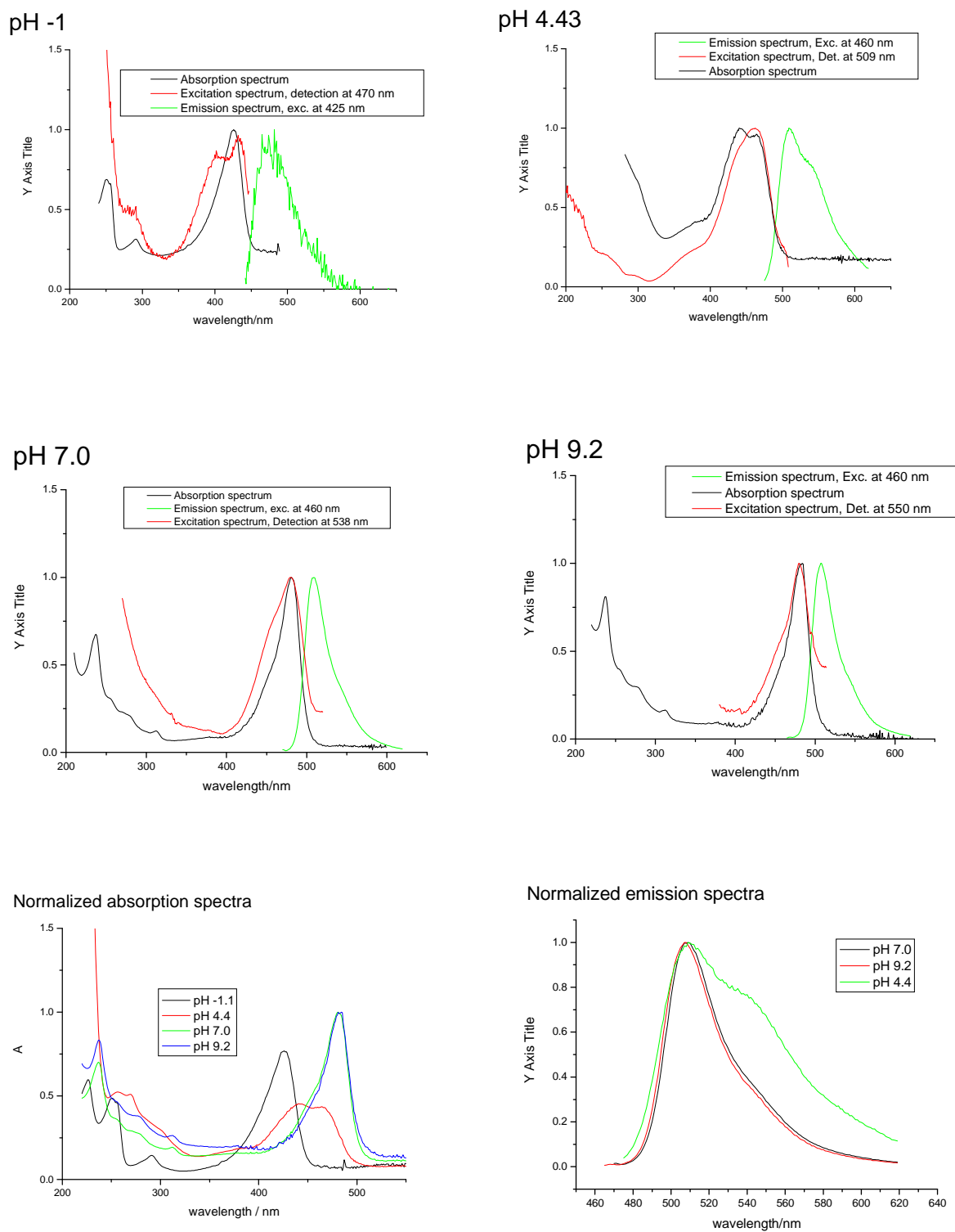
◀▲ 2D and 3D courses of fluorometric titration of $1^*/1^{-*}$ in a phosphate buffer solution ($I = 0.1$ M, pH 7) by 0.1 M HCl (normalized spectra).

◀ Resolved emission spectra of 1^* (A) and 1^{-*} (B).



◀ Relative contributions to fluorescence by 1^* (A) and 1^{-*} (B). The intercept at pH 5.37 gives the apparent pK_a^* value mentioned in the text.

Fig. 4 Fluorescence Spectra of **1** at different pH (SPEX)



The $pK_{a,1}^*$ (i.e. the pK_a of deprotonation of the cationic form in the excited state) is predicted to be -0.76 (Förster cycle, see below). Our fluorescence experiments indicated a value between 1.7 and -1.1 . Therefore the fluorescence spectrum of the cation begins to appear only under strongly acidic conditions, e.g. in concentrated H_2SO_4 or HCl (we have observed it in a 27 % HCl). This emission, which is a mirror image of the cation absorption spectrum, has a peak at 470 – 480 nm.

Estimates of $pK_{a,1}^*$ and $pK_{a,2}^*$ of **1**

$$\text{Förster equation: } pK_a^* = pK_a - \frac{N_A h}{2.3RT} (\nu_1 - \nu_2) \quad (\text{eq. 1})$$

$$\text{For } T = 293.15 \text{ K: } pK_a^* = pK_a - 7.118 \times 10^{-14} \text{ s} \times (\nu_1 - \nu_2) \text{ s}^{-1} \quad (\text{eq. 2})$$

| Species | $\lambda_{\text{max}}/\text{nm}$ | ν/s^{-1} |
|-----------|----------------------------------|-------------------------|
| Monoanion | 481 | 6.2327×10^{14} |
| Neutral | 465 | 6.4471×10^{14} |
| Cation | 426 | 7.0374×10^{14} |

$$pK_{a,1}^* = pK_{a,1} - 7.118 \text{ s} \times (7.0374 - 6.4471) \text{ s}^{-1}$$

$$pK_{a,1}^* = 3.44 - 4.20 = -0.76$$

$$pK_{a,2}^* = pK_{a,2} - 7.118 \text{ s} \times (6.4471 - 6.2327) \text{ s}^{-1}$$

$$pK_{a,2}^* = 6.31 - 1.53 = 4.78$$

Klonis and Martin^{89, 90} give following quantum yields of fluorescence and lifetimes of the fluorescent species of **2** obtained by a phase modulation method using a glycogen suspension as a reference (Table 3).

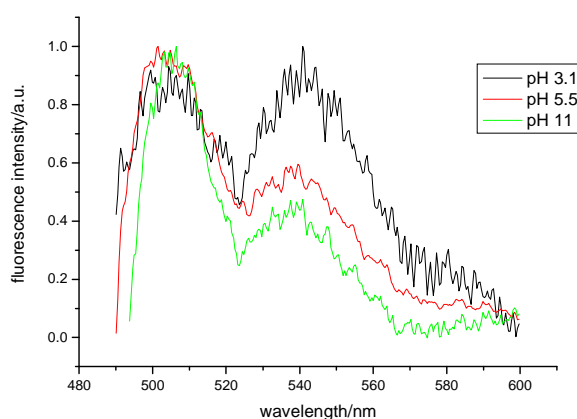
Table 3 Quantum yields and lifetimes of **2**⁺, **2**, **2**⁻ and **2**²⁻ according to Klonis and Martin^{89, 90}

| Species / conditions | Fluorescence quantum yield | Lifetime / ns |
|----------------------------|----------------------------|-----------------|
| Cation / 3M H_2SO_4 | 0.9 – 1.0 | 3.5 – 4.4 |
| Neutral (Quinoid) / pH 1.6 | 0.29 | 2.97 ± 0.02 |
| Monoanion / pH 4.5 | 0.36 | 3.37 ± 0.02 |
| Dianion / 0.01 M NaOH | 0.93 | 4.06 ± 0.02 |

Alvarez-Pez and coworkers⁹¹ claim to have resolved the lifetimes of the mono- and dianionic forms of **2** present at pH around 7 (in 1 mM and 1 M phosphate buffer). They report somewhat longer lifetimes: 4.34 ns for the dianion and 3.70 ns for the monoanion.

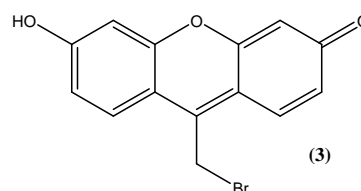
Our time-resolved experiments (Clark-MXR Ti:Sa laser CPA 2001 coupled to a noncollinear optical parametric amplifier (NOPA), excitation light of 490 nm, detection by streak camera) yielded lifetimes of (3.5 ± 0.1) ns for both neutral and anionic forms of **1**, independently of the pH (in the interval 3 – 11). In these experiments, the band at 545 nm was much better resolved and its relative intensity to the band at 505 nm varied depending on the pH from 1:1 (pH 4 and lower) to 2:5 (pH 9 and higher). At pH 5.5 and lower, an additional indistinct band at 580 appeared (Fig. 5). The kinetics of its decay was, however, the same as that of the other two bands.

Fig. 5 Fluorescence Spectra of **1** (streak camera)



3.2. Time-resolved Fluorescence Experiments

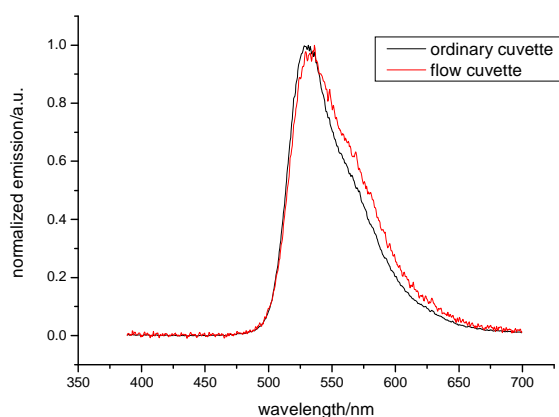
Compound **3** was subjected to a time-resolved experiment similar to the one described above. The excitation wavelength used was 515 nm and the repetition frequency of the laser was lowered by about 90 % to 40 Hz. The solution of **3** in phosphate buffer ($I = 0.1$ M, pH 7.0) flowed through a 2-mm thick cuvette with a flow speed of 1 ml per second. The laser was focused to a spot of ca 1 mm in diameter. In this



arrangement, each recorded spectrum should correspond to a fresh (i.e. non-irradiated) solution. The goal was to observe only the fluorescence of **3** and not that of its photoproduct.

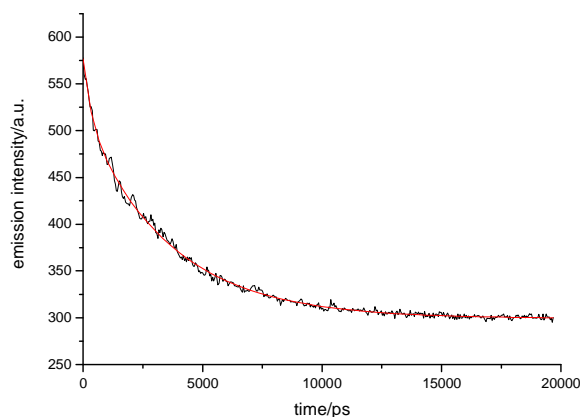
When an ordinary (non-flow) cuvette was used (i.e. the photoproduct was irradiated), we have obtained fluorescence emission spectra similar to those of **1** but with maxima at 530 and 570 nm. The fluorescence decayed monoexponentially, again with a similar lifetime of (3.55 ± 0.10) ns.

Fig. 6 Emission spectra of **3** and its (photo-)product



In a flow cuvette, however, even though the spectra did not change very much, we could clearly see kinetics of two processes (biexponential decay, see Fig. 7). The slower component $\tau = (3.54 \pm 0.04)$ ns seemed to be that of the product, the faster component had a lifetime of (331 ± 30) ps. The measurement was repeated three times for time windows of 20, 5, and 2 ns.

Fig. 7 Decay of fluorescence of **3** (streak camera, 20 ns time window)



$$y = A_1 e^{(-x/\tau_1)} + A_2 e^{(-x/\tau_2)} + y_0;$$

$$y_0 = 299.1 \pm 0.3;$$

$$R^2 = 0.996$$

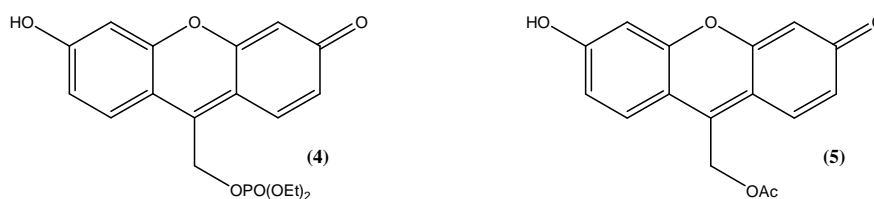
$$A_1 = 220.1 \pm 1.7; \quad \tau_1 = 3540 \pm 38$$

$$A_2 = 57.4 \pm 2.5; \quad \tau_2 = 331 \pm 30$$

We attribute the shorter lifetime to **3**, the longer one to its product. It seems that even though we have prepared a fresh solution for the measurements, there was already a noticeable amount of the product (which apparently fluoresces much more strongly than **3** itself; the fluorescence of the product will be discussed later in more detail). Another possible reason could have been the laminar flow of the liquid in the cuvette causing a repeated irradiation of the same solution near the cell inner surface. Unfortunately, we could neither increase the flow speed, nor decrease the frequency of the laser any further for technical reasons.

3.3. Quantum Yield Measurements

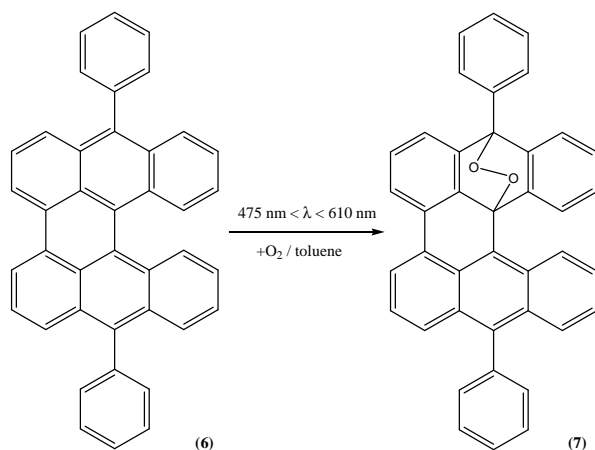
We have determined the quantum yields of photoconversion of **3**, **4** and **5** to their common (but still unknown) photoproduct.



The actinometer used was meso-diphenylhelianthrene (MHD (**6**)), which undergoes a uniform and well-described⁹² self-sensitized photo-oxidation reaction in a solution of air-saturated toluene to form **7** (MDHPO). A singlet excited state ¹MDH intersystem-crosses to triplet ³MDH, which sensitizes oxygen that is present in the solution, thus forming singlet oxygen, which reacts with a molecule of MDH to form an endo-peroxide MDHPO.

A 10⁻³ M solution of **6** in toluene totally absorbs incident radiation between 475 and 610 nm (1 cm path length). For this concentration, the formation of MDHPO is independent of the MDH concentration and the photo-oxidation can be followed photometrically at 429 nm, where MDHPO absorbs considerably (and MDH does not); see Fig. 8.

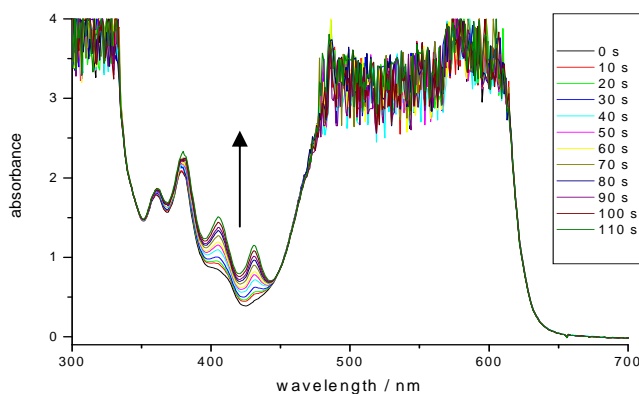
Knowing the amount of **7** formed per time interval and the quantum yield of its formation, one can easily determine the number of photons that enter the sample per given time interval (linear regression, R² ≥ 0.99).



Once we know the number of photons that enter the sample per second and the absorbance of our sample, we can also determine the quantum yield of the formation of our product (indeed the light has to be monochromatic and both the actinometer and our compound have to absorb at the same wavelength).

The wavelength of the irradiation light (Clark-MXR Ti:Sa laser CPA 2001 coupled to NOPA) was $538 \pm 7 \text{ nm}$ (bandwidth at half height) and the number of photons entering the sample cell were around $4.8 \times 10^{-9} \text{ einsteins s}^{-1}$ (the quantum flux was determined with more precision before and after each measurement and the average of the two measurements was used for the calculation of the quantum yield).

Fig. 8 Self-sensitized photooxidation of **6** to **7**



The quantum yields of photoreaction of **3** - **5** listed in Table 4 were calculated from the measured quantum flux through the cuvette and from the decrease in absorbance at $\lambda = 538 \text{ nm}$ in time. 2D- and 3D-courses of the photoreactions of **3**, **4** and **5** are shown in Fig. 9 to Fig. 11.

Fig. 9 Compound **3** irradiated at $\lambda = 538$ nm in water pH = 7 (phosphate buffer, $I = 0.1$ M)

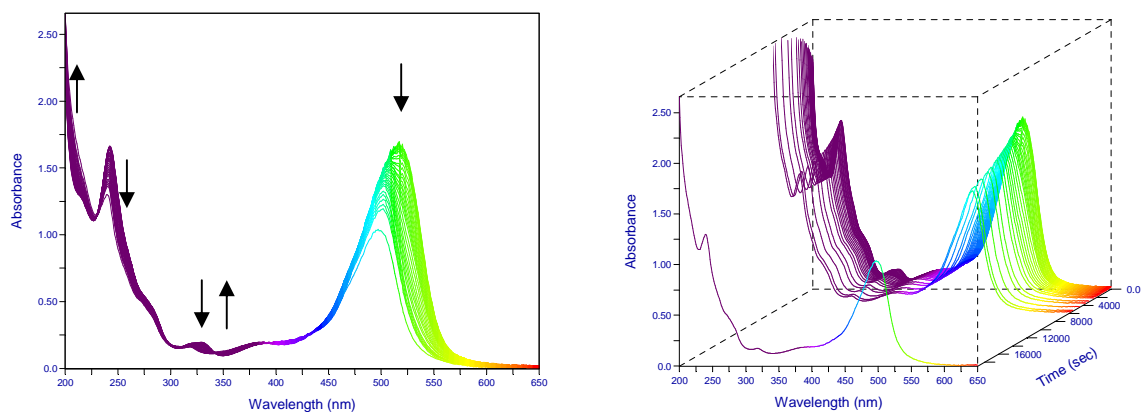


Fig. 10 Compound **4** irradiated at $\lambda = 538$ nm in water pH = 7 (phosphate buffer, $I = 0.1$ M)

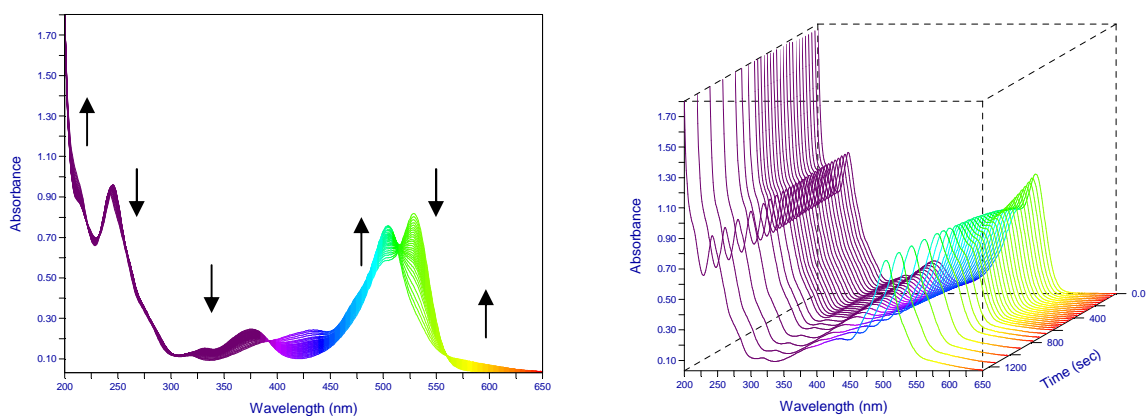


Fig. 11 Compound **5** irradiated at $\lambda = 538$ nm in water pH = 7 (phosphate buffer, $I = 0.1$ M)

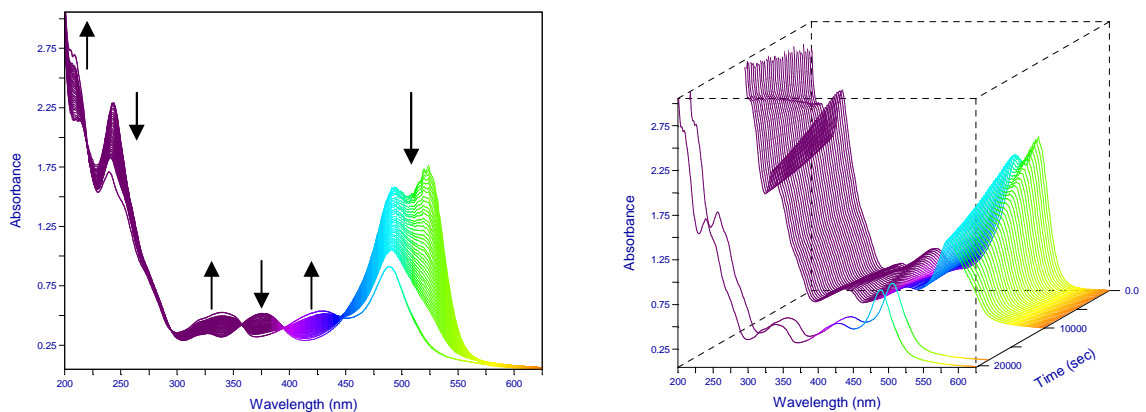
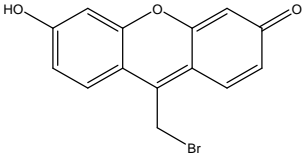
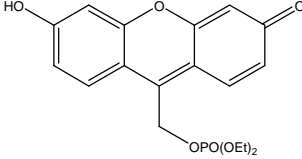
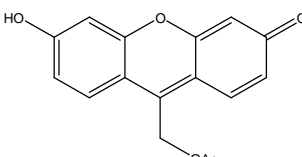


Table 4 Quantum yields of dissociation for compounds **3**, **4** and **5** in phosphate buffer ($I = 0.1$ M, pH 7)

| Compound | Quantum yield Φ |
|---|----------------------|
|  | $(4.2 \pm 0.2) \%$ |
|  | $(2.7 \pm 0.3) \%$ |
|  | $(0.48 \pm 0.08) \%$ |

The quantum yields of the photoreactions of **3**, **4** and **5** decrease from **3** to **5**. This may be attributed to the difference in pK_a of the conjugated acids of the leaving anions: HBr (-9.0), $(EtO)_2POOH$ (0.71) and AcOH (4.76). The higher the stability of the anion, the better the leaving group.

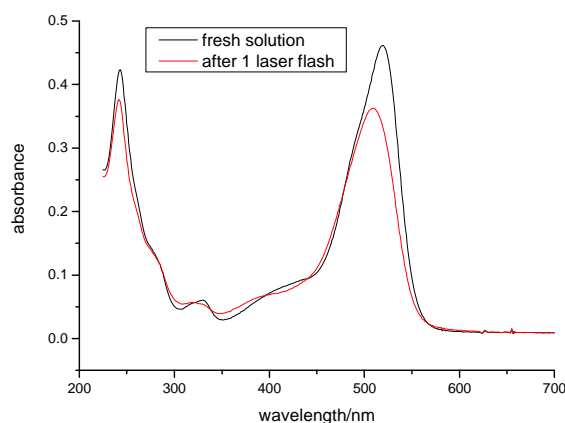
Schade *et al.*⁴⁶ determined quantum yields of similar (7-methoxycoumarin-4-yl)methyl-caged acids (MCM-esters). The quantum yield of the ester photocleavage of MCM-OPO(OEt)₂ (equivalent of **4**) was reported to be 3.7 %, and that of MCM-benzoates to be around 0.5 %. Furuta and coworkers⁴⁸ give a quantum yield of HCM-acetate of 2.5 %.

Schmidt and coworkers⁹³ have recently reported on the mechanism of photocleavage of several (coumarin-4-yl)methyl esters of biologically active acids (CM-A). The initial step of the photoreaction is a formation of a singlet ion pair $^1[CM^+ A^-]$. They authors have found out that the stabilization of the free ions CM^+ and A^- (using electron-donating substituents on the CM unit and/or increasing the acid strength of HA) leads to a strong enhancement of the rate of ion pair formation and to a diminution of the rate of recombination, which consequently leads to an increase of the efficiency of product formation. Recombination of the initial ion pair is also most likely to be the reason for relatively low quantum yields of our (6-hydroxy-3-oxo-3H-xanthen-9-yl)methyl cages.

3.4. Laser Flash Photolysis (LFP)

Several LFP experiments have been carried out with solutions of compound **3** in a phosphate buffer. Nevertheless, considering the lifetime of the excited species ($\tau_{fl} = (330 \pm 30)$ ps), the quantum yield of the photoreaction (4.2 %), and the duration of the excimer laser pulse (60 ns, which corresponds to ca 200 lifetimes), the phenomena observed after the laser pulse can hardly be attributed to the compound **3** itself, but mostly to its product. Fig. 12 shows that most of the compound **3** is converted to its product by a single flash.

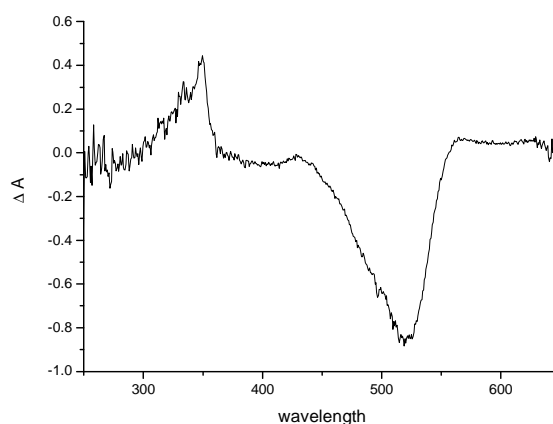
Fig. 12 Absorption spectrum of **3** measured before and after one laser flash (UV-Vis spectrophotometer)



The excitation wavelength used for all LFP experiments was 248 nm (KrF excimer laser, Compex 205, Lambda Physik).

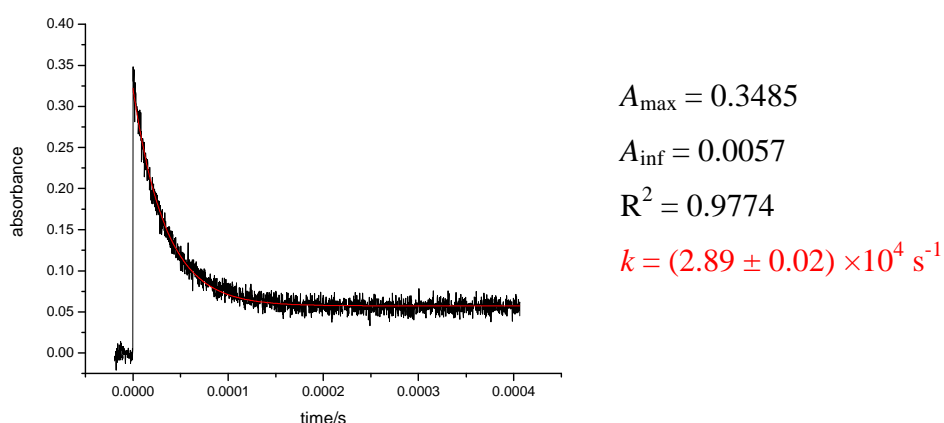
Unlike in the case of irradiation by visible light, the chromophore seems to be destroyed when irradiated by UV light. Further flashes result in a complete disappearance of the product.

Fig. 13 Absorption difference spectrum of **3** at the end of the laser flash (phosph. buffer $I = 0.1$ M, pH 7, ICCD camera)



The absorption difference spectrum measured by an ICCD camera at the end of the first laser flash (with a fresh solution of **3** as reference and excitation wavelength of 248 nm) contains “negative bands” in the visible region, where the fresh solution originally absorbed (bleaching), see Fig. 13. There is also a new absorption band appearing in the UV region having a maximum at 350 nm. Its kinetics is shown in Fig. 14.

Fig. 14 Monoexponential decay of the absorption band at 350 nm right after the laser flash (phosph. buffer $I = 0.1$ M, pH 7)



The amplitude of the signal becomes smaller with subsequent laser flashes (complete disappearance of the signal within 10 flashes). The decay obeys first-order kinetics. The end-absorption at 350 nm (measured about 1 minute after the laser flash) can also be seen in Fig. 12.

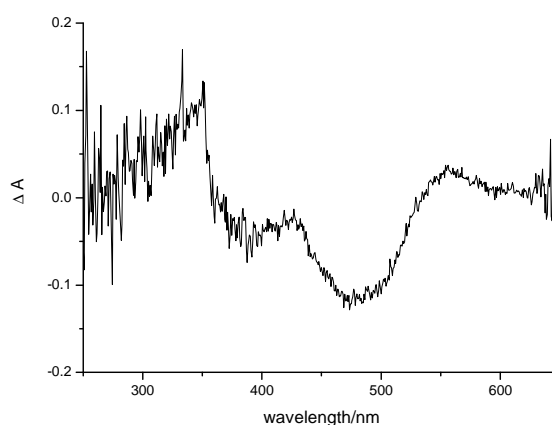
Bubbling the solution of **3** by O_2 for 15 minutes results in no observable change in the absorption spectrum of the transient (350 nm), the kinetics of its decay, however, becomes almost two times faster ($k = 5.41 \times 10^4 \text{ s}^{-1}$). Degassing of the solution, on the other hand, leads to a slight slowdown of the decay ($k = 1.95 \times 10^4 \text{ s}^{-1}$).

The decay of the transient seems to be, to a small extent, dependent on oxygen concentration. The observed constant of quenching by oxygen $k_q[\text{O}_2]$ is ca $3 \times 10^7 \text{ M}^{-1} \text{ s}^{-1}$, which is by three orders of magnitude less than a diffusion-controlled energy transfer to oxygen ($\sim 10^{10} \text{ M}^{-1} \text{ s}^{-1}$). This might imply the oxygen either reacts with the transient with certain activation barrier or it just catalyses the product formation in some way. Nevertheless, the rate constants differ

only slightly in degassed and oxygen-saturated solutions and it would be inappropriate to make any firm conclusions based on this small difference.

The transient absorption spectrum recorded straight after the LFP (< 20 ns) of a solution of **3** in acetate buffer (pH 4.46) also contains negative bands due to the bleaching (corresponding to the absorption of the neutral **3**, which was used as a reference) and the band at 350 nm (Fig. 15). Its kinetics also obeys the first-order law but it becomes slightly slower ($k = 2.37 \times 10^4 \text{ s}^{-1}$) than at pH 7.

Fig. 15 Absorption difference spectrum of **3** at the end of the laser flash (acetate buffer $I = 0.1$ M, pH 4.46, ICCD camera)

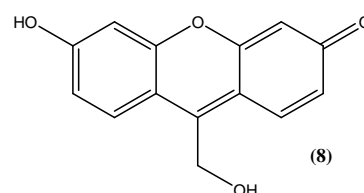


As at pH 7, bubbling of the solution of **3** in acetate buffer also resulted in a noticeable increase of the decay rate ($k = 5.56 \times 10^4 \text{ s}^{-1}$).

The observed transient is probably the cation formed by a photocleavage of the bromide anion. Quenching experiments with high concentrations of a base (e.g. N_3^-), which should confirm or refute this notion, are going to be carried out in the near future.

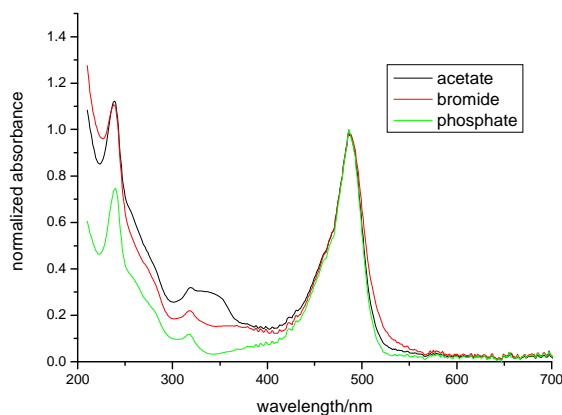
3.5. Photoproduct

No matter if converted by irradiation or just left in an aqueous solution for several days, all three compounds (**3–5**) finally



yield the same main product with characteristic bands at 239 and 488 nm. The spectra (Fig. 16) are also not dissimilar to the anionic forms of **3–5**, suggesting both the photoproduct and/or the product of spontaneous decomposition in aqueous solutions still contain the original chromophore.

Fig. 16 Spectra of **3**, **4** and **5** in phosphate buffer ($I = 0.1$ M, pH 7) 10 days after irradiation



The primary product of the reaction is most probably 9-(hydroxymethyl)-6-hydroxy-3*H*-xanthen-3-one (**8**). This notion is based on the fact, that a drop in pH can be observed upon photolysis in non-buffered solutions (the anion of the LG is substituted in the molecule by OH⁻ from water, thus leaving H⁺LG⁻ acids, which depending on their strength partially or completely dissociate). The formation of an analogous alcohol in water or mixed H₂O/CH₃CN solutions has also been described for the coumarinyl PPG^{46-48, 53, 94-96} (see Scheme 9).

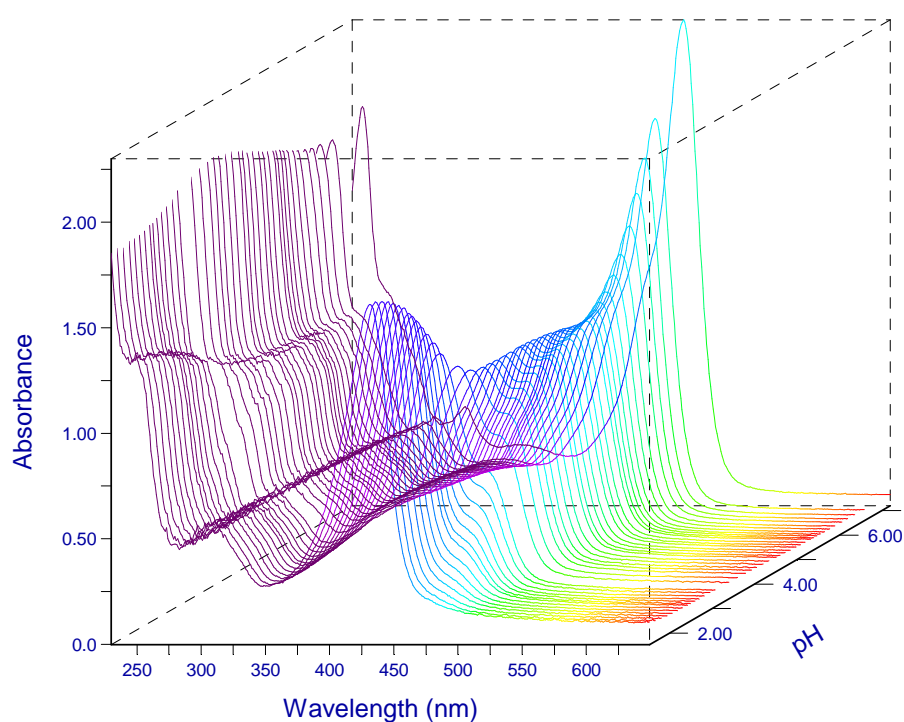
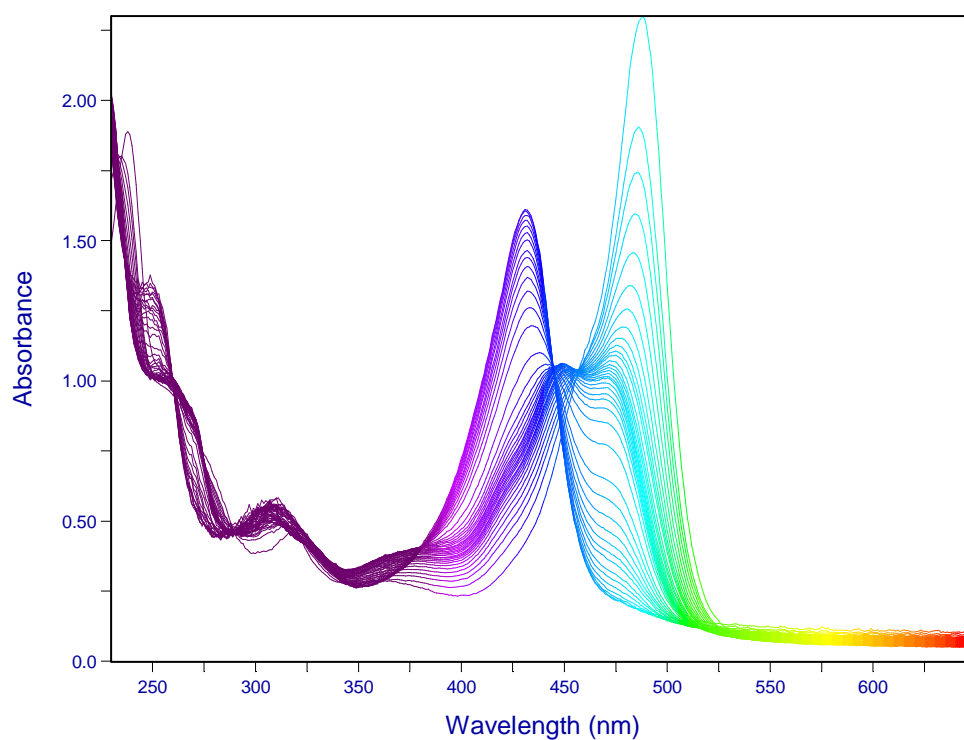
The absorption maximum of **8** is blue-shifted with respect to the caged compounds to 505 nm. Similarly to hydroxymethylcoumarin, this compound is also highly-fluorescent (which is not the case for the original caged substances **3**, **4** and **5**).

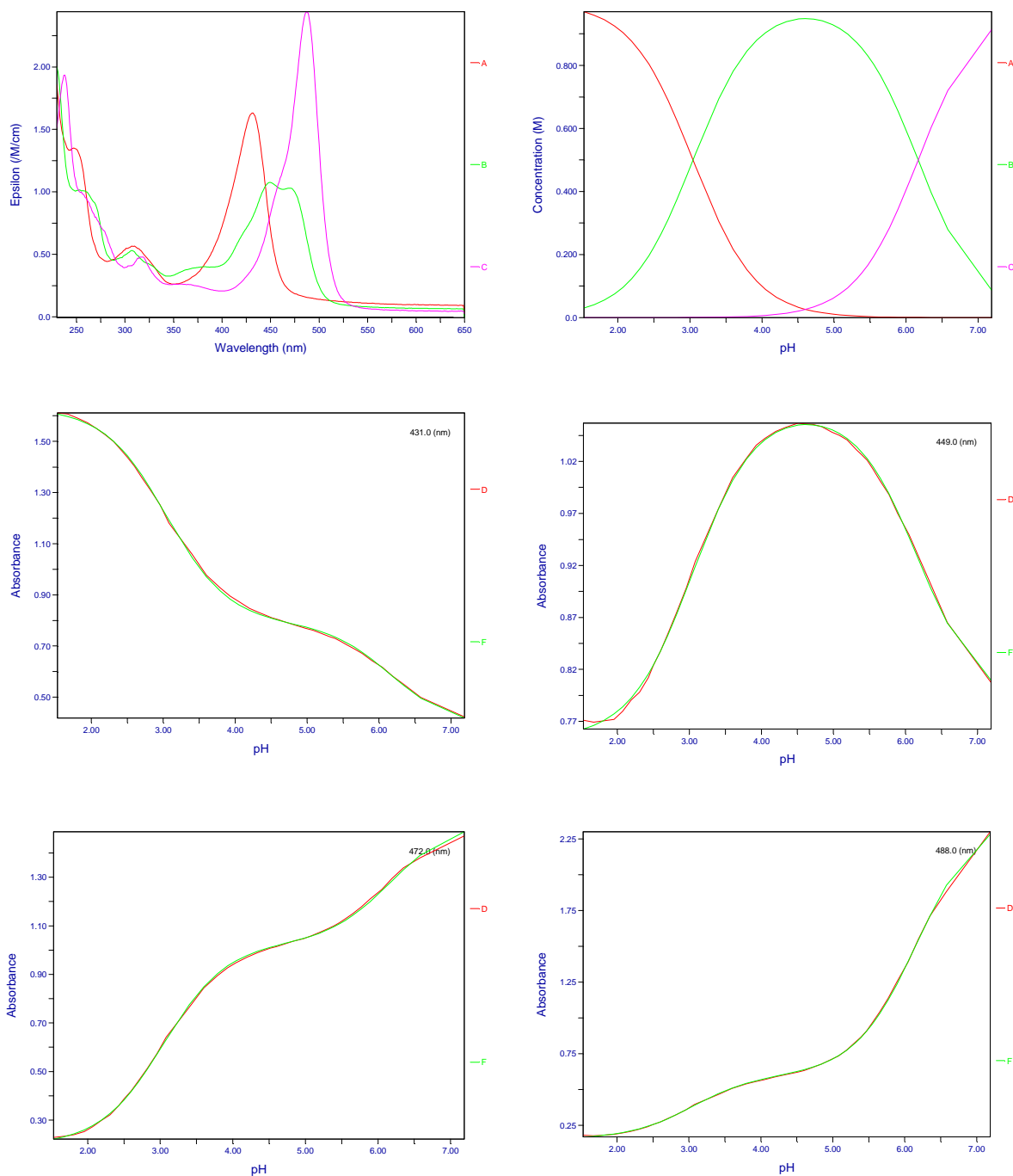
The primary photoproduct **8** is in equilibrium with its two colorless tautomers, 9-(hydroxymethylene)-9*H*-xanthene-3,6-diol and 3,6-dihydroxy-9*H*-xanthene-9-carbaldehyde (see Table 5 in the next chapter). One or more of these tautomers react further to give the final photoproduct, which is, as well as **8**, highly fluorescent. Upon spectrophotometrical titration, it follows the same acid dissociation pattern as the compounds **1**, **3**, **4** and **5**⁸⁸.

The titration spectra obey the acid dissociation model with two p*K*_a's, p*K*_{a,1} being 3.04 ± 0.02 and p*K*_{a,2} equal to 6.17 ± 0.02 . At pH 7, where the monoanion prevails, one can observe

a distinct absorption band with $\lambda_{\text{max}} = 488$ nm. The neutral form has its absorption maxima at 450 and 472 nm and the cation at 433 nm.

Fig. 17 2D and 3D courses of spectrophotometric titration of the final photoproduct, electronic spectra of the prototropic forms, species distribution in the pH interval 1.5 – 7 and model fit for several significant wavelengths





In theory, a dianion could also be formed in strongly basic solutions; nonetheless, it was not detected even at pH as high as 13.5. The value of $pK_{a,3}$ is thus irrelevant for potential biochemical applications and it cannot be determined in aqueous solutions.

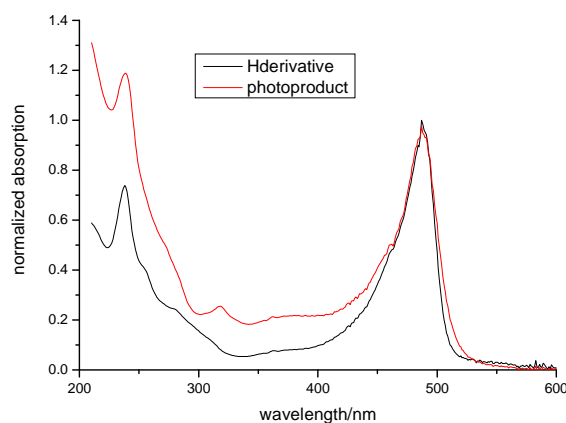
Also the final photoproduct is blue-shifted with respect to its precursors **3**, **4** and **5**. This is very convenient since the interference with the absorption of the starting material can be avoided if the chosen irradiation wavelength is 525 nm or higher (the absorption maxima of **3**, **4** and **5** are between 519 and 530 nm).

Isolation and Identification of the Photoproduct

The compounds **3**, **4** and **5** were irradiated in non-buffered solutions by a conventional medium–pressure mercury lamp with a 430 nm filter. The drop in pH due to the formation of the free acids was compensated for by adding dropwise a diluted solution of NaOH so that the pH values were kept between 6 and 8. After complete conversion (monitoring by means of UV-Vis spectroscopy), the solvent was evaporated, the final photoproduct was washed several times with chloroform and dried. The photoproduct was analyzed by the following techniques: UV – Vis (titration, see Fig. 17), NMR, IR, and MS.

The UV-Vis spectrum of the photoproduct is very much alike that of 6-hydroxy-3*H*-xanthen-3-one (a compound with a hydrogen atom in the 9-position), see Fig. 18, but the direct comparison by NMR spectroscopy proved the photoproduct is not identical to 6-hydroxy-3*H*-xanthen-3-one.

Fig. 18 UV-Vis spectra of 6-hydroxy-3*H*-xanthen-3-one (“Hderivative”) and of the photoproduct at pH 7



Nuclear Magnetic Resonance

^1H , ^{13}C , NOESY (H–H interactions over space), COSY (H–H interactions over 3 to 4 bonds), HMQC (direct C–H interactions over one bond) and HMBC (C–H interactions over 2 or more bonds) spectra of the photoproduct formed from **5** were recorded. The spectra are shown in figures 19 to 21.

¹H NMR (600 MHz, δ , DMSO-d₆, 25°C): 7.72 (d, H8), 7.31 (d, H1), 6.48 (d, H7), 6.34 (s, H5), 6.23 (d, H2), 5.99 (s, H4) ppm;

¹³C NMR (600 MHz, δ , DMSO-d₆, 25°C): 180.9 (C3), 174.0 (C6), 168.8 (C10a), 159.1 (C9), 154.7 (C4a), 131.6 (C1), 127.7 (C8), 123.4 (C2), 116.1 (C7), 112.2 (C8a), 105.6 (C9a), 103.6 (C4), 102.8 (C5);

NOESY interactions: H1↔H2, H7↔H8;

COSY interactions: H1↔H2, H2↔H4, H5↔H7, H7↔H8;

HMOC interactions: H1↔C1, H2↔C2, H3↔C3, H4↔C4, H5↔C5, H6↔C6;

HMBC interactions:

H1 ↔ C3, C4, C4a, C9, C9a

H2 ↔ C1, C4, C9, C9a

H4 ↔ C2, C3, C9, C9a

H5 ↔ C6, C7, C8a, C9, C10a

H7 ↔ C5, C8, C8a, C9

H8 ↔ C5, C6, C9, C10a

The NMR experiments together with UV-Vis spectroscopy have confirmed that the original chromophore is still preserved in the photoproduct. The question that remains unanswered is the X substituent on the carbon C9 of the final product. Considering the conditions of the experiment, the only conceivable substituents are the following: -H, -OH, -CH₂OH (primary photoproduct, compound **8**), -CHO, and -COO(H).

Neither CH₂ protons, nor a CH₂ carbon (APT NMR experiment) were found in the NMR spectra of the final product, which rules out the -CH₂OH substituent. An aldehydic proton of a -CHO group was not observed either. 6-Hydroxy-3*H*-xanthen-3-one (i.e. the compound with hydrogen atom in the 9-position) was added to a previously measured sample of the photoproduct but the direct comparison clearly showed two different substances, which excluded also this option. The only two possible substituents left at this point were -OH and -COO(H).

Fig. 19 ^1H NMR spectrum of the photoproduct in DMSO. The peak at 1.70 ppm was attributed to the CH_3 group of the free acetate, the one at 2.54 to DMSO and the one at 3.60 to residual water.

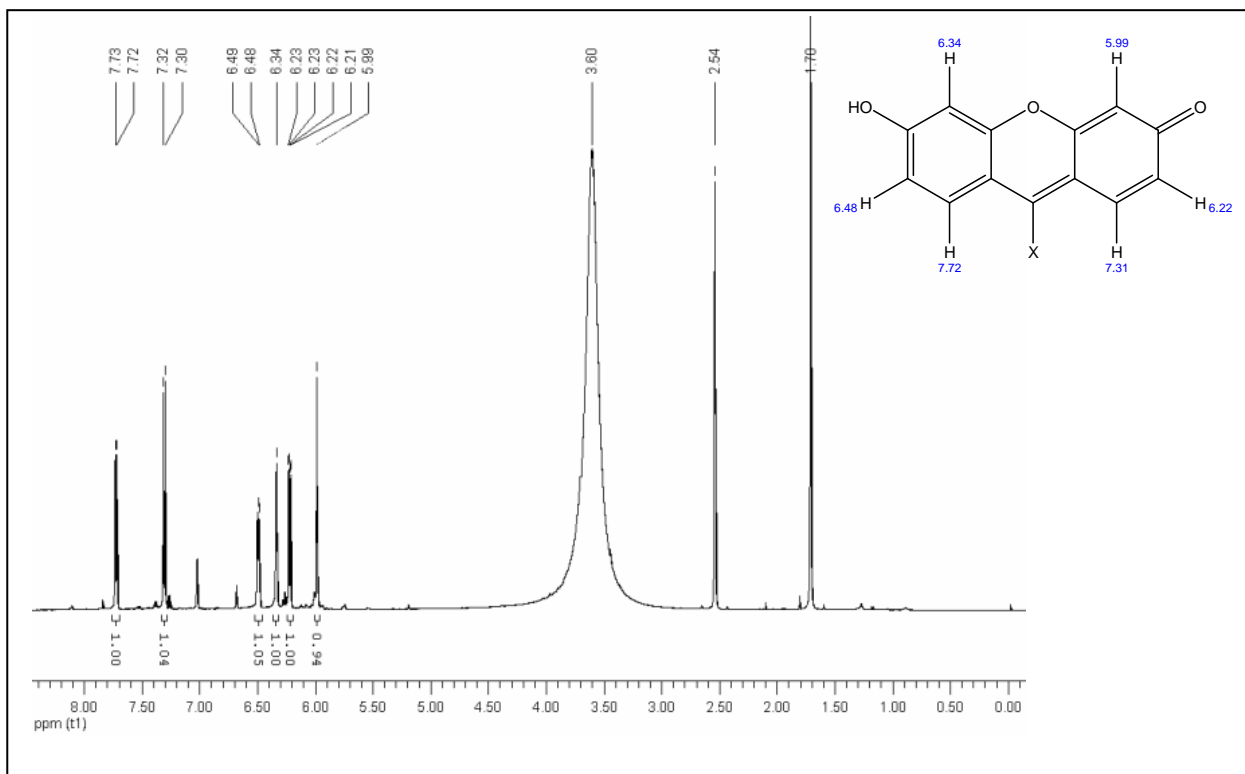


Fig. 20 Detail of the ^1H NMR spectrum of the photoproduct in DMSO

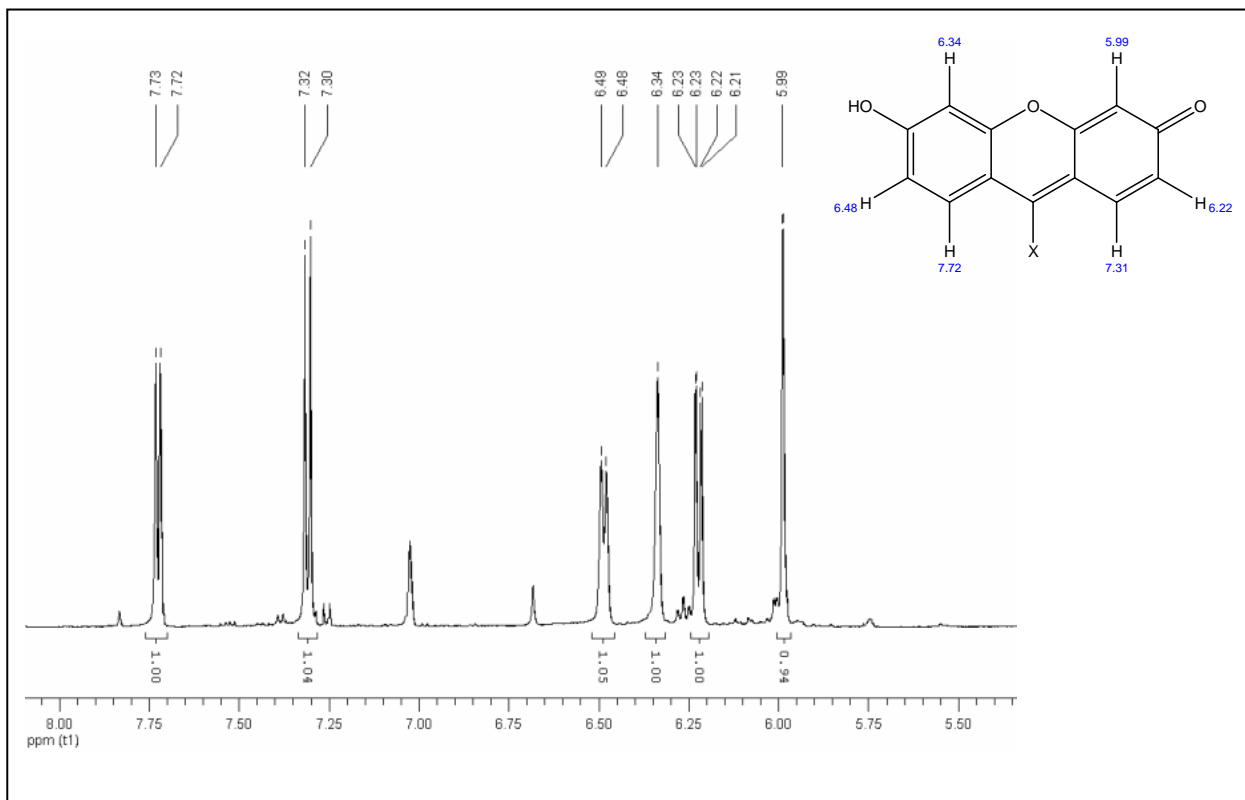
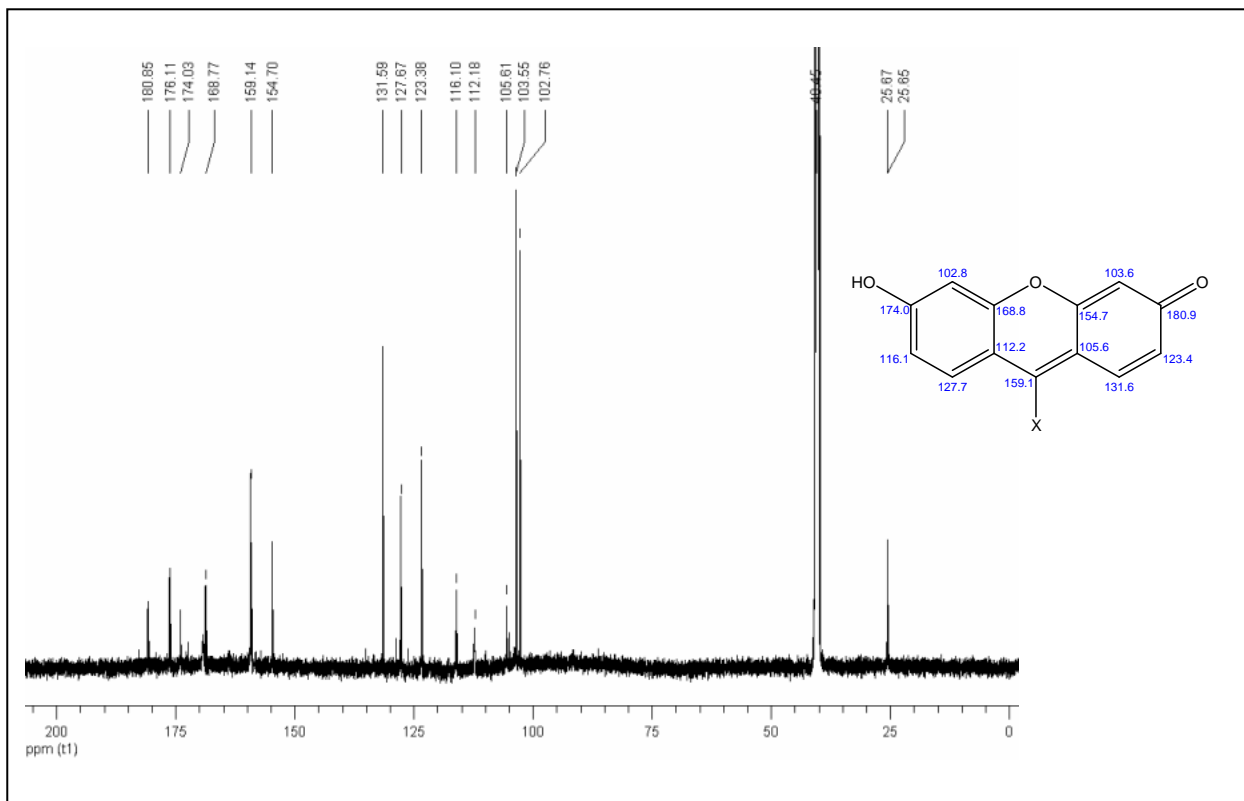


Fig. 21 ^{13}C NMR spectrum of the photoproduct in DMSO. The peaks at 25.7 and 176.1 belong to the free acetate, the heptet at 40.45 to DMSO



Finally, the compound with an -OH substituent in the 9-position (6,9-dihydroxy-3H-xanthen-3-one) would be transformed to its much more stable keto-tautomer (3,6-dihydroxy-9H-xanthen-9-one, see Table 6), which has a different UV-Vis spectrum (it is colorless) and also a different NMR spectrum⁸⁸.

The only candidate left is the corresponding carboxylic acid originating by an oxidation of the primary photoproduct **8** or one of its tautomers. Even though no C \leftrightarrow H interactions with the carboxylic carbon were found in the HMBC spectrum, it does not necessarily mean that there is no carboxylic carbon since these interactions over 4 bonds may sometimes be difficult to observe with low sample concentrations.

Mass Spectroscopy

So far, all of the attempts to determine the mass of the photoproduct failed or gave no convincing results. The problem appears to be the very low tendency of the photoproduct to

go to the gas phase (melting points of the derivatives of 6-hydroxy-3*H*-xanthen-3-one are usually higher than 250 °C and they tend to decompose at these temperatures⁸⁸).

The EI (electron ionisation) experiment at 300 °C (maximum temperature) gave a few peaks of very low intensity (by about 3 orders of magnitude lower than the usual signal intensities). Small peaks appeared at 212 M/z (~ 6-hydroxy-3*H*-xanthen-3-one), 213 M/z, 226 M/z (~ 6-hydroxy-9-methyl-3*H*-xanthen-3-one), and 228 M/z (~ 6, 9-dihydroxy-3*H*-xanthen-3-one). Since the mass spectroscopy gives only little or no information about the relative abundance of the individual components in the sample, and since the obtained signals were very weak, the major photoproduct could not be distinguished from the side-products or impurities or, perhaps, it was not even detected.

The MALDI-TOF (Matrix-Assisted Laser Desorption/Ionization – Time Of Flight) experiment using 2,5-dihydroxybenzoic acid (pK_a 2.97) as matrix gave rise to four peaks in the positive mode: 213 M/z (~ protonated 6-hydroxy-3*H*-xanthen-3-one), 214 M/z, 227 M/z (~ protonated 6-hydroxy-9-methyl-3*H*-xanthen-3-one), and 242 M/z (~ 9-(hydroxymethyl)-6-hydroxy-3*H*-xanthen-3-one (**8**)). For similar reasons as in the case of EI, the MALDI-TOF experiment also did not give us an unequivocal answer to our problem.

3.6. Stability Tests

Solutions of **3**, **4** and **5** in phosphate buffer (pH 7, $I = 0.1$ M) were subjected to stability tests in the dark. Fig. 22 to Fig. 24 show the courses of spontaneous conversions (i.e. conversions in the absence of light) of **3**, **4** and **5** (**A**) to their primary products (**B**), the resolved spectra of **A**'s and **B**'s and the fit of the calculated kinetics. In all three cases, the kinetics (**A** → **B**) obeyed the 1st-order law. The rate constants and the lifetimes of the species **3** to **5** under given conditions are also given in the figures.

The spectra of **B**'s, however, were not those of the final product. After a couple of more days, the absorption spectra of the samples were very much alike those shown in Fig. 16. (see Fig. 25).

Fig. 22 Absorption spectra and the course of a monoexponential non-photochemical conversion of **3** to its product

$$k = (4.81 \pm 0.33) \times 10^{-5} \text{ s}^{-1}; \tau = 5.78 \text{ hours}$$

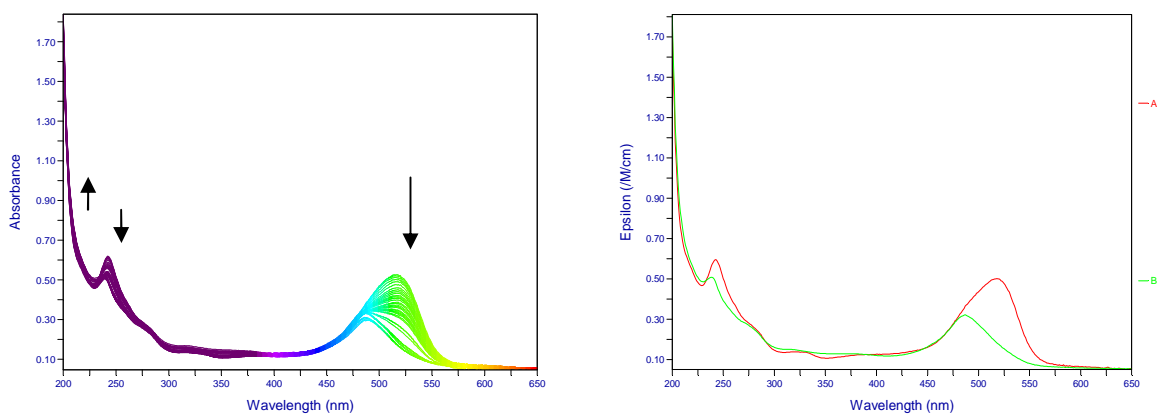


Fig. 23 Absorption spectra and the course of a monoexponential non-photochemical conversion of **4** to its product

$$k = (1.36 \pm 0.07) \times 10^{-5} \text{ s}^{-1}; \tau = 20.5 \text{ hours}$$

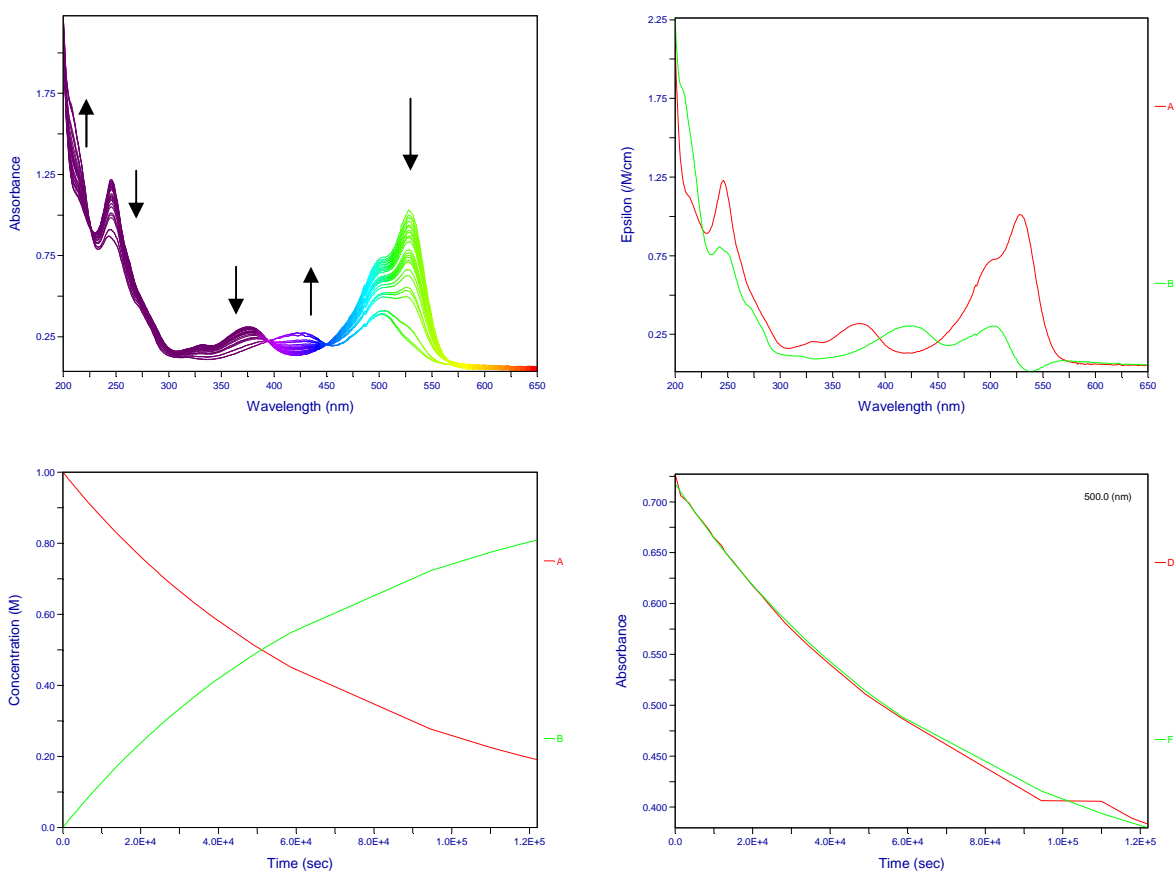


Fig. 24 Absorption spectra and the course of a monoexponential non-photochemical conversion of **5** to its product

$$k = (1.15 \pm 0.06) \times 10^{-5} \text{ s}^{-1}; \tau = 24.2 \text{ hours}$$

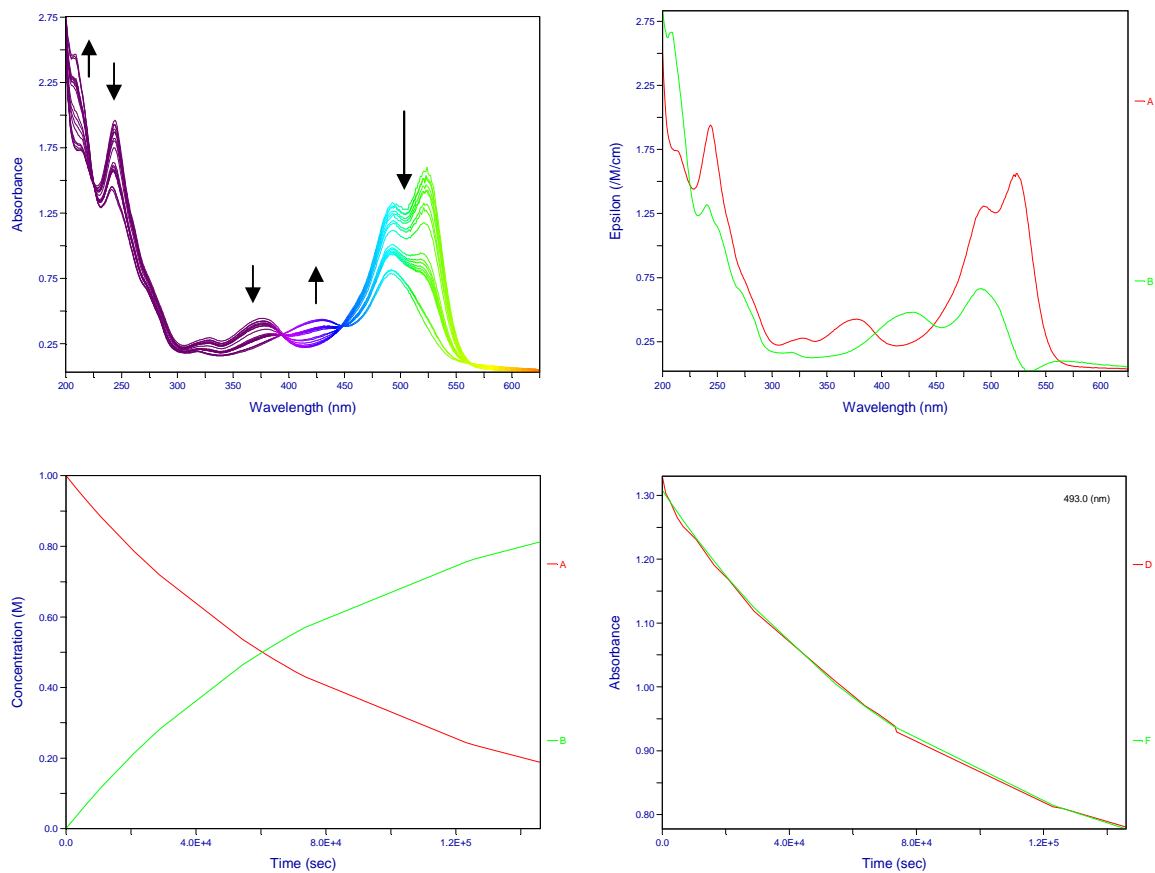
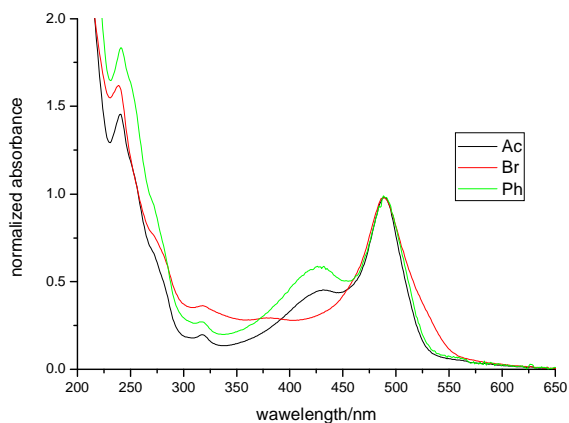


Fig. 25 Normalized absorption spectra of the products of thermal decomposition of **3**, **4** and **5** after 1 week (*conversion not complete yet*)



3.7. Calculations

DFT calculations were performed using the Gaussian03 software package. The chosen method was a restricted B3LYP with the basis set 6-31+g(d). Before the solvent field was added, the molecules were optimized in the gas phase. Energies of several compounds of interest (i.e. model compounds and possible photoproducts and/or reaction intermediates) and their tautomers were calculated. The results are summarized in Tables 5 to 7.

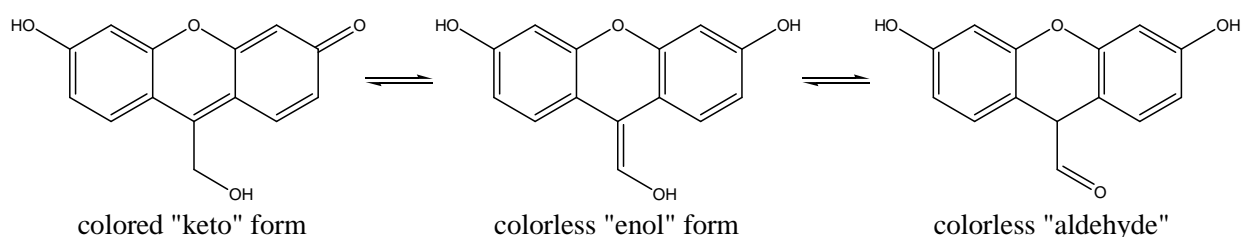


Table 5 Calculated energies of the primary photoproduct **8** and its tautomers. The energy values are given both for the neutral and the anionic forms (which prevail at pH 7). The last column shows the energy differences among the three tautomers under given conditions (gas phase/water; neutral species/anion). The colors correspond to the tautomers, which are to be compared.

| Compound | Phase | Charge | Form | Energy / (kJ.mol ⁻¹) | Energy difference / (kJ.mol ⁻¹) |
|---|-------|--------|----------|----------------------------------|---|
| 3,6-dihydroxy-9H-xanthen-9-carbaldehyde | gas | 0 | aldehyde | -2206509.6 | 0 |
| | water | 0 | aldehyde | -2206612.9 | 0 |
| | gas | -1 | aldehyde | -2205087.4 | 43.0 |
| | water | -1 | aldehyde | -2205364.8 | 22.1 |
| 6-hydroxy-9-(hydroxymethyl)-3H-xanthen-3-one (8) | gas | 0 | keto | -2206477.3 | 32.3 |
| | gas | 0 | enol | -2206490.4 | 19.2 |
| | water | 0 | keto | -2206594.9 | 18.0 |
| | water | 0 | enol | -2206602.7 | 10.2 |
| | gas | -1 | keto | -2205130.4 | 0 |
| | gas | -1 | enol | -2205055.3 | 75.1 |
| | water | -1 | keto | -2205386.9 | 0 |
| | water | -1 | enol | -2205353.8 | 33.1 |

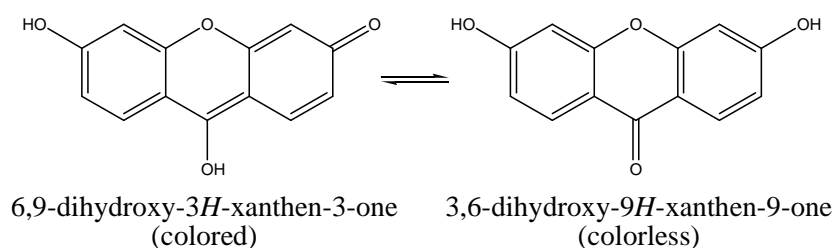


Table 6 Comparison of calculated energies of 6,9-dihydroxy-3*H*-xanthen-3-one and 3,6-dihydroxy-9*H*-xanthen-9-one

| Compound | Phase | Charge | Form | Energy / (kJ.mol ⁻¹) | Energy difference / (kJ.mol ⁻¹) |
|---|-------|--------|------|----------------------------------|---|
| 6,9-dihydroxy-3 <i>H</i> -xanthen-3-one | gas | 0 | - | -2103301.7 | 79.3 |
| | water | 0 | - | -2103421.0 | 58.4 |
| | gas | -1 | - | -2101958.6 | 34.0 |
| | water | -1 | - | -2102209.2 | 46.8 |
| 3,6-dihydroxy-9 <i>H</i> -xanthen-9-one | gas | 0 | - | -2103381.0 | 0 |
| | water | 0 | - | -2103479.4 | 0 |
| | gas | -1 | - | -2101992.6 | 0 |
| | water | -1 | - | -2102256.0 | 0 |

Table 7 Comparison of the calculated energies of the keto end enol forms of the compounds 1, 3 and 5.

| Compound | Phase | Charge | Form | Energy / (kJ.mol ⁻¹) | Energy difference / (kJ.mol ⁻¹) |
|--|-------|--------|------|----------------------------------|---|
| 6-hydroxy-9-methyl-3 <i>H</i> -xanthen-3-one | gas | 0 | keto | -2009024.1 | 0 |
| | gas | 0 | enol | -2009009.7 | 14.4 |
| | water | 0 | keto | -2009116.1 | 0 |
| | water | 0 | enol | -2009091.6 | 24.5 |
| | gas | -1 | keto | -2007676.5 | 0 |
| | gas | -1 | enol | -2007591.0 | 85.5 |
| | water | -1 | keto | -2007905.4 | 0 |
| | water | -1 | enol | -2007850.6 | 54.8 |
| 9-(bromomethyl)-6-hydroxy-3 <i>H</i> -xanthen-3-one | gas | 0 | keto | -8759507.6 | 0 |
| | gas | 0 | enol | -8759492.1 | 15.6 |
| | water | 0 | keto | -8759602.2 | 0 |
| | water | 0 | enol | -8759576.9 | 25.3 |
| | gas | -1 | keto | -8758175.6 | 0 |
| | gas | -1 | enol | -8758085.1 | 90.5 |
| | water | -1 | keto | -8758397.1 | 0 |
| | water | -1 | enol | -8758339.4 | 57.7 |
| (6-hydroxy-3-oxo-3 <i>H</i> -xanthen-9-yl)methyl acetate | gas | 0 | keto | -2607288.7 | 13.7 |
| | gas | 0 | enol | -2607302.4 | 0 |
| | water | 0 | keto | -2607409.0 | 0 |
| | water | 0 | enol | -2607404.9 | 4.1 |
| | gas | -1 | keto | -2605957.6 | 0 |
| | gas | -1 | enol | -2605897.8 | 59.8 |
| | water | -1 | keto | -2606204.3 | 0 |
| | water | -1 | enol | -2606164.9 | 39.4 |

Table 5 compares the energies for the three tautomers of the primary photoproduct **8**. According to the calculations, the colored anionic keto form would be the prevalent form in aqueous solutions at pH 7. Out of the neutral forms, the “aldehyde” seems to be the most stable. The experiment shows a substantial decrease (to about 40 % of the original intensity) of the absorption band in the visible region (505 nm) at pH 7. As the final photoproduct is formed, this band eventually shifts towards shorter wavelengths (488 nm) and gains in intensity again.

Table 6 indicates the colorless 3,6-dihydroxy-9*H*-xanthen-9-one is much more stable under all conditions than 6,9-dihydroxy-3*H*-xanthen-3-one. This is in agreement with our observation. When dissolved in water or aqueous buffers, 3,6-dihydroxy-9*H*-xanthen-9-one stays colorless and does not tautomerize to 6,9-dihydroxy-3*H*-xanthen-3-one.

Table 7 shows that although the “aromaticity” of the system is disturbed in the keto forms, these forms are still lower in energy than the enol forms in aqueous media. The equilibria are therefore shifted towards the keto species. This is also in accord with our observations and it is very convenient since the keto form is the one that absorbs in the visible region (the enol form absorbs only in the UV). The opposite is true in DMSO – there the colorless forms prevail.

4. Summary

A new water-soluble photoremovable protecting group for carboxylic acids and phosphates with high molar extinction coefficients ($\epsilon_{\lambda_{\max}} \sim 25\,000 \text{ dm}^3\text{mol}^{-1}\text{cm}^{-1}$) in the visible region (above 520 nm) was designed and tested. The suggested concept based on the photochemistry of coumarinyl PPG proved to work also for the compounds derived from 6-hydroxy-3-oxo-3*H*-xanthen-9-yl)methyl. The introduction of an additional aromatic core to the coumarinyl unit resulted in a substantial shift of the absorption towards longer wavelengths and also caused a drop in $\text{p}K_{\text{a}}$ of the phenolic protons to about 6, which then caused the anionic form of the molecule to be the prevalent species at neutral pH. This is of advantage since it improves the solubility of these compounds in aqueous media and also because the anionic forms of the cages are even further red-shifted with respect to the neutral ones.

The model cages released the protected bromide, acetate and/or diethylphosphate upon irradiation by visible light in neutral aqueous solutions (the cleavage of the free anions was indicated by a drop in pH and confirmed by NMR).

The quantum yields of photodeprotection of the model compounds were relatively low but still comparable to those of coumarinyl cages. The quantum yields could probably be enhanced by a suitable substitution. The efficiency of the photoreaction is also likely to be higher in the case of cages of other phosphates and/or acyls of biochemical interest, which are better leaving groups than diethyl phosphate or acetate.

In the dark, the model compounds were stable for several hours (up to 1 day) in aqueous solutions at room temperature. The stability should thus be sufficient for potential biochemical applications.

The fluorescence lifetime of one of the model compounds, 9-(bromomethyl)-6-hydroxy-3*H*-xanthen-3-one was found to be $(331 \pm 30) \text{ ps}$.

The last problem that remains to be solved is an unequivocal identification of the final photoproduct and of the reaction intermediates. The first step of the photoreaction is most probably analogous to that of coumarinyl cages, i.e. the elimination of the protected species

(free acids) and the nucleophilic attack of the resulting cation by water, which leads to the formation of the primary photoproduct, 6-hydroxy-9-(hydroxymethyl)-3*H*-xanthen-3-one. This compound is in equilibrium with its enol tautomer and also with another tautomer: 3,6-dihydroxy-9*H*-xanthene-9-carbaldehyde. One or more of these tautomers react further to give a final product, in which the original chromophore is restored again (testified by UV-Vis spectroscopy and NMR). The UV-Vis spectrum of the final photoproduct overlaps with the spectrum of 6-hydroxy-3*H*-xanthen-3-one but the NMR analysis revealed that the two compounds were not identical. Further analyses and attempts to identify the photoproduct and the reaction intermediates are still in progress.

5. Experimental

5.1. Instruments

UV/Vis Spectrophotometry:

- *Agilent 8453* UV-Vis spectrophotometer (routine measurements, quantum yield determination),
- *Perkin-Elmer Lambda 9* UV-Vis spectrophotometer (spectrophotometric titration).

IR:

- *Perkin Elmer 1600 Series* FTIR.

NMR:

- *Bruker AVANCE400* – 400 MHz (routine 1D measurements),
- *Bruker DRX600* – 600 MHz (thorough analysis of the photoproduct, 2D spectra; measurements at this instrument were performed by Dr. Daniel Häussinger at the Institute of Organic Chemistry, University of Basel).

MS:

- *Mat95* (measurements at this instrument were performed by Dr. Heinz Nadig at the Institute of Organic Chemistry, University of Basel).

MALDI-TOF:

- *MALDI Mass Spectrometer Voyager-DE-PRO*: matrix – 2,5-dihydroxybenzoic acid

Ultrasonics:

- *Telsonic Ultrasonics TPC-15*.

pH Measurements:

- *Metrohm 654* pH-meter with *Metrohm LL micro* pH glass electrode (*Biotrode*).

Evaporation, Drying and Degassing:

- rotavapor *Büchi R 200* with *Büchi B-490* water bath connected to *Vacuumbrand* diaphragm vacuum pump *Type MZ 2*,
- oil pumps *Balzors DUO 004 B*,
- high vacuum pump *Balzors PDI 063*.

Laser Flash Photolysis:

- excitation by *Lambda-Physik Compex 205* excimer laser operating at 248 nm (KrF), 308 nm (XeCl), and 351 nm (XeF); pulse energy ~ 100 mJ, pulse duration ~ 50 ns,
- probing light: pulsable Xe-arc lamp oriented perpendicularly to the excitation light,
- transient spectra captured by an ICCD camera *iStar 720*, *Andor Tech.*, optical resolution 2 nm, time of accumulation 20 – 50 ns,
- kinetics measurements: *Hamamatsu IP28* photomultiplier, *Tektronix TDS 540* 500 MHz oscilloscope, *Brandenburg* photomultiplier power supply,
- quartz cuvettes (1×1 cm wide, 4.5 cm long), light shutters, cut-off filters.

Fluorimetry:

- *Spex Fluorolog 111C* instrument with 150 W Xe-lamp light source, quartz cells.

Time-Resolved Fluorimetry and Quantum Yield Determination:

- light source - *Clark-MXR* Ti:Sa laser *CPA 2001* coupled to a noncollinear optical parametric amplifier (NOPA), wavelengths set to 490 nm, 515 nm (time-resolved fluorescence), or 538 nm (quantum yield measurements); bandwidth at half height ca 15 nm,
- time-resolved fluorescence spectra recorded by *Hamamatsu C5680* streak camera preceded by a *Chromex 250IS* polychromator, and synchronized with the light source by a delay unit *C1097*.

Irradiation and Isolation of the Photoproduct:

- *Hanau* medium pressure lamp,
- cut-off filter (530 nm), quartz beaker (500 ml), magnetic stirrer, rotavapor.

5.2. Chemicals

| Chemical | Formula | $M / \text{g} \cdot \text{mol}^{-1}$ | Quality | Producer |
|--------------------------------------|---|--------------------------------------|-----------------------|-------------------------|
| acetone | $\text{C}_3\text{H}_6\text{O}$ | 58.08 | c. p. | Schweizerhall Chemie AG |
| acetonitrile | $\text{C}_2\text{H}_3\text{N}$ | 41.05 | HPLC grade | Scharlau |
| argon | Ar | 39.95 | 4.6 | Linde |
| dimethylformamide-d ₇ | $\text{HCON}(\text{CH}_3)_2$ | 73.09 | 99.5 % | Cambridge Iso. Lab. |
| dimethyl sulfoxide-d ₆ | $\text{SO}(\text{CD}_3)_2$ | 78.13 | 99.98 % | Cambridge Iso. Lab. |
| hydrochloric acid | HCl | 36.46 | 36-38% | Merck |
| sodium acetate anhydrous | CH_3COONa | 82.03 | u. | Fluka |
| sodium chloride | NaCl | 58.44 | p. a. | Merck |
| sodium dihydrogenphosphate dihydrate | $\text{NaH}_2\text{PO}_4 \cdot 2\text{H}_2\text{O}$ | 137.99 | p.a., $\geq 99.0\%$ | Fluka |
| sodium hydrogenphosphate dihydrate | $\text{HN}_2\text{PO}_4 \cdot 2\text{H}_2\text{O}$ | 177.96 | p.a., $\geq 99.0\%$ | Fluka |
| sodium hydroxide | NaOH | 40 | p. a. | Fluka |
| water | H_2O | 18.02 | bidistilled $>99.9\%$ | UniBasel |
| water-d ₂ | D_2O | 20.04 | d. 99.9 % | Cambridge Iso. Lab. |

Abbreviations:

| | | | |
|-------|-----------------|----|-------|
| c. p. | chemically pure | d. | dried |
| p. a. | pro analysis | u. | ultra |

5.3. Data Analysis

The measured spectra were normalized (fluorescence) or corrected for dilution (UV/Vis spectrophotometric titration) using *Origin* or *MS Excel* and exported to *SPECFIT32*, a multivariate data analysis program for modeling and fitting chemical kinetics and a variety of equilibrium titration 3D data sets that are obtained from multi-wavelength spectrophotometric measurements.

6. Index of Symbols and Abbreviations

| | |
|---------------|--|
| δ | chemical shift |
| δ_u | two-photon action cross section |
| ε | molar absorption coefficient |
| λ | wavelength |
| ν | frequency |
| τ | lifetime |
| Φ | quantum yield |
| 2D | two-dimensional |
| 2PE | two-photon excitation |
| 3D | three-dimensional |
| A | absorption |
| AMP | adenosine monophosphate |
| ATP | adenosine triphosphate |
| B3LYP | Becke, three-parameter, Lee-Yang-Parr exchange-correlation functional |
| BAPTA | (1,2-bis(2-aminophenoxy)ethane- <i>N,N,N',N'</i> -tetraacetic acid |
| BCMB | 3',5'-bis(carboxymethoxy)benzoin-group |
| Bz | benzoin group |
| cAMP | cyclic adenosine monophosphate |
| CD | circular dichroism |
| cGMP | cyclic guanosin monophosphate |
| COSY | correlation (NMR) spectroscopy |
| d | doublet (multiplicity in NMR spectroscopy) |
| DEPT | distortionless enhancement by polarization transfer |
| DFT | density functional theory |
| DMBz | dimethoxybenzoin group |
| DMF | dimethyl formamide |
| DMP | dimethylphenacyl group |
| DMSO | dimethyl sulfoxide |
| DNA | deoxyribonucleic acid |
| E | enol form or “entgegen” isomer (the substituents on a double bond having the highest priorities point in different directions) |

| | |
|-------------------|---|
| e.g. | exempli gratia (= for example) |
| EDTA | ethylenediamine tetraacetic acid |
| EI | electron impact/ionisation |
| <i>et al.</i> | et alia (= and others) |
| EtOH | ethanol |
| Fig(s). | figure(s) |
| FRAP | fluorescence recovery after photobleaching |
| GABA | γ -aminobutyric acid |
| GM | 1 Göppert-Mayer = 10^{-50} cm ³ s photon ⁻¹ |
| GMP | guanosine monophosphate |
| GTP | guanosine triphosphate |
| HCM | hydroxycoumarin group |
| HMBC | heteronuclear multiple bond correlation |
| HMQC | heteronuclear multiple quantum coherence |
| <i>hν</i> | quantum of energy/photon (Planck constant × frequency) |
| <i>I</i> | light intensity or ionic strength |
| IC | internal conversion |
| ICCD | intensified charge-coupled device |
| IgG | immunoglobulin G |
| InsP ₃ | inositol trisphosphate |
| IR | infrared spectroscopy or infrared radiation |
| ISC | intersystem crossing |
| <i>k</i> | rate constant |
| K | keto form |
| LFP | laser flash photolysis |
| LG | leaving group |
| M/z | mass per charge |
| MALDI-TOF | matrix-assisted laser desorption/ionization – time of flight |
| MCM | methoxycoumarin group |
| MeOH | methanol |
| MS | mass spectroscopy |
| NMR | nuclear magnetic resonance |
| NOESY | nuclear Overhauser enhancement spectroscopy |
| NOPA | noncollinear optical parametric amplifier |

| | |
|--------------|---|
| <i>o</i> -NB | 2-nitrobenzyl group |
| PAF | photoactivation of fluorescence |
| PG | protecting group |
| PPG | photoremovable protecting group |
| pH | pH-value |
| <i>p</i> -HP | parahydroxyphenacyl group |
| pK_a | pK_a -value |
| <i>p</i> -MP | paramethoxyphenacyl group |
| R^2 | square of the Pearson product moment correlation coefficient |
| s | second or singlet (multiplicity in NMR spectroscopy) |
| <i>T</i> | temperature |
| UV/Vis | ultraviolet/visible |
| Z | “zusammen” isomer (the substituents on a double bond having the highest priorities point in the same direction) |

7. References

1. Fischer, E., *Ber. Dtsch. Chem. Ges.* **1895**, 28, (1145), 1145-1165.
2. Greene, T. W.; Wuts, P. G. M., *Greene's Protective Groups in Organic Synthesis*, 4th Edition; ISBN: 978-0-471-69754-1. **2006**.
3. Grossweiner, L. I., *The Science of Phototherapy: An Introduction*, ISBN 978-1-4020-2885-4. **2005**.
4. Barltrop, J. A.; Schofield, P., Photosensitive protecting groups. *Tetrahedron Letters* **1962**, 697-9.
5. Kaplan, J. H.; Forbush, B., 3rd; Hoffman, J. F., Rapid photolytic release of adenosine 5'-triphosphate from a protected analogue: utilization by the Na:K pump of human red blood cell ghosts. *Biochemistry FIELD Full Journal Title:Biochemistry* **1978**, 17, (10), 1929-35.
6. Barltrop, J. A.; Plant, P. J.; Schofield, P., Photosensitive protective groups. *Chemical Communications (London)* **1966**, (22), 822-3.
7. Pillai, V. N. R., Photoremovable protecting groups in organic synthesis. *Synthesis* **1980**, (1), 1-26.
8. Chee, M.; Yang, R.; Hubbell, E.; Berno, A.; Huang, X. C.; Stern, D.; Winkler, J.; Lockhart, D. J.; Morris, M. S.; Fodor, S. P. A., Accessing genetic information with high-density DNA arrays. *Science* **1996**, 274, (5287), 610-614.
9. Pelliccioli Anna, P.; Wirz, J., Photoremovable protecting groups: reaction mechanisms and applications. *Photochemical & photobiological sciences : Official journal of the European Photochemistry Association and the European Society for Photobiology* **2002**, 1, (7), 441-58.
10. Adams, S. R.; Kao, J. P. Y.; Tsien, R. Y., Biologically useful chelators that take up calcium(2+) upon illumination. *Journal of the American Chemical Society* **1989**, 111, (20), 7957-68.
11. Amit, B.; Patchornik, A., Photorearrangement of N-Substituted Orthonitroanilides and Nitroveratramides - Potential Photosensitive Protecting Group. *Tetrahedron Letters* **1973**, (24), 2205-2208.
12. Blanc, A.; Bochet, C. G., Bis(o-nitrophenyl)ethanediol: A Practical Photolabile Protecting Group for Ketones and Aldehydes. *Journal of Organic Chemistry* **2003**, 68, (3), 1138-1141.

13. Hasan, A.; Stengele, K. P.; Giegrich, H.; Cornwell, P.; Isham, K. R.; Sachleben, R. A.; Pfeleiderer, W.; Foote, R. S., Photolabile protecting groups for nucleosides: Synthesis and photodeprotection rates. *Tetrahedron* **1997**, 53, (12), 4247-4264.
14. Wettermark, G., Photochromism of O-Nitrotoluenes. *Nature* **1962**, 194, (4829), 677.
15. Il'ichev Yuri, V.; Schworer Markus, A.; Wirz, J., Photochemical reaction mechanisms of 2-nitrobenzyl compounds: methyl ethers and caged ATP. *J Am Chem Soc FIELD Full Journal Title:Journal of the American Chemical Society* **2004**, 126, (14), 4581-95.
16. Pirrung, M. C.; Lee, Y. R.; Park, K.; Springer, J. B., Pentadienylnitrobenzyl and Pentadienylnitropiperonyl Photochemically Removable Protecting Groups. *Journal of Organic Chemistry* **1999**, 64, (14), 5042-5047.
17. Givens, R. S.; Jung, A.; Park, C.-H.; Weber, J.; Bartlett, W., New Photoactivated Protecting Groups. 7. p-Hydroxyphenacyl: A Phototrigger for Excitatory Amino Acids and Peptides. *Journal of the American Chemical Society* **1997**, 119, (35), 8369-8370.
18. Conrad, P. G., II; Givens, R. S.; Hellrung, B.; Rajesh, C. S.; Ramseier, M.; Wirz, J., p-Hydroxyphenacyl Phototriggers: The Reactive Excited State of Phosphate Photorelease. *Journal of the American Chemical Society* **2000**, 122, (38), 9346-9347.
19. Sheehan, J. C.; Umezawa, K., Phenacyl photosensitive blocking groups. *Journal of Organic Chemistry* **1973**, 38, (21), 3771-4.
20. Givens, R. S.; Park, C.-H., Hydroxyphenacyl ATP: a new phototrigger. V. *Tetrahedron Letters* **1996**, 37, (35), 6259-6262.
21. Givens, R. S.; Weber, J. F. W.; Conrad, P. G., II; Orosz, G.; Donahue, S. L.; Thayer, S. A., New Phototriggers 9: p-Hydroxyphenacyl as a C-Terminal Photoremovable Protecting Group for Oligopeptides. *Journal of the American Chemical Society* **2000**, 122, (12), 2687-2697.
22. Kamdzhilov, Y.; Wirz, J., Unpublished work.
23. Ma, C. S.; Chan, W. S.; Kwok, W. M.; Zuo, P.; Phillips, D. L., Time-resolved resonance Raman study of the triplet state of the p-hydroxyphenacyl acetate model phototrigger compound. *Journal of Physical Chemistry B* **2004**, 108, (26), 9264-9276.
24. Ma, C. S.; Kwok, W. M.; Chan, W. S.; Zuo, P.; Kan, J. T. W.; Toy, P. H.; Phillips, D. L., Ultrafast time-resolved study of photophysical processes involved in the photodeprotection of p-hydroxyphenacyl caged phototrigger compounds. *Journal of the American Chemical Society* **2005**, 127, (5), 1463-1472.

25. Banerjee, A.; Falvey, D. E., Protecting groups that can be removed through photochemical electron transfer: Mechanistic and product studies on photosensitized release of carboxylates from phenacyl esters. *Journal of Organic Chemistry* **1997**, 62, (18), 6245-6251.
26. Banerjee, A.; Lee, K.; Yu, Q.; Fang, A. G.; Falvey, D. E., Protecting group release through photoinduced electron transfer: Wavelength control through sensitized irradiation. *Tetrahedron Letters* **1998**, 39, (26), 4635-4638.
27. Banerjee, A.; Lee, K.; Falvey, D. E., Photoreleasable protecting groups based on electron transfer chemistry. Donor sensitized release of phenacyl groups from alcohols, phosphates and diacids. *Tetrahedron* **1999**, 55, (44), 12699-12710.
28. Conrad, P. G., 2nd; Givens, R. S.; Weber, J. F.; Kandler, K., New phototriggers: extending the p-hydroxyphenacyl pi-pi absorption range. *Org Lett FIELD Full Journal Title:Organic letters* **2000**, 2, (11), 1545-7.
29. Klan, P.; Zabadal, M.; Heger, D., 2,5-Dimethylphenacyl as a New Photoreleasable Protecting Group for Carboxylic Acids. *Organic Letters* **2000**, 2, (11), 1569-1571.
30. Klan, P.; Paola Pelliccioli, A.; Pospisil, T.; Wirz, J., 2,5-Dimethylphenacyl esters: A photoremovable protecting group for phosphates and sulfonic acids. *Photochemical & Photobiological Sciences* **2002**, 1, (11), 920-923.
31. Bergmark, W. R.; Barnes, C.; Clark, J.; Papanian, S.; Marynowski, S., Photoenolization with Alpha-Chloro Substituents. *Journal of Organic Chemistry* **1985**, 50, (26), 5612-5615.
32. Bergmark, W. R., Photolysis of Alpha-Chloro-O-Methylacetophenones. *Journal of the Chemical Society-Chemical Communications* **1978**, (2), 61-62.
33. Sheehan, J. C.; Wilson, R. M.; Oxford, A. W., Photolysis of methoxy-substituted benzoin esters. Photosensitive protecting group for carboxylic acids. *Journal of the American Chemical Society* **1971**, 93, (26), 7222-8.
34. Rajesh, C. S.; Givens, R. S.; Wirz, J., Kinetics and Mechanism of Phosphate Photorelease from Benzoin Diethyl Phosphate: Evidence for Adiabatic Fission to an a-Keto Cation in the Triplet State. *Journal of the American Chemical Society* **2000**, 122, (4), 611-618.
35. Corrie, J. E. T.; Trentham, D. R., Synthetic, Mechanistic and Photochemical Studies of Phosphate-Esters of Substituted Benzoin. *Journal of the Chemical Society-Perkin Transactions 1* **1992**, (18), 2409-2417.

36. Pirrung, M. C.; Huang, C. Y., Photochemical Deprotection of 3',5'-Dimethoxybenzoin (Dmb) Carbamates Derived from Secondary-Amines. *Tetrahedron Letters* **1995**, 36, (33), 5883-5884.
37. Peach, J. M.; Pratt, A. J.; Snaith, J. S., Photolabile Benzoin and Furoin Esters of a Biologically-Active Peptide. *Tetrahedron* **1995**, 51, (36), 10013-10024.
38. Pirrung, M. C.; Bradley, J.-C., Dimethoxybenzoin Carbonates: Photochemically-Removable Alcohol Protecting Groups Suitable for Phosphoramidite-Based DNA Synthesis. *Journal of Organic Chemistry* **1995**, 60, (5), 1116-17.
39. Pirrung, M. C.; Shuey, S. W., Photoremovable Protecting Groups for Phosphorylation of Chiral Alcohols - Asymmetric-Synthesis of Phosphotriesters of (-)-3',5'-Dimethoxybenzoin. *Journal of Organic Chemistry* **1994**, 59, (14), 3890-3897.
40. Shi, Y.; Corrie, J. E. T.; Wan, P., Mechanism of 3',5'-Dimethoxybenzoin Ester Photochemistry: Heterolytic Cleavage Intramolecularly Assisted by the Dimethoxybenzene Ring Is the Primary Photochemical Step. *Journal of Organic Chemistry* **1997**, 62, (24), 8278-8279.
41. Givens, R. S.; Athey, P. S.; Kueper, L. W.; Matuszewski, B.; Xue, J. Y., Photochemistry of Alpha-Keto Phosphate-Esters - Photorelease of a Caged Camp. *Journal of the American Chemical Society* **1992**, 114, (22), 8708-8710.
42. Boudebous, H.; Kosmrlj, B.; Sket, B.; Wirz, J., Primary photoreactions of the 3',5'-dimethoxybenzoin cage and determination of the release rate in polar media. *Journal of Physical Chemistry A* **2007**, 111, (15), 2811-2813.
43. Givens, R. S.; Matuszewski, B., Photochemistry of phosphate esters: an efficient method for the generation of electrophiles. *Journal of the American Chemical Society* **1984**, 106, (22), 6860-1.
44. Matuszewska, B.; Borchardt, R. T., Guinea-Pig Brain Histamine N-Methyltransferase - Purification and Partial Characterization. *Journal of Neurochemistry* **1983**, 41, (1), 113-118.
45. Furuta, T.; Torigai, H.; Sugimoto, M.; Iwamura, M., Photochemical Properties of New Photolabile cAMP Derivatives in a Physiological Saline Solution. *Journal of Organic Chemistry* **1995**, 60, (13), 3953-6.
46. Schade, B.; Hagen, V.; Schmidt, R.; Herbrich, R.; Krause, E.; Eckardt, T.; Bendig, J., Deactivation Behavior and Excited-State Properties of (Coumarin-4-yl)methyl Derivatives. 1. Photocleavage of (7-Methoxycoumarin-4-yl)methyl-Caged Acids with Fluorescence Enhancement. *Journal of Organic Chemistry* **1999**, 64, (25), 9109-9117.

47. Schonleber, R. O.; Bendig, J.; Hagen, V.; Giese, B., Rapid photolytic release of cytidine 5'-diphosphate from a coumarin derivative: a new tool for the investigation of ribonucleotide reductases. *Bioorganic & Medicinal Chemistry* **2002**, 10, (1), 97-101.
48. Furuta, T.; Wang, S. S.; Dantzker, J. L.; Dore, T. M.; Bybee, W. J.; Callaway, E. M.; Denk, W.; Tsien, R. Y., Brominated 7-hydroxycoumarin-4-ylmethyls: photolabile protecting groups with biologically useful cross-sections for two photon photolysis. *Proc Natl Acad Sci U S A FIELD Full Journal Title:Proceedings of the National Academy of Sciences of the United States of America* **1999**, 96, (4), 1193-200.
49. Hagen, V.; Bendig, J.; Frings, S.; Eckardt, T.; Helm, S.; Reuter, D.; Kaupp, U. B., Highly efficient and ultrafast phototriggers for cAMP and cGMP by using long-wavelength UV/vis-activation. *Angewandte Chemie-International Edition* **2001**, 40, (6), 1046-+.
50. Papageorgiou, G.; Ogden, D. C.; Barth, A.; Corrie, J. E. T., Photorelease of carboxylic acids from 1-acyl-7-nitroindolines in aqueous solution: Rapid and efficient photorelease of L-glutamate. *Journal of the American Chemical Society* **1999**, 121, (27), 6503-6504.
51. Ellis-Davies, G.; Momotake, A. Synthesis of nitrodibenzofuran chromophore for photodeprotection of organic molecules. 2006-US13634 2006110804, 20060412., 2006.
52. Singh Anil, K.; Khade Prashant, K., Synthesis and photochemical properties of nitro-naphthyl chromophore and the corresponding immunoglobulin bioconjugate. *Bioconjug Chem FIELD Full Journal Title:Bioconjugate chemistry* **2002**, 13, (6), 1286-91.
53. Fedoryak, O. D.; Dore, T. M., Brominated Hydroxyquinoline as a Photolabile Protecting Group with Sensitivity to Multiphoton Excitation. *Organic Letters* **2002**, 4, (20), 3419-3422.
54. Lukeman, M.; Scaiano Juan, C., Carbanion-mediated photocages: rapid and efficient photorelease with aqueous compatibility. *J Am Chem Soc FIELD Full Journal Title:Journal of the American Chemical Society* **2005**, 127, (21), 7698-9.
55. Engels, J.; Schlaeger, E. J., Synthesis, Structure, and Reactivity of Adenosine Cyclic 3',5'-Phosphate Benzyl Triesters. *Journal of Medicinal Chemistry* **1977**, 20, (7), 907-911.
56. Walker, J. W.; McCray, J. A.; Hess, G. P., Photolabile Protecting Groups for an Acetylcholine-Receptor Ligand - Synthesis and Photochemistry of a New Class of

- Ortho-Nitrobenzyl Derivatives and Their Effects on Receptor Function. *Biochemistry* **1986**, 25, (7), 1799-1805.
57. Kramer, R. H.; Chambers, J. J.; Trauner, D., Photochemical tools for remote control of ion channels in excitable cells. *Nature Chemical Biology* **2005**, 1, (7), 360-365.
58. Goeldner, M.; Givens, R., Dynamic Studies in Biology. 2005. XXVII, 557 Pages, Hardcover Handbook/Reference Book **2005**, 1. Edition, 557 Pages.
59. <http://freednerd.wordpress.com/tag/the-brain/solitary-tract/>.
60. <http://kph12.myweb.uga.edu/cellcommunication.html>.
61. Somlyo, A. P.; Somlyo, A. V., Signal-Transduction and Regulation in Smooth-Muscle. *Nature* **1994**, 372, (6503), 231-236.
62. Kaplan, J. H.; Ellis-Davies, G. C., Photolabile chelators for the rapid photorelease of divalent cations. *Proc Natl Acad Sci U S A FIELD Full Journal Title:Proceedings of the National Academy of Sciences of the United States of America* **1988**, 85, (17), 6571-5.
63. Adams, S. R.; Kao, J. P. Y.; Gryniewicz, G.; Minta, A.; Tsien, R. Y., Biologically useful chelators that release Ca²⁺ upon illumination. *Journal of the American Chemical Society* **1988**, 110, (10), 3212-20.
64. Adams, S. R.; Lev-Ram, V.; Tsien, R. Y., A new caged Ca²⁺, azid-1, is far more photosensitive than nitrobenzyl-based chelators. *Chem Biol FIELD Full Journal Title:Chemistry & biology* **1997**, 4, (11), 867-78.
65. Brown, E. B.; Shear, J. B.; Adams, S. R.; Tsien, R. Y.; Webb, W. W., Photolysis of caged calcium in femtoliter volumes using two-photon excitation. *Biophysical Journal* **1999**, 76, (1), 489-499.
66. Adams, S. R.; Tsien, R. Y., Controlling cell chemistry with caged compounds. *Annual Review of Physiology* **1993**, 55, 755-84.
67. Terrett, N. K.; Bell, A. S.; Brown, D.; Ellis, P., Sildenafil (VIAGRA(TM)), a potent and selective inhibitor of type 5 cGMP phosphodiesterase with utility for the treatment of male erectile dysfunction. *Bioorganic & Medicinal Chemistry Letters* **1996**, 6, (15), 1819-1824.
68. Janeway, C. A. e. a., Immunobiology: the immune system in health and disease, 6th ed.; ISBN 0-8153-4101-6. *New York: Garland Science*. **2005**.
69. Makings, L. R.; Tsien, R. Y., Caged Nitric-Oxide - Stable Organic-Molecules from Which Nitric-Oxide Can Be Photoreleased. *Journal of Biological Chemistry* **1994**, 269, (9), 6282-6285.

70. Goppert-Mayer, M., Elementary processes with two quantum jumps. *Annalen der Physik (Berlin, Germany)* **1931**, 9, 273-94.
71. Kaiser, W.; Garrett, C. G. B., Two-photon excitation in CaF₂:Eu⁺⁺. *Physical Review Letters* **1961**, 7, 229-31.
72. Krafft, G. A.; Sutton, W. R.; Cummings, R. T., Photoactivable Fluorophores .3. Synthesis and Photoactivation of Fluorogenic Difunctionalized Fluoresceins. *Journal of the American Chemical Society* **1988**, 110, (1), 301-303.
73. Zhao, Y. R.; Zheng, Q.; Dakin, K.; Xu, K.; Martinez, M. L.; Li, W. H., New caged coumarin fluorophores with extraordinary uncaging cross sections suitable for biological imaging applications. *Journal of the American Chemical Society* **2004**, 126, (14), 4653-4663.
74. Theriot, J. A.; Mitchison, T. J.; Tilney, L. G.; Portnoy, D. A., The rate of actin-based motility of intracellular *Listeria monocytogenes* equals the rate of actin polymerization. *Nature FIELD Full Journal Title:Nature* **1992**, 357, (6375), 257-60.
75. Reinsch, S. S.; Mitchison, T. J.; Kirschner, M., Microtubule Polymer Assembly and Transport During Axonal Elongation. *Journal of Cell Biology* **1991**, 115, (2), 365-379.
76. Moffat, K., Time-resolved biochemical crystallography: A mechanistic perspective. *Chemical Reviews* **2001**, 101, (6), 1569-1581.
77. Schlichting, I.; Almo, S. C.; Rapp, G.; Wilson, K.; Petratos, K.; Lentfer, A.; Wittinghofer, A.; Kabsch, W.; Pai, E. F.; Petsko, G. A.; Goody, R. S., Time-Resolved X-Ray Crystallographic Study of the Conformational Change in Ha-Ras P21 Protein on Gtp Hydrolysis. *Nature* **1990**, 345, (6273), 309-315.
78. Šrajer, V.; Teng, T. Y.; Ursby, T.; Pradervand, C.; Ren, Z.; Adachi, S.; Schildkamp, W.; Bourgeois, D.; Wulff, M.; Moffat, K., Photolysis of the carbon monoxide complex of myoglobin: Nanosecond time-resolved crystallography. *Science* **1996**, 274, (5293), 1726-1729.
79. Cohen, B. E.; Stoddard, B. L.; Koshland, D. E., Caged NADP and NAD. Synthesis and characterization of functionally distinct caged compounds. *Biochemistry* **1997**, 36, (29), 9035-9044.
80. Volk, M.; Kholodenko, Y.; Lu, H. S. M.; Gooding, E. A.; DeGrado, W. F.; Hochstrasser, R. M., Peptide conformational dynamics and vibrational stark effects following photoinitiated disulfide cleavage. *Journal of Physical Chemistry B* **1997**, 101, (42), 8607-8616.

81. Lu, H. S. M.; Volk, M.; Kholodenko, Y.; Gooding, E.; Hochstrasser, R. M.; DeGrado, W. F., Aminothietyrosine disulfide, an optical trigger for initiation of protein folding. *Journal of the American Chemical Society* **1997**, 119, (31), 7173-7180.
82. Hansen, K. C.; Rock, R. S.; Larsen, R. W.; Chan, S. I., A Method for Photoinitiating Protein Folding in a Nondenaturing Environment. *Journal of the American Chemical Society* **2000**, 122, (46), 11567-11568.
83. Abbruzzetti, S.; Viappiani, C.; Small, J. R.; Libertini, L. J.; Small, E. W., Kinetics of local helix formation in poly-L-glutamic acid studied by time-resolved photoacoustics: Neutralization reactions of carboxylates in aqueous solutions and their relevance to the problem of protein folding. *Biophysical Journal* **2000**, 79, (5), 2714-2721.
84. Diaspro, A.; Federici, F.; Viappiani, C.; Krol, S.; Pisciotta, M.; Chirico, G.; Cannone, F.; Gliozzi, A., Two-photon photolysis of 2-nitrobenzaldehyde monitored by fluorescent-labeled nanocapsules. *Journal of Physical Chemistry B* **2003**, 107, (40), 11008-11012.
85. Fodor, S. P.; Read, J. L.; Pirrung, M. C.; Stryer, L.; Lu, A. T.; Solas, D., Light-directed, spatially addressable parallel chemical synthesis. *Science FIELD Full Journal Title: Science* **1991**, 251, (4995), 767-73.
86. Vossmeier, T.; DeIono, E.; Heath, J. R., Light-directed assembly of nanoparticles. *Angewandte Chemie, International Edition in English* **1997**, 36, (10), 1080-1083.
87. Pirrung, M. C.; Fallon, L.; McGall, G., Proofing of Photolithographic DNA Synthesis with 3',5'-Dimethoxybenzoinyloxycarbonyl-Protected Deoxynucleoside Phosphoramidites. *Journal of Organic Chemistry* **1998**, 63, (2), 241-246.
88. Wintner, J., Synthesis and investigations of (6-hydroxy-3-oxo-3H-xanthen-9-yl)methyl derivatives. A new photoremovable protecting group. *Dissertation, Universität Basel, Switzerland* **2007**.
89. Klonis, N.; Sawyer, W. H., Spectral properties of the prototropic forms of fluorescein in aqueous solution. *Journal of Fluorescence* **1996**, 6, (3), 147-157.
90. Martin, M. M.; Lindqvist, L., Ph-Dependence of Fluorescein Fluorescence. *Journal of Luminescence* **1975**, 10, (6), 381-390.
91. Alvarez-Pez, J. M.; Ballesteros, L.; Talavera, E.; Yguerabide, J., Fluorescein Excited-State Proton Exchange Reactions: Nanosecond Emission Kinetics and Correlation with Steady-State Fluorescence Intensity. *Journal of Physical Chemistry A* **2001**, 105, (26), 6320-6332.

92. Schmidt, R.; Brauer, H. D., Self-sensitized photo-oxidation of aromatic compounds and photocycloreversion of endoperoxides: applications in chemical actinometry. *Journal of Photochemistry* **1984**, 25, (2-4), 489-99.
93. Schmidt, R.; Geissler, D.; Hagen, V.; Bendig, J., Mechanism of photocleavage of (coumarin-4-yl)methyl esters. *Journal of Physical Chemistry A* **2007**, 111, (26), 5768-5774.
94. Eckardt, T.; Hagen, V.; Schade, B.; Schmidt, R.; Schweitzer, C.; Bendig, J., Deactivation Behavior and Excited-State Properties of (Coumarin-4-yl)methyl Derivatives. 2. Photo-Cleavage of Selected (Coumarin-4-yl)methyl-Caged Adenosine Cyclic 3',5'-Monophosphates with Fluorescence Enhancement. *Journal of Organic Chemistry* **2002**, 67, (3), 703-710.
95. Suzuki Akinobu, Z.; Watanabe, T.; Kawamoto, M.; Nishiyama, K.; Yamashita, H.; Ishii, M.; Iwamura, M.; Furuta, T., Coumarin-4-ylmethoxycarbonyls as phototriggers for alcohols and phenols. *Org Lett FIELD Full Journal Title:Organic letters* **2003**, 5, (25), 4867-70.
96. Geissler, D.; Antonenko, Y. N.; Schmidt, R.; Keller, S.; Krylova, O. O.; Wiesner, B.; Bendig, J.; Pohl, P.; Hagen, V., (Coumarin-4-yl)methyl esters as highly efficient, ultrafast phototriggers for protons and their application to acidifying membrane surfaces. *Angewandte Chemie, International Edition* **2005**, 44, (8), 1195-1198.

8. Appendix

During my PhD studies at the University of Basel, I have worked on two other projects:

1. Aqueous Oxidation of Phenylurea Herbicides by Triplet Aromatic Ketones,
2. Inverted Region Behavior in Proton Transfer to Carbanions.

The results from the two projects are summarized in the following subchapters.

8.1. Aqueous Oxidation of Phenylurea Herbicides by Triplet Aromatic Ketones

Environ. Sci. Technol. 2006, 40, 6636–6641

Aqueous Oxidation of Phenylurea Herbicides by Triplet Aromatic Ketones

SILVIO CANONICA,*† BRUNO HELLRUNG,‡ PAVEL MÜLLER,‡ AND JAKOB WIRZ‡

Eawag, Swiss Federal Institute of Aquatic Science and Technology, 8600 Dübendorf, Switzerland, and Departement Chemie, Universität Basel, Klingelbergstrasse 80, CH-4056 Basel, Switzerland

Excited triplet states of dissolved natural organic matter (DOM) are important players for the transformation of organic chemical contaminants in sunlit natural waters. The present study focuses on kinetics and mechanistic aspects of the transformation of phenylurea herbicides induced by well-defined excited triplet states, which have been chosen to model DOM triplet states having oxidative character. The aromatic ketones benzophenone, 3'-methoxyacetophenone, and 2-acetonaphthone were used to photogenerate their triplet states and oxidize a series of eleven substituted phenylureas. Quenching of the excited triplet states by the phenylureas was measured using laser flash photolysis in the microsecond time domain, while the oxidation kinetics of the phenylureas was followed under steady-state irradiation. Second-order rate constants for quenching and oxidation were largely identical for a given pair of ketone and phenylurea. They reached the diffusion-controlled limit ($\approx 4 \times 10^9 \text{ M}^{-1} \text{ s}^{-1}$) and decreased with increasing free energy of electron transfer from the phenylurea to the ketone triplet. These results confirm those already obtained using phenols as the substrates to be oxidized and suggest that oxidation rates are mainly determined by the bimolecular rate constant for electron transfer, a rule that can possibly be extended to various organic contaminants. A refined estimate of the effective reduction potential of DOM excited triplet states was also obtained.

Introduction

Since the first report that phenols might be efficiently oxidized by excited triplet states of dissolved natural organic matter (DOM) (1), various pieces of evidence appeared indicating that such triplet states might be responsible for the depletion of several organic contaminants in sunlit natural waters. These contaminants include phenylurea herbicides (2, 3), the pharmaceuticals mefenamic acid (4) and a series of sulfa drugs containing six-membered heterocyclic groups (5), and the phenolic endocrine disruptor bisphenol A (6). Due to a lack of information about the structure of the supposedly very variable chromophores of the DOM, one practicable way to assess the chemical reactivity of DOM excited triplet

states is to determine that of some model chromophores in the triplet state. Using a series of substituted phenols and three aromatic ketones, we have demonstrated that the excited triplet states of these ketones efficiently oxidize the phenols in aqueous solution. The dependence of the reactivity on energetics suggested an initial one-electron-transfer process (7). Reaction of quinone and aromatic carbonyl triplets through electron or hydrogen atom transfer from organic (8–13) or inorganic (14) substrates is a very well-known process in photochemistry. Unfortunately, data concerning organic compounds in wholly aqueous solution (water fraction >95% vol/vol) are quite scarce (12, 15). Kinetics data obtained using organic solvents or solvent-water mixtures cannot be used to assess aqueous oxidation rate constants owing to the high solvent-sensitivity of electron and hydrogen atom transfer processes (7).

Phenylurea herbicides were selected for this study because, as a result of their widespread use in agriculture and other activities, they are ubiquitous in surface waters (3) and indirect photochemical transformation, most probably induced by excited triplet states of the DOM, constitutes a major removal pathway for these herbicides (3). In the present investigation, we wished to determine second-order rate constants for the reaction of excited triplet states of select aromatic ketones with a series of substituted phenylureas and to establish whether initial oxidation of the phenylureas leads to their efficient depletion. Another important goal was to verify that the measured reaction rate constants follow the trend expected for an electron-transfer process, as was found to be the case for phenols (7). Such a behavior would offer the advantage of providing a predictive tool for the quantification of triplet-induced oxidation of various organic contaminants in water.

Experimental Section

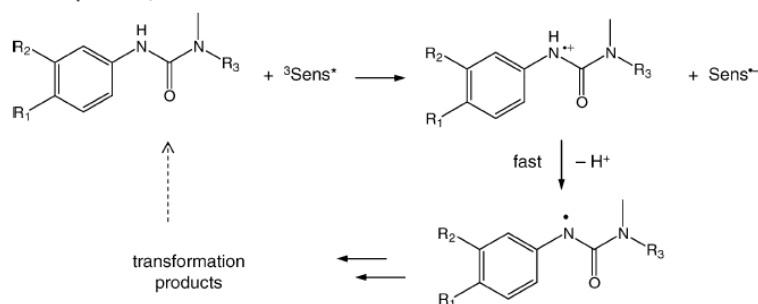
Chemicals. Commercially available phenylurea pesticides, i.e., metoxuron (99.6%), isoproturon (99%), fenuron (99%), chlorotoluron (99%), diuron (99%), and fluometuron (99%) were purchased from Riedel-de Haën, Seelze, Germany (Pestanal quality). The other phenylurea derivatives, i.e., CGA 16519, CGA 17092, CGA 17667, CGA 18414, and CGA 24482, were a gift from Syngenta AG, Basel, Switzerland. The aromatic ketones used were benzophenone (BP, Fluka, >99%), 3'-methoxyacetophenone (3'-MAP, Fluka, 99%), and 2-acetonaphthone (2-AN, Aldrich, 99%). The above compounds and 3,4-dimethoxyphenol (DMOP, Aldrich, 99%) and 2,4,6-trimethylphenol (TMP, EGA-Chemie, 99%), employed as reference substrates in photosensitized depletion experiments, were all used as received. Methanol and acetonitrile applied for high-performance liquid chromatography (HPLC) were both of multisolvent quality from Scharlau (Barcelona, Spain). Aqueous solutions for flash photolysis were made with bidistilled water, while those used for steady-state irradiations were prepared with deionized water treated with a Milli-Q water purification device (Millipore). This water was also used as an HPLC eluent. All other chemicals used were analytical grade.

Laser Flash Photolysis. The nanosecond apparatus for kinetic measurements was of standard design (16). Excitation was done with 351 or 308-nm pulses (pulse width ≈ 25 ns, ≈ 140 mJ per pulse) from an excimer laser (Lambda Physik COMPEX 205), which allowed for selective excitation of the aromatic ketones. A pulsed 150-W xenon arc was used as the monitoring light source. The beam was passed through the sample cell, focused onto a monochromator, and recorded by an RCA 1P28 photomultiplier. The signal was taken from

* Corresponding author phone: +41-1-823-5453; fax: +41-1-823-5210; e-mail: canonica@eawag.ch.

† Eawag, Swiss Federal Institute of Aquatic Science and Technology.
‡ Universität Basel.

SCHEME 1. Proposed Reaction Mechanism for the Oxidation of Phenylureas by the Excited Triplet State of an Aromatic Ketone (Photosensitizer, Denoted by "Sens").



the fifth dynode of the photomultiplier and fed into the 50- Ω terminated amplifier of a Tektronix TDS 540 transient digitizer (500 MHz, 1 G sample/s). The rise time of this detection system was determined as 2.5 ns using a picosecond probe pulse. The parameters of the rate laws described in the text were fitted to the observed kinetic traces using an iterative Marquardt least-squares procedure, where the linear parameters (amplitudes) were determined by linear regression for each trial set of the nonlinear parameters (rate constants) (16). The following probe wavelengths were employed for observing the triplet decays: for BP $\lambda_{\text{obs}} = 350$ nm, 420–450 nm, and 520–530 nm; for 3'-MAP $\lambda_{\text{obs}} = 380$ –440 nm; for 2-AN $\lambda_{\text{obs}} = 440$ nm. All measurements were performed at room temperature (22–24 °C) using a 4.5-cm path length quartz cell connected to the degassing device. Solutions containing a given aromatic ketone (50–300 μM , concentration adjusted to enable formation of 2–3 μM triplet state), 2.0% vol/vol acetonitrile or methanol as a solubilizing agent, and variable concentrations of a given phenylurea were degassed by three freeze–pump–thaw cycles. All compounds were present at concentrations that were clearly below their aqueous solubility limits and no precipitation during degassing was observed. Transient absorption spectra were recorded for aerated solutions buffered at pH = 8.0 with 5 mM phosphate. Excitation of solutions containing potassium peroxydisulfate was performed using 248-nm laser pulses.

Steady-State Irradiation. A DEMA 125 merry-go-round photoreactor (Hans Mangels, Bornheim-Roisdorf, Germany) equipped with a Hanau TQ 718 medium-pressure mercury lamp driven at a power of 500 W, a Pyrex glass cooling jacket, and appropriate filter solutions were used. The experimental setup is described in detail elsewhere (1, 17). Temperature was kept at 25.0 ± 0.2 °C throughout all experimental series. In most cases, irradiations were performed using a 0.25 M sodium nitrate filter solution (irradiation wavelength >320 nm). To determine the second-order reaction rate constant of TMP with triplet BP and 3'-MAP, irradiations were performed using a filter solution containing 0.15 M sodium nitrate and 0.76 M nickel sulfate, which resulted in an effectively monochromatic irradiation at 334 nm. Fluence rate was determined by *p*-nitroanisole (5 μM)/pyridine (10 mM) actinometry (18) assuming a quantum yield of 0.0038 (1). Solutions to be irradiated were aerated and contained 10–50 μM of a given ketone (BP, 13.5 μM ; 3'-MAP, 50 μM ; 2-AN, 10 μM), 5 μM of target compound (phenylurea or reference phenol), and 5.0 mM phosphate buffer (final pH = 8.0). They also contained a small amount of methanol ($\leq 0.1\%$ vol/vol) from the BP and 2-AN stock solutions, which was previously shown not to affect triplet lifetimes in aerated water (7). The depletion kinetics of the target compounds was followed by taking 0.5 mL samples from the irradiated solution (20 mL), contained in a glass-stoppered quartz tube (1.5 cm i.d., 1.8 cm o.d.) at different time increments and subsequent analysis was performed by HPLC as detailed

elsewhere (19, 20). For phenylurea analysis, samples were immediately cooled in an ice bath and transferred to the autosampler chamber of the HPLC system cooled at 4 °C to avoid re-formation of the parent compound by decomposition of unstable photoproducts. Direct phototransformation of all target compounds and aromatic ketones was checked and found to be negligible within the exposure times required for the kinetics experiments.

Results

Triplet Quenching Rate Constants. In degassed aqueous solutions containing BP or 3'-MAP and one of the phenylureas (PU), the excited triplet states of the aromatic ketones, ³BP* and ³3'-MAP*, were observed immediately after the laser flash. Under the present experimental conditions, triplet lifetimes in the absence of phenylurea were determined to be 9.5 ± 0.5 μs for both aromatic ketones. Quenching of the ketone triplets by the phenylureas gave the corresponding ketyl radicals (cf. Discussion, Scheme 1). Due to the large excess of the phenylureas over the excited triplet ketones, the quenching reactions were taken to obey first-order rate laws with rate constants $k_{\text{q}}[\text{PU}]$, where k_{q} is the second-order quenching rate constant and [PU] is the concentration of phenylurea. The subsequent decay of the ketyl radicals was well described by a second-order rate law.

The triplet and ketyl radical absorption spectra overlap at all wavelengths. Thus, the absorbance decay traces $A(t)$ were analyzed by combining a first-order rate law to describe the triplet decay and a second-order rate law to account for the ketyl radical decay, $A(t)/\{d c_{\text{triplet}}(t=0)\} = (\epsilon_{\text{triplet}} - \epsilon_{\text{ketyl}}) \exp(-k_{\text{q}}[\text{PU}]t) + \epsilon_{\text{ketyl}}/(1 + \epsilon_{\text{ketyl}}kt)$. Here, d is the cell path length in cm and $\epsilon_{\text{triplet}}$ and ϵ_{ketyl} are the molar absorbance coefficients of the ketone triplet and ketyl radical, respectively, in units of $\text{M}^{-1} \text{cm}^{-1}$. The above absorbance decay function is not the correct integrated rate law for the envisaged sequence of a first- and a second-order reaction. The differential equations describing such a reaction sequence can only be integrated numerically. The integral rate law given above assumes (wrongly) that the decay of the ketyl radicals starts at $t = 0$ with $c_{\text{ketyl}}(t=0) = c_{\text{triplet}}(t=0)$. This is a satisfactory approximation to determine $k_{\text{q}}[\text{PU}]$ at sufficiently high phenylurea concentrations, where the triplet lifetimes become much shorter than the half-lives of the ketyl radicals, as was confirmed by comparison of traces calculated by numerical integration with experimental traces.

The first-order rate constants $k_{\text{q}}[\text{PU}]$ obtained in this way were plotted against phenylurea concentration, and the corresponding second-order rate constants, k_{q} , for quenching of the excited triplet ketone by the phenylurea were obtained from the slopes of linear regressions to 10–20 data points (Table 1). For BP, k_{q} values varied only within a narrow range of 2.0 – $4.2 \times 10^9 \text{ M}^{-1} \text{ s}^{-1}$, close to the diffusion limit, as was previously observed with a series of phenols (7). By contrast,

TABLE 1. Chemical Structure, Substituent Constants, and Second-Order Rate Constants of Phenylureas for the Reaction with ³BP* and ³3'-MAP*

| compound ^a | substituent | | $\Sigma\sigma^+$ ^b | ³ BP* | | ³ 3'-MAP* | |
|------------------------|-----------------------------------|-----------------|-------------------------------|-----------------------------|-----------------------------|-----------------------------|-----------------------------|
| | R ₁ | R ₂ | | k _q ^c | k _r ^c | k _q ^c | k _r ^c |
| metoxuron | OCH ₃ | Cl | -0.41 | 26(±2) | 31(±2) | 26(±2) | 20(±3) |
| CGA 24482 | 3,4-tetramethylene | | -0.37 | 41(±2) | 37(±2) | 25(±2) | 19(±3) |
| CGA 16519 | CH ₂ CH ₃ | H | -0.30 | 42(±2) | 34(±2) | 14(±1) | 9.5(±1.3) |
| isoproturon | CH(CH ₃) ₂ | H | -0.28 | 40(±2) | 32(±1) | 9.0(±1) | 8.2(±0.9) |
| CGA 17667 ^d | CH(CH ₃) ₂ | H | -0.28 | 39(±2) | 38(±3) | 11(±1) | 8.5(±1.0) |
| CGA 17092 | C(CH ₃) ₃ | H | -0.26 | 38(±2) | 33(±4) | 10(±1) | 8.4(±1.4) |
| fenuron | H | H | 0.00 | 38(±2) | 20(±2) | 1.1(±0.2) | 0.81(±0.13) |
| chlorotoluron | CH ₃ | Cl | 0.06 | 34(±4) | 27(±2) | 1.0(±0.3) | 2.7(±0.3) |
| CGA 18414 ^d | CH(CH ₃) ₂ | Cl | 0.09 | 30(±6) | 28(±3) | < 1 | 1.8(±0.4) |
| fluometuron | H | CF ₃ | 0.43 | 32(±2) | 7.1(±0.8) | < 1 | < 0.08 |
| diuron | Cl | Cl | 0.48 | 20(±4) | 5.2(±0.8) | < 1 | 0.09(±0.02) |

^aSubstituent R₃=CH₃ unless when noted. ^b See ref 3 for calculation. ^c k_q: Quenching rate constant; k_r: rate constant for reaction of the triplets with the phenylureas (obtained from depletion kinetics); units: 10⁸ M⁻¹ s⁻¹, 95% confidence intervals in parenthesis. ^d Substituent R₃=CH₂CH₃.

the quenching rate constants of ³3'-MAP* varied by nearly 2 orders of magnitude, with a maximum of 2.6 × 10⁹ M⁻¹ s⁻¹ for metoxuron and constants lower than 1 × 10⁸ M⁻¹ s⁻¹ for three phenylureas, including diuron. For 2-AN no triplet quenching by any of the phenylureas could be observed and k_q may be considered to be well below 1 × 10⁸ M⁻¹ s⁻¹.

Phenylurea Depletion by Steady-State Irradiation. A pseudo-first-order kinetics behavior was expected because of the low phenylurea concentration (which cannot affect the excited triplet concentration) and of the photostability of the used aromatic ketones, which undergo a photocatalytic cycle in the presence of oxygen (1). However, preliminary steady-state irradiation experiments using 3'-MAP as the photosensitizer revealed, especially for the phenylureas bearing electron donating substituents, depletion kinetics that deviated from the expected behavior: The residual concentration of a given phenylurea that was left after extended irradiation was higher than that predicted by first-order extrapolation of the initial depletion kinetics. The cause of this anomaly could be attributed to an unstable product of the photosensitized reaction, which was more hydrophilic than the parent phenylurea (shorter HPLC retention time) and slowly disappeared with a concomitant increase of the parent compound concentration. These unstable photoproducts, possibly peroxides (see Discussion), disappeared with half-lives of 0.8, 37, and 105 h in the dark at 25 °C and pH = 8, yielding the parent compounds metoxuron, isoproturon, and chlorotoluron, respectively. The deviation from first-order kinetics could be eliminated by cooling the samples of solution to be analyzed in an ice bath immediately after withdrawal from the photoreactor and keeping them cooled at 4 °C in the HPLC autosampler until injection. Figure 1 displays a series of depletion curves obtained using 3'-MAP as the photosensitizer. The depletion of all eleven phenylureas was investigated using the photosensitizers BP, 3'-MAP, and 2-AN. Depletion of the photosensitizers during irradiations was negligible. Pseudo-first-order rate constants were determined by linear regression of logarithmic phenylurea concentration values for each kinetics run and corrected for fluence rate variations (<±9%) within a given photosensitizer series (the average fluence rate at the wavelength of 366 nm was 2.5 mEinstein m⁻² s⁻¹). This enabled us to obtain, for each photosensitizer separately, a set of relative pseudo-first-order rate constants. Control irradiation experiments were also carried out in the absence of photosensitizer, which led to first-order depletion rate constants (due to direct or impurity-induced phototransformation of the phenylureas) that were much smaller than those determined in the

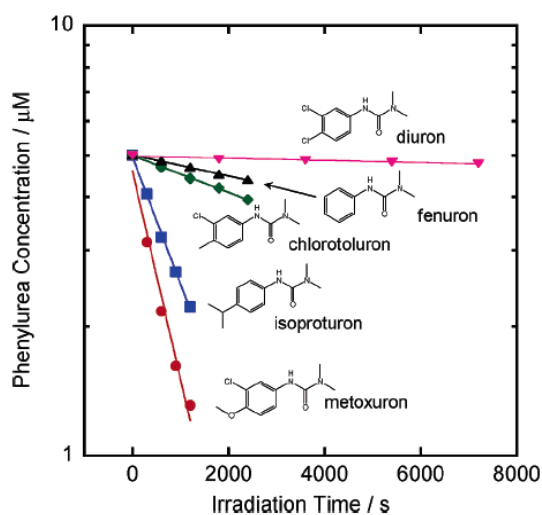


FIGURE 1. Depletion of selected phenylureas irradiated in buffered aqueous solution (pH = 8.0) containing 3'-methoxyacetophenone (50 μM). Note that the concentrations are plotted on a logarithmic scale.

presence of the photosensitizer, except with 2-AN. For the latter aromatic ketone, no appreciable sensitized degradation of the phenylureas was found. To obtain second-order rate constants for the reaction of phenylureas with ³BP* and ³3'-MAP*, a monochromatic irradiation experiment (λ = 334 nm) was carried out using TMP as a reference compound, which was chosen for its fast reaction even at the low fluence rates used. The method for calculating these constants has been described in detail elsewhere (7). The second-order rate constants for depletion of the phenylureas, k_r (given in Table 1), where calculated based on the k_r ratios between TMP and isoproturon, which were determined to be 1.3 and 2.2 for ³BP* and ³3'-MAP*, respectively. By comparison with the first-order depletion rate constant of DMOP, the following upper limit was determined in the case of ³2-AN*: k_r < 2 × 10⁷ M⁻¹ s⁻¹.

Time-Resolved Spectra. To allow observation of primary oxidation products of the phenylureas, laser flash photolysis was applied to aerated aqueous solutions containing BP as the photosensitizer and fenuron or metoxuron, present at a concentration of 0.5 mM to serve as the main quencher for

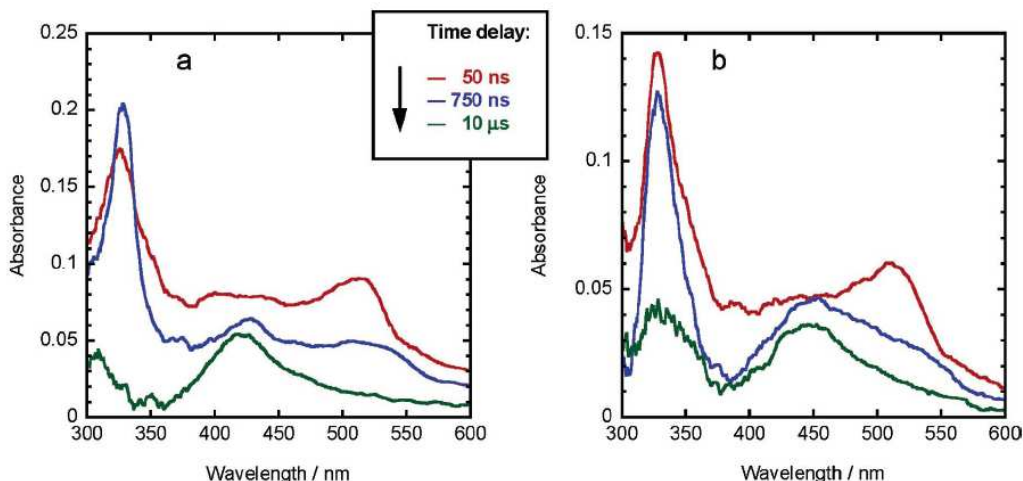


FIGURE 2. Time-resolved absorption spectra obtained after laser flash photolysis (excitation at 308 nm) of 300 μM aerated aqueous benzophenone solutions buffered at pH = 8.0, containing (a) 0.5 mM fenuron and (b) 0.5 mM metoxuron. Spectra were taken at delay times of 50 ns (red line), 750 ns (blue line), and 10 μs (green line).

$^3\text{BP}^*$. Figure 2 shows for the two phenylureas a set of time-resolved absorption spectra. Immediately after the laser flash (50 ns delay), the main contribution to absorbance is given by $^3\text{BP}^*$, with characteristic absorption maxima at ≈ 335 and ≈ 515 nm. At 750 ns delay the 515 nm band has essentially disappeared, while a shoulder, assigned to the BP ketyl radical (21), has appeared at ≈ 520 –530 nm. The 335 nm band is still present, but should now be assigned mainly to the ketyl radical, and two new local maxima at ≈ 430 and ≈ 450 nm have formed, which we assign to fenuron radical and metoxuron radical, respectively. The third spectrum of each series was taken 10 μs after the laser pulse, when complete relaxation of both $^3\text{BP}^*$ and BP ketyl radical should have taken place (the BP ketyl radical is scavenged by molecular oxygen to form BP in its ground state and superoxide radical anion, and its relaxation rate constant in aerated water was determined to be $5.8 \times 10^5 \text{ s}^{-1}$ (7)), and should reflect the absorption spectrum of the phenylurea radical. This assignment is supported by the good match with the spectra (data not shown) obtained after flash photolysis of aqueous solutions of the same phenylureas in the presence of peroxodisulfate, which generates the strong oxidizing sulfate radical and leads to the corresponding phenylurea radicals (22). The spectrum obtained for the fenuron radical formed by reaction of $^3\text{BP}^*$ with fenuron also matches well the published spectra for the same radical obtained by two different methods, i.e., photoionization by laser flash photolysis and reaction with sulfate radical generated by pulse radiolysis (22).

Discussion

Excited triplet states of aromatic ketones are well-known to be strong oxidants, which react in particular with aromatic compounds that are activated by electron-donating substituents. Phenols (9), phenoxide ions (23), methoxybenzenes (10), but also amines (8, 24) (including anilines), amino acids, and aminopolycarboxylic acids (11), were shown to undergo oxidation by triplet aromatic ketones. In the presence of easily abstractable hydrogen atoms, oxidation of organic substrates may be postulated to occur by a range of mechanisms between the two extremes of “pure” hydrogen atom transfer and “pure” electron transfer. While hydrogen atom abstraction may be the energetically most favorable pathway in nonpolar solvents, electron transfer was shown to be the probable mechanism for the oxidation of phenols by triplet

aromatic ketones in aqueous solution (7). In the case of phenylureas, a quantitative analysis of oxidation rate constants based on the Marcus theory of electron transfer cannot be performed currently because oxidation potentials of phenylureas are not available. We analyze instead the oxidation rate data by means of Hammett relationships using σ^+ resonance substituent constants, which have been proven to be efficient descriptor variables for electron-deficient transition states as in one-electron oxidation reactions (25, 26). Hammett plots of second-order rate constants for triplet state quenching by phenylureas, k_q , and reaction with phenylureas, k_r , are given in Figure 3.

For $^3\text{BP}^*$, quenching rate constants exhibit a very minor decrease with increasing $\Sigma\sigma^+$ ($= \sigma_p^+ + \sigma_m^+$ for the present series of phenylureas; the subscripts “p” and “m” indicate para and meta positions of the substituents on the benzene ring, respectively, relative to the urea functional group), while k_r follows a more pronounced negative dependence which significantly deviates from linearity. Looking in more detail at individual k_q – k_r pairs, one can notice that the values are essentially identical except for fluometuron and diuron, for which $k_r \approx k_q/4$. By contrast, Hammett plots for $^33'$ -MAP* yield good linear relationships with much the same results for k_q and k_r (eqs 1 and 2).

$$\log k_q(^33'\text{-MAP}^*) = 8.14(\pm 0.10) - 3.21(\pm 0.34) \Sigma\sigma^+ \\ n = 8, r^2 = 0.989, s = 0.06 \quad (1)$$

$$\log k_r(^33'\text{-MAP}^*) = 8.26(\pm 0.16) - 2.54(\pm 0.54) \Sigma\sigma^+ \\ n = 10, r^2 = 0.936, s = 0.20 \quad (2)$$

Unfortunately, it is not possible to compare k_q and k_r of fluometuron and diuron for their reaction with $^33'$ -MAP*, because the k_q values lie below our quantification limit. The reason for the difference between k_q and k_r observed for these two phenylureas for the reaction with $^3\text{BP}^*$ remains uncertain. It may be due to a minimized phenylurea radical yield or reduction of the phenylurea radical to reform the parent compound.

By analogy with the reaction between phenols and triplet aromatic ketones (7) we propose an initial electron-transfer step for the oxidation of the phenylureas (see Scheme 1) leading to ketyl radicals and phenylurea radical cations, which are known to be strong acids ($-1.5 < \text{pK}_a < 0.5$) (22, 27) and

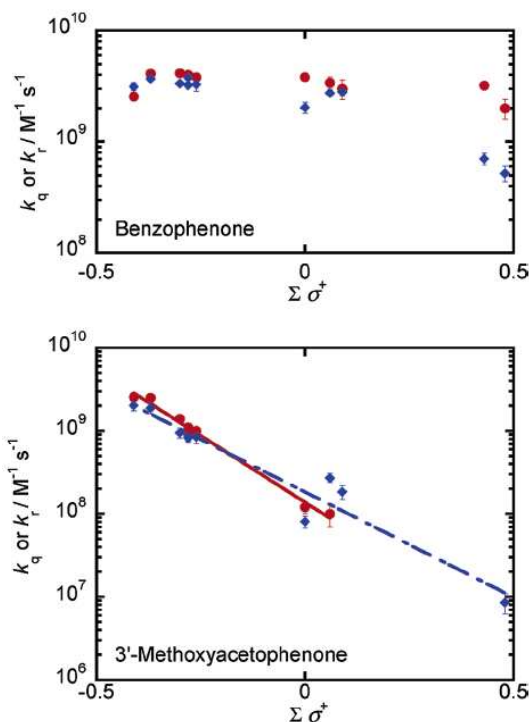


FIGURE 3. Hammett plots of rate constants for quenching of excited triplet aromatic ketones (k_q , circles) and their reaction with phenylureas (k_r , squares). The straight lines, eq 1 (continuous line) and eq 2 (dashed line), were obtained by linear regression.

should therefore deprotonate rapidly to yield neutral phenylurea radicals. This mechanism explains why only the phenylurea radicals, but not the phenylurea radical cations (27), are observed at neutral pH (Figure 2). The phenylurea radicals react further to yield not yet identified oxidation products that may partially undergo transformation to regenerate the parent phenylurea. The direct formation of phenylurea radicals by hydrogen abstraction cannot be excluded based on the evidence from time-resolved spectra, however the high second-order rate constants obtained for the reaction of the phenylureas with $^3\text{BP}^*$ tend to support electron transfer.

Assuming that the one-electron-transfer process is the rate determining step for the oxidation of the phenylureas, it is possible to make some predictions of their hitherto unknown standard oxidation potentials. As a measure of the oxidation potential of phenylureas (PU) we take the standard reduction potential of the corresponding radical cations ($\text{PU}^{*\cdot}$), $E_{\text{red}}^{\text{PU}^{*\cdot}/\text{PU}}$, and express it in the following in V versus the normal hydrogen electrode (NHE). A lower limit to $E_{\text{red}}^{\text{PU}^{*\cdot}/\text{PU}}$ for the series of studied phenylureas is given by the reduction potential of $^3\text{2-AN}^*$, which amounts to 1.34 V [value extracted from (14), Table 1; note the very good agreement with the value calculated from Marcus analysis of rate constants for quenching of $^3\text{BP}^*$ and $^3\text{2-AN}^*$ by phenols (7)]. Considering that $^3\text{BP}^*$ reacts with the phenylureas at rates that approach the diffusion limit, its reduction potential of 1.79 V (14) can be taken as an upper limit for the potential of the compounds studied. We conclude that $E_{\text{red}}^{\text{PU}^{*\cdot}/\text{PU}}$ is comprised in the range of ≈ 1.4 –1.8 V. This assignment is reasonable if one considers the second-order rate constants for the reaction of phenylureas with various oxidants, which are summarized graphically in Figure

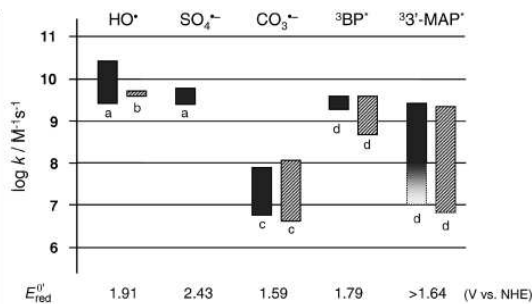


FIGURE 4. Summary of second-order rate constants for the reaction of phenylureas with various oxidants. Rate constants, obtained by microsecond time-resolved techniques (gray bars) or steady-state irradiation (hatched bars), are taken from (a) ref 22, (b) ref 28, (c) ref 20, and (d) this study. One-electron standard reduction potentials of the oxidants are also given.

4. In particular, the carbonate radical ($\text{CO}_3^{\cdot-}$) and $^3\text{3'-MAP}^*$, which have reduction potentials within the proposed range, also exhibit selective reactivity with the phenylureas (20).

The selectivity of a reaction may be expressed by means of the reaction constant ρ^+ , which is the slope of the corresponding Hammett regression line when the $\Sigma\sigma^+$ descriptor variable is used. By considering the selectivity ($\rho^+ = -1.16$) previously obtained for the photosensitized transformation of phenylureas by Suwannee River fulvic acid (SRFA) ($^3\text{SRFA}^*$) (3), one can note that it lies between the selectivity of $^3\text{3'-MAP}^*$ and that of $^3\text{BP}^*$ determined in this study. Evidence was presented that the photosensitized transformation of the phenylureas was brought about by excited triplet states of SRFA ($^3\text{SRFA}^*$) (3). Based on this hypothesis one can conclude that the standard one-electron reduction potential of $^3\text{SRFA}^*$ should lie between that of $^3\text{3'-MAP}^*$ and that of $^3\text{BP}^*$, i.e., in the range of ≈ 1.6 –1.8 V. This estimate is consistent with, but more accurate than the previous lower limit of 1.36 V obtained from our analogous study on phenol photosensitized oxidation (1, 7). Of course, such an estimate cannot be assumed to hold for every type of DOM, and more work is needed for an appropriate verification. The remarkably high one-electron reduction potential estimated in this study for excited triplet states of the DOM, $^3\text{DOM}^*$, leads us to conclude that there must be various classes of organic chemical contaminants which undergo oxidation initiated by $^3\text{DOM}^*$. For contaminants that are recalcitrant to biological degradation and are inefficiently depleted by direct photochemical transformation, this indirect photochemical transformation might constitute the main depletion process taking place in surface waters.

Acknowledgments

We thank Andreas Gerecke for fruitful discussions.

Literature Cited

- (1) Canonica, S.; Jans, U.; Stemmler, K.; Hoigné, J. Transformation kinetics of phenols in water: Photosensitization by dissolved natural organic material and aromatic ketones. *Environ. Sci. Technol.* **1995**, *29*, 1822–1831.
- (2) Aguer, J. P.; Richard, C. Transformation of fenuron induced by photochemical excitation of humic acids. *Pestic. Sci.* **1996**, *46*, 151–155.
- (3) Gerecke, A. C.; Canonica, S.; Müller, S. R.; Schärer, M.; Schwarzenbach, R. P. Quantification of dissolved natural organic matter (DOM) mediated phototransformation of phenylurea herbicides in lakes. *Environ. Sci. Technol.* **2001**, *35*, 3915–3923.
- (4) Werner, J. J.; McNeill, K.; Arnold, W. A. Environmental photodegradation of mefenamic acid. *Chemosphere* **2005**, *58*, 1339–1346.
- (5) Boreen, A. L.; Arnold, W. A.; McNeill, K. Triplet-sensitized photodegradation of sulfa drugs containing six-membered

- heterocyclic groups: Identification of an SO₂ extrusion photoproduct. *Environ. Sci. Technol.* **2005**, *39*, 3630–3638.
- (6) Chin, Y. P.; Miller, P. L.; Zeng, L. K.; Cawley, K.; Weavers, L. K. Photosensitized degradation of bisphenol A by dissolved organic matter. *Environ. Sci. Technol.* **2004**, *38*, 5888–5894.
 - (7) Canonica, S.; Hellrung, B.; Wirz, J. Oxidation of phenols by triplet aromatic ketones in aqueous solution. *J. Phys. Chem. A* **2000**, *104*, 1226–1232.
 - (8) Cohen, S. G.; Parola, A.; Parsons, G. H. Photoreduction by amines. *Chem. Rev.* **1973**, *73*, 141–161.
 - (9) Das, P. K.; Encinas, M. V.; Scaiano, J. C. Laser flash photolysis study of the reactions of carbonyl triplets with phenols and photochemistry of *p*-hydroxypropiophenone. *J. Am. Chem. Soc.* **1981**, *103*, 4154–4162.
 - (10) Das, P. K.; Bobrowski, K. Charge transfer reactions of methoxybenzenes with aromatic carbonyl triplets. A laser flash photolytic study. *J. Chem. Soc.-Faraday Trans. II* **1981**, *77*, 1009–1027.
 - (11) Bhattacharyya, S. N.; Das, P. K. Photoreduction of benzophenone by amino acids, aminopolycarboxylic acids and their metal complexes. A laser flash photolysis study. *J. Chem. Soc.-Faraday Trans. II* **1984**, *80*, 1107–1116.
 - (12) Encinas, M. V.; Lissi, E. A.; Olea, A. F. Quenching of triplet benzophenone by vitamins E and C and by sulfur-containing amino acids and peptides. *Photochem. Photobiol.* **1985**, *42*, 347–352.
 - (13) Marciniak, B.; Bobrowski, K.; Hug, G. L. Quenching of triplet states of aromatic ketones by sulfur-containing amino acids in solution. Evidence for electron transfer. *J. Phys. Chem.* **1993**, *97*, 11937–11943.
 - (14) Loeff, I.; Rabani, J.; Treinin, A.; Linschitz, H. Charge-transfer and reactivity of $n\pi^*$ and $\pi\pi^*$ organic triplets, including anthraquinonesulfonates, in interactions with inorganic anions: A comparative study based on classical Marcus theory. *J. Am. Chem. Soc.* **1993**, *115*, 8933–8942.
 - (15) Encinas, M. V.; Lissi, E. A.; Vasquez, M.; Olea, A. F.; Silva, E. Photointeraction of benzophenone triplet with lysozyme. *Photochem. Photobiol.* **1989**, *49*, 557–563.
 - (16) Bonneau, R.; Wirz, J.; Zuberbühler, A. D. Methods for the analysis of transient absorbance data. *Pure Appl. Chem.* **1997**, *69*, 979–992.
 - (17) Wegelin, M.; Canonica, S.; Mechsner, K.; Fleischmann, T.; Pesaro, F.; Metzler, A. Solar water disinfection: Scope of the process and analysis of radiation experiments. *J. Water Supply Res. Technol. - Aqua* **1994**, *43*, 154–169.
 - (18) Dulin, D.; Mill, T. Development and evaluation of sunlight actinometers. *Environ. Sci. Technol.* **1982**, *16*, 815–820.
 - (19) Canonica, S.; Freiburghaus, M. Electron-rich phenols for probing the photochemical reactivity of freshwaters. *Environ. Sci. Technol.* **2001**, *35*, 690–695.
 - (20) Canonica, S.; Kohn, T.; Mac, M.; Real, F. J.; Wirz, J.; Von Gunten, U. Photosensitizer method to determine rate constants for the reaction of carbonate radical with organic compounds. *Environ. Sci. Technol.* **2005**, *39*, 9182–9188.
 - (21) Hayon, E.; Ibata, T.; Lichtin, N. N.; Simic, M. Electron and hydrogen atom attachment to aromatic carbonyl compounds in aqueous solution. Absorption spectra and dissociation constants of ketyl radicals. *J. Phys. Chem.* **1972**, *76*, 2072–2078.
 - (22) Canle Lopez, M.; Fernandez, M. I.; Rodriguez, S.; Santaballa, J. A.; Steenken, S.; Vuilliet, E. Mechanisms of direct and TiO₂-photocatalysed UV degradation of phenylurea herbicides. *ChemPhysChem* **2005**, *6*, 2064–2074.
 - (23) Das, P. K.; Bhattacharyya, S. N. Laser flash photolysis study of electron transfer reactions of phenolate ions with aromatic carbonyl triplets. *J. Phys. Chem.* **1981**, *85*, 1391–1395.
 - (24) Bhattacharyya, K.; Das, P. K. Nanosecond transient processes in the triethylamine quenching of benzophenone triplets in aqueous alkaline media. Substituent effect, ketyl radical deprotonation, and secondary photoreduction kinetics. *J. Phys. Chem.* **1986**, *90*, 3987–3993.
 - (25) Hansch, C.; Leo, A.; Taft, R. W. A survey of Hammett substituent constants and resonance and field parameters. *Chem. Rev.* **1991**, *91*, 165–195.
 - (26) Hansch, C.; Gao, H. Comparative QSAR: Radical reactions of benzene derivatives in chemistry and biology. *Chem. Rev.* **1997**, *97*, 2995–3059.
 - (27) Canle, M.; Rodriguez, S.; Vazquez, L. F. R.; Santaballa, J. A.; Steenken, S. First stages of photodegradation of the urea herbicides Fenuron, Monuron and Diuron. *J. Mol. Struct.* **2001**, *565*, 133–139.
 - (28) De Laat, J.; Maouala Makata, P.; Doré, M. Rate constants for reactions of ozone and hydroxyl radicals with several phenylureas and acetamides. *Environ. Technol.* **1996**, *17*, 707–716.

Received for review May 11, 2006. Revised manuscript received July 19, 2006. Accepted August 17, 2006.

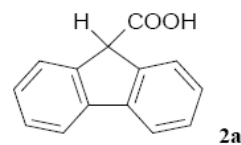
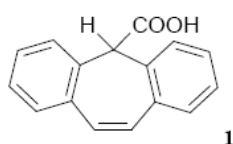
ES0611238

8.2. Inverted Region Behavior in Proton Transfer to Carbanions

Introduction

Recently, J. M. Savéant and his coworkers^{1,2} predicted an inverted region behavior in proton transfer to carbanions. There are a few ways to generate carbanions, one of which is a photochemical decarboxylation of deprotonated forms of the corresponding carboxylic acids. One of the first detailed mechanistic studies of photodecarboxylation was reported by Margerum and Petrusis³ in 1969.

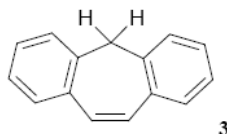
In the late 80's and early 90's, P. Wan et al. published two papers^{4,5} describing a photodissociation of a series of diarylacetic acids both in pure and in aqueous CH₃CN (typically 60% (v/v) H₂O-CH₃CN) at different pH's. Photolysis of the acids in D₂O-CH₃CN solutions having a pH > pK_a resulted in an exclusive formation of the corresponding monodeuterated hydrocarbons in high yields. However, at pH's < pK_a, most of the acids were completely nonreactive, the only exception being suberene-5-carboxylic acid (IUPAC: 5*H*-dibenzo[*a,d*][7]annulene-5-carboxylic acid) (**1**).



The photolysis of **1** (10^{-3} M solution in 40 % CH₃CN) displayed no measurable pH effect (within the range of pH = -1 to +11) on the quantum yield of decarboxylation ($\Phi = 0.6 \pm 0.05$). **1** was also the most reactive compound of all tested acids. Similarly to other tested compounds, the photodecarboxylation of **1** is supposed to proceed via a carbanion intermediate, which, in this case, would involve eight π ($4n$) electrons in the “internal cyclic array” (ICA) and would thus be formally anti-aromatic in the ground state and hence highly reactive.

9*H*-fluorene-9-carboxylic acid (**2a**), on the other hand, proved to be the least reactive compound from the whole series. The carbanion intermediate derived from **2a** involves six π ($4n + 2$) electrons in the ICA and is therefore aromatic in the ground state.

In the later works⁶⁻¹¹, P. Wan and co-workers also reported on an unusual C-acidity of suberene (**3**) in its excited state. They observed a photochemical proton-deuterium exchange (in both directions) at the terminal 5-carbon upon irradiation and suggested a mechanism involving a carbanion intermediate.



The unique photoreactivity of **1** and **3** described by P. Wan et al. would open up an easy way to generate carbanions and to determine rate constants and KIE for carbanion protonation by acids of various pK_a values. A systematic study of the reactivity of the carbanions in both protic and aprotic solvents was to shed more light on the validity of Savéant's inverted region theory.

Triphenylacetic Acid and its Sodium Salt

| | | |
|------------------------|--------------------------------|---|
| Formula: | 4a | 4b |
| Molecular Formula: | $C_{20}H_{16}O_2$ | $C_{20}H_{15}O_2Na$ |
| Molecular weight: | 288.35 g/mol | 310.33 g/mol |
| Molecular composition: | C 83.31 %; H 5.59 %; O 11.10 % | C 77.41 %; H 4.87 %; Na 7.41 %; O 10.30 % |
| Producer: | Aldrich | - |
| Purity: | 99 % | - |

The commercial triphenylacetic acid (**4a**) was transformed to its Na^+ -salt (**4b**), since it is easier to control the amount of water in a CH_3CN solution of **4b** than in case of NaOH-solution added to a solution of **4a** (to ensure $pH > pK_a$ and stimulate the decarboxylation of the acid).

Preparation of 4b

0.5 g (1.735×10^{-3} mol) of **4a** were dissolved in 10 ml of 0.2 M aqueous NaOH (2×10^{-3} mol NaOH). The stirred mixture was heated (until the organic fraction dissolved completely) and then cooled down in a freezer. The precipitate (**4b**) was filtered, washed with ice-cold distilled water and dried.

LFP experiments

A few nanoseconds after irradiation of a solution of **4b** in CH₃CN with laser light (248 nm), two distinct absorption bands could be observed (see **Fig. 1**). The first band (max. at 330 nm) was assigned to a triphenylmethyl radical¹² and the second band (max. at 485 nm) to a triphenylmethyl carbanion¹³. Irradiation of **4a** in pure CH₃CN did not result in formation of any of the two bands.

A series of kinetics measurements were carried out. Kinetic traces were recorded (at 485 nm) for 1.5×10^{-4} M solutions of **4b** containing different concentrations of added H₂O (0.00 to 1.00 M). The obtained data is shown in more detail in the following table (**Table 1**) and depicted in **Fig. 2**.

Table 1

| $c(\text{Ph}_3\text{CCOONa}) /$ (mol/l) | $c(\text{H}_2\text{O}) /$ (mol/l) | A_{248} (against CH ₃ CN) | k / s^{-1} |
|--|-----------------------------------|--|---------------------|
| 1.50E-04 | 0.00 | 0.34 | 3.454E+06 |
| 1.50E-04 | 0.05 | 0.38 | 3.894E+06 |
| 1.50E-04 | 0.15 | 0.36 | 4.452E+06 |
| 1.50E-04 | 0.30 | 0.36 | 5.902E+06 |
| 1.50E-04 | 0.50 | 0.37 | 9.251E+06 |
| 1.50E-04 | 1.00 | 0.37 | 2.669E+07 |

Fig. 1 A UV-vis absorption spectrum of a non-degassed 1.5×10^{-4} M solution of **4b** in CH₃CN recorded a few ns after the laser flash (248 nm).

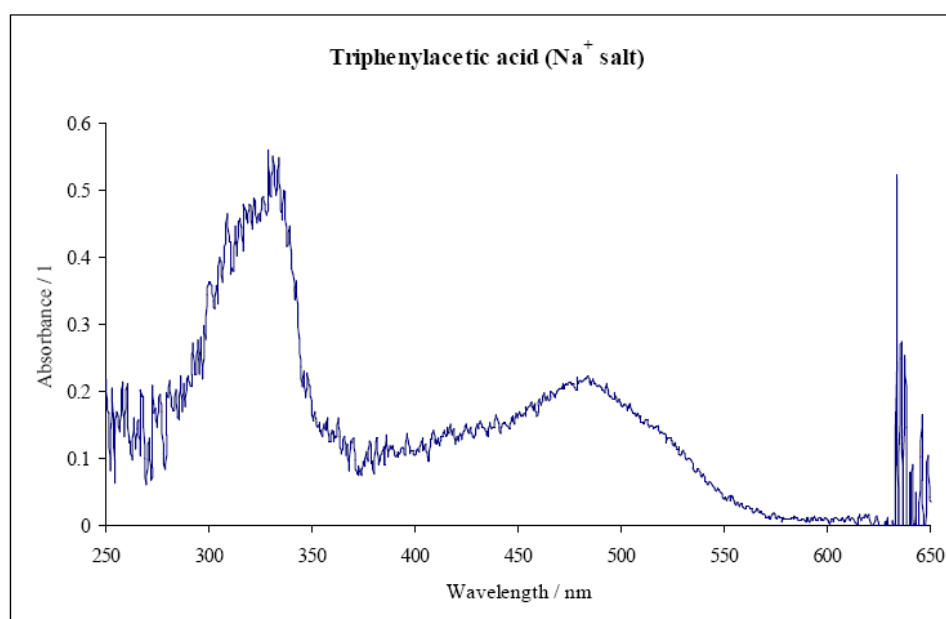
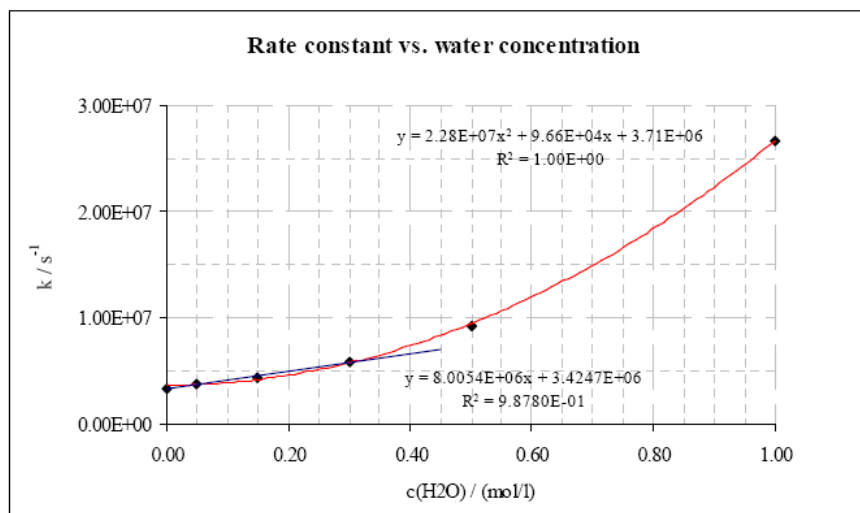


Fig. 2 1st-order rate constants obtained from the kinetics measurements of the solutions of **4b** in CH₃CN plotted against added H₂O concentration.



Diphenylacetic Acid and its Sodium Salt

| | | |
|------------------------|--|---|
| Formula: | | |
| Molecular Formula: | C ₁₄ H ₁₂ O ₂ | C ₁₄ H ₁₁ O ₂ Na |
| Molecular weight: | 212.25 g/mol | 234.23 g/mol |
| Molecular composition: | C 79.22 %; H 5.70 %; O 15.08 % | C 71.79 %; H 4.74 %; Na 9.81 %; O 13.66 % |
| Producer: | Fluka | - |
| Purity: | Puriss. | - |

For the same reason **4a** was transformed to its Na⁺-salt (**4b**), the commercially available diphenylacetic acid (**5a**) was transformed to **5b**.

Preparation of 5b

0.5 g (2.356 x 10⁻³ mol) of **5a** were dissolved in 10 ml of 0.25 M aqueous NaOH (2.5 x 10⁻³ mol NaOH). The stirred mixture was heated (until the organic fraction dissolved completely) and then cooled down in a freezer. The precipitate (**5b**) was filtered, washed with ice-cold distilled water and dried.

LFP experiments

A few nanoseconds after irradiation of a solution of **5b** in CH₃CN with laser light (248 nm), again, two distinct absorption bands could be observed (see **Fig. 3**). The first band (max. at 330 nm) was assigned to a diphenylmethyl radical and the second one (max. at 440 nm) to a diphenylmethyl carbanion^{13, 14}. Again, the irradiation of **5a** in pure CH₃CN did not result in formation of any of the two bands.

As in the previous case, kinetic traces were recorded (this time at 440 nm) for 1.5×10^{-4} M solutions of **5b** containing different concentrations of added H₂O (0.00 to 0.50 M). The obtained data is shown in more detail in **Table 2** and depicted in **Fig. 4**.

Table 2

| $c(\text{Ph}_2\text{CCOONa}) /$ (mol/l) | $c(\text{H}_2\text{O}) /$ (mol/l) | A_{248} (against CH ₃ CN) | k / s^{-1} |
|--|-----------------------------------|--|---------------------|
| 1.50E-04 | 0.00 | 0.08 | 4.047E+06 |
| 1.50E-04 | 0.05 | 0.12 | 5.085E+06 |
| 1.50E-04 | 0.10 | 0.11 | 6.084E+06 |
| 1.50E-04 | 0.15 | 0.10 | 7.952E+06 |
| 1.50E-04 | 0.30 | 0.12 | 1.455E+07 |
| 1.50E-04 | 0.50 | 0.11 | 3.944E+07 |

Fig. 3 A UV-vis absorption spectrum of a non-degassed 1.5×10^{-4} M solution of **5b** in CH₃CN recorded a few ns after the laser flash (248 nm).

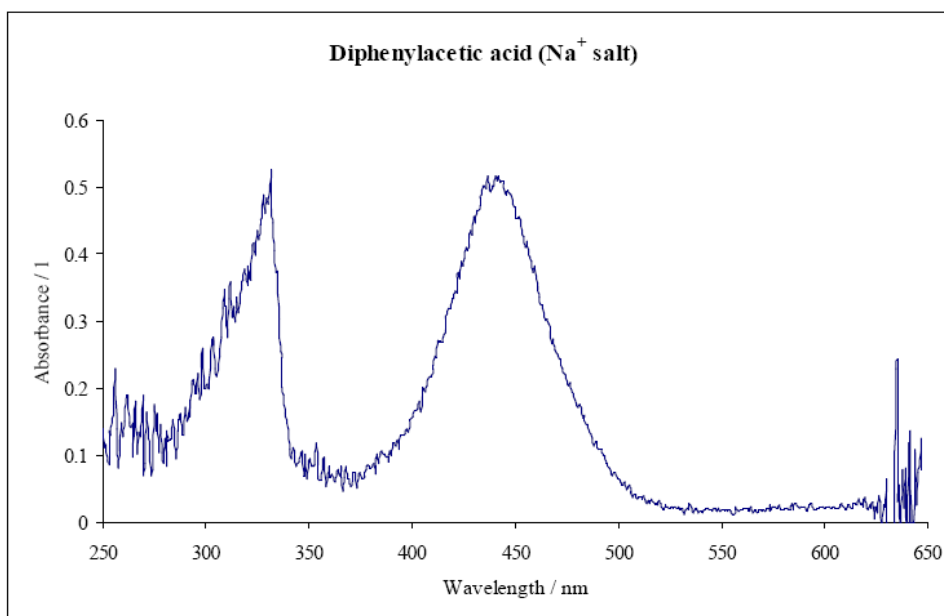
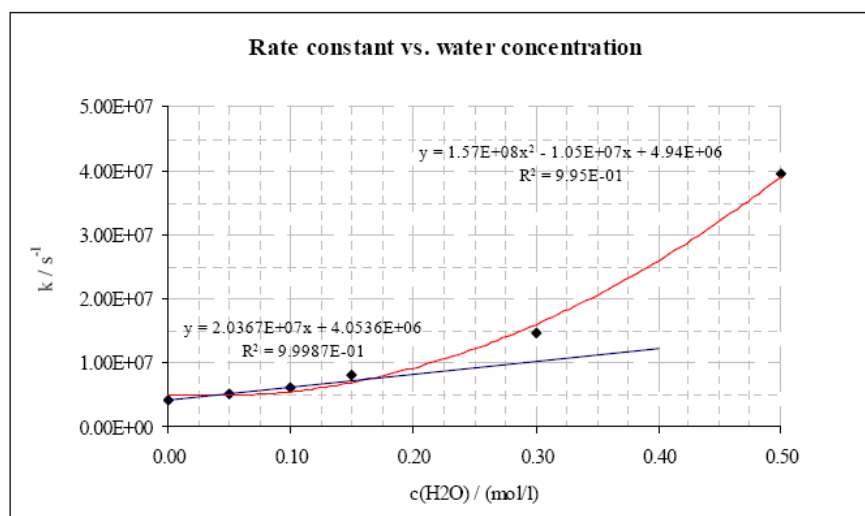


Fig. 4 1st-order rate constants obtained from the kinetics measurements of the solutions of **5b** in CH₃CN plotted against added H₂O concentration.



9H-Fluorene-9-carboxylic Acid and its Sodium Salt

| | | |
|------------------------|--|--|
| Formula: | | |
| Molecular Formula: | C ₁₄ H ₁₀ O ₂ | C ₁₄ H ₉ O ₂ Na |
| Molecular weight: | 210.23 g/mol | 232.22 g/mol |
| Molecular composition: | C 79.98 %; H 4.79 %; O 15.23 % | C 72.41 %; H 3.91 %; Na 9.90 %; O 13.78 % |
| Producer: | Fluka | - |
| Purity: | Purum >96.0 % | - |

As in the previous two cases, also the commercial **2a** was transformed to its Na⁺-salt (**2b**).

Preparation of 2b

0.5 g (2.381×10^{-3} mol) of **2a** were dissolved in 10 ml of 0.25 M aqueous NaOH (2.5×10^{-3} mol NaOH). The stirred mixture was heated (until the organic fraction dissolved completely) and then cooled down in a freezer. The precipitate (**2b**) was filtered, washed with ice-cold distilled water and dried.

LFP experiments

Irradiation of a **2b** solution in CH₃CN with laser light (248 nm) again led to a formation of two absorption bands (see **Fig. 5**). The first band (max. at 370 nm) was most likely a fluorenyl radical and the second one (max. at 430 nm) corresponds to a fluorene-9-carbanion¹⁵. As in previous two cases, the irradiation of **2a** in pure CH₃CN did not result in a formation of any observable transients.

Again, kinetic traces were recorded (at 430 nm) for 1.5×10^{-4} M solutions of (**2b**) containing different concentrations of added H₂O (0.00 to 0.30 M). For more details see **Table 3** and **Fig.. 6**.

Table 3

| $c(\text{fl. carb. acid}) / (\text{mol/l})$ | $c(\text{H}_2\text{O}) / (\text{mol/l})$ | A_{248} (against CH ₃ CN) | k / s^{-1} |
|---|--|--|---------------------|
| 1.50E-05 | 0.00 | 0.08 | 4.739E+06 |
| 1.50E-05 | 0.05 | 0.12 | 4.862E+06 |
| 1.50E-05 | 0.10 | 0.11 | 5.102E+06 |
| 1.50E-05 | 0.15 | 0.10 | 5.564E+06 |
| 1.50E-05 | 0.30 | 0.12 | 7.318E+06 |

Fig. 5 A UV-vis absorption spectrum of a non-degassed 1.5×10^{-5} M solution of **2b** in CH₃CN recorded a few ns after the laser flash (248 nm).

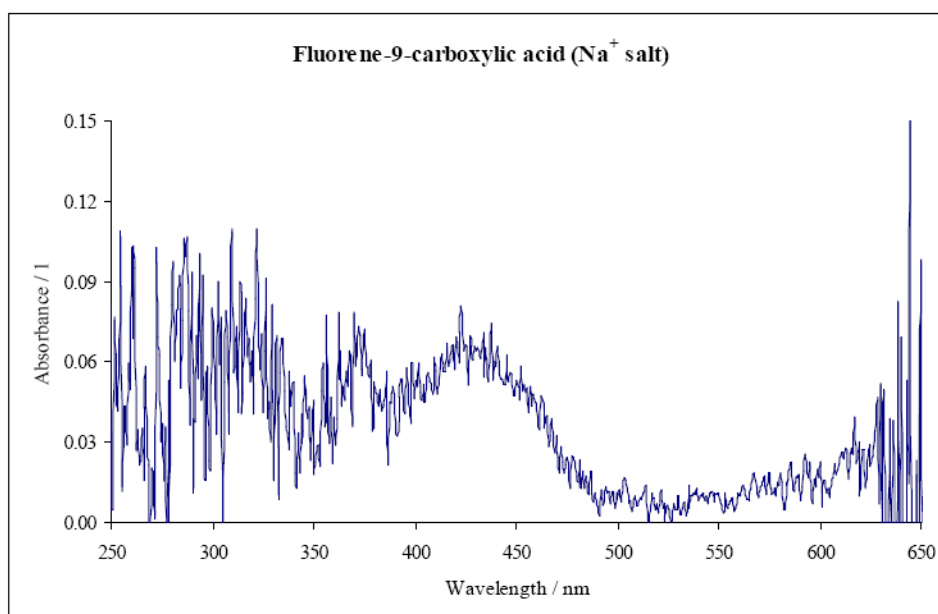
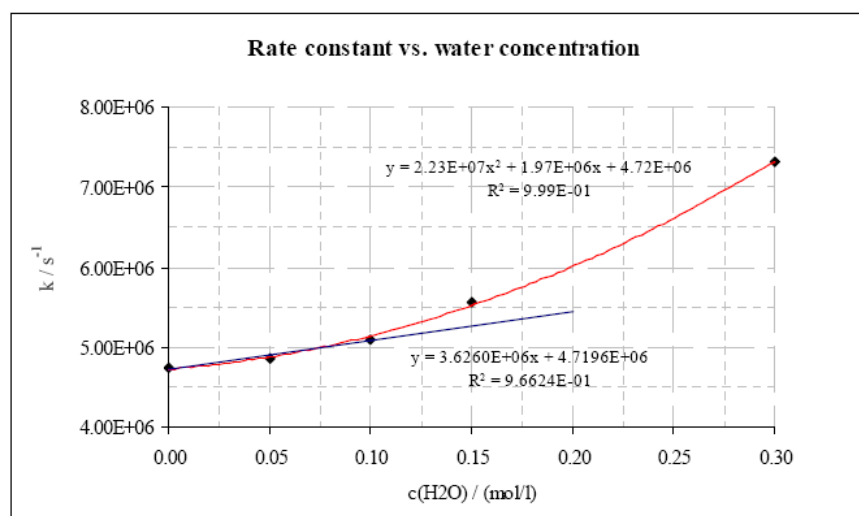
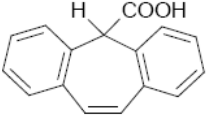
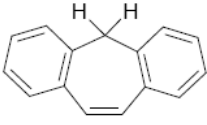


Fig. 6 1st-order rate constants obtained from the kinetics measurements of the solutions of **2b** in CH₃CN plotted against added H₂O concentration.

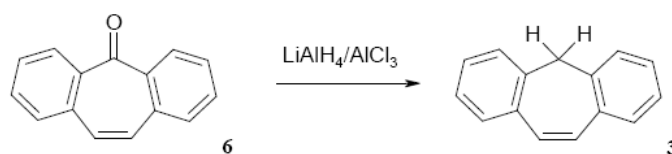


Photochemistry of 5*H*-Suberene-5-carboxylic acid and Suberene

| | | |
|------------------------|--|---|
| Formula: |  1 |  3 |
| Molecular Formula: | C ₁₆ H ₁₂ O ₂ | C ₁₅ H ₁₂ |
| Molecular weight: | 236.27 g/mol | 192.26 g/mol |
| Molecular composition: | C 81.34 %; H 5.12 %; O 13.54 % | C 93.71 %; H 6.29 %; |

Since neither **1** nor **3** are commercially available, they had to be synthesized. **3** can be readily prepared by a reduction of the corresponding ketone (dibenzosuberene-5-one; (**6**)) using lithium aluminium hydride¹⁶. **1** is formed from **3** by its deprotonation with butyllithium and a subsequent addition of CO₂ (g) to the resulting anion^{5,17}.

Synthesis of 3



Chemicals:

5-dibenzosuberone (Fluka, pure > 97%), Ether (Fluka, puriss., dried over molecular sieve, H₂O < 0.005 %), THF (Fluka, puriss., dried over molecular sieve, H₂O < 0.005 %), LiAlH₄ (Fluka, pure > 97 %), AlCl₃ (Fluka, anhydrous, puriss. > 99 %), bidistilled H₂O, H₂SO₄ (Baker, 95-98%), Na₂SO₄.

Procedure:

To a suspension of 1.00 g (0.026 mol) LiAlH₄ in 15 ml ether under argon atmosphere a solution of 3.42 g (0.026 mol) AlCl₃ in 20 ml ether was added dropwise. After 10 minutes, 4.8 g of **6** (dissolved in 25 ml THF) were added and the mixture was refluxed for 2 hours.

After cooling to 0 °C, 35 ml of water were added. The precipitate was dissolved in aqueous 10% H₂SO₄. The organic phase was separated from the water phase and the water phase was shaken once more with ether. The combined ether fractions were shaken with water until pH = 7.

The mixture was rid of water with Na₂SO₄, filtered, and the liquid was evaporated. After vacuum drying, 4.4 g of light-yellow crystals (**3**) were isolated (95 % yield).

Product identification:

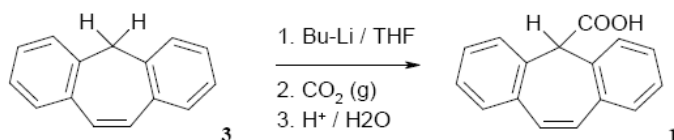
mp: 127-129 °C;

¹H-NMR (400 MHz, CDCl₃): 3.76 (s, 2H, -CH₂-); 7.05 (s, 2H, -CH=CH-); 7.22-7.33 (m, 8H, arom. H);

¹³C-NMR (400 MHz, CDCl₃): 42.0 (1C, -CH₂-); 126.5-131.9 (5 x 2C, 8 arom. C-H and 2 -CH=CH-); 135.6, 138.5 (2 x 2C, arom. C_{quart.});

MS (GC-MS): M/Z = 192.

Synthesis of 1



Chemicals:

Suberene (synthesized), THF (Fluka, puriss., dried over molecular sieve, H₂O < 0.005 %), Butyllithium (Aldrich, 2.5M solution in hexane), CH₂Cl₂, Ethanol, bidistilled H₂O, HCl (Prolabo, 37%), NaOH (Riedel-de Haën, puriss.), MgSO₄ (Fluka, puriss.), Ar, CO₂ (g).

Procedure:

A solution of 2 g (10 mmol) of suberene (**3**) in 100 ml of dry THF under argon was cooled to 0 °C, and 15 mmol of a 2.5 M solution of n-BuLi (Aldrich) were added dropwise via syringe. The solution was heated to reflux for 1 h and then cooled to room temperature before purging with dry CO₂ (g) via syringe.

The reaction was worked up by reducing the THF to 15 ml, diluting with 100 ml of CH₂Cl₂ and subsequent extracting with a 0.1 M NaOH solution (3 x 100 ml). The combined aqueous fractions were acidified, and the cloudy precipitate was extracted into CH₂Cl₂ (2 x 100 ml).

The organic layer was dried over MgSO₄, filtered, and reduced under vacuum to yield 1.3 g of a bright-yellow solid, which was recrystallized (5 times) from 1:2 H₂O-ethanol to yield 0.62 g (25% yield) of fine white needles.

Product identification:

mp: 234-238 °C (lit. 239-241 °C);

¹H-NMR (400 MHz, D₆-acetone): 5.16 (s, 1 H, -CHCOO-), 7.00 (s, 2 H, -CH=CH-), 7.25-7.50 (m, 8H, arom. H);

¹³C-NMR (400 MHz, D₆-acetone): 57.6 (1C, term. C); 127.1-131.2 (5 x 2C, 8 arom. C-H and 2 -CH=CH-); 135.1, 137.9 (2 x 2C, arom. C_{quart.}); 172.0 (1C, -COOH)

MS (GC-MS): M/Z = 236.

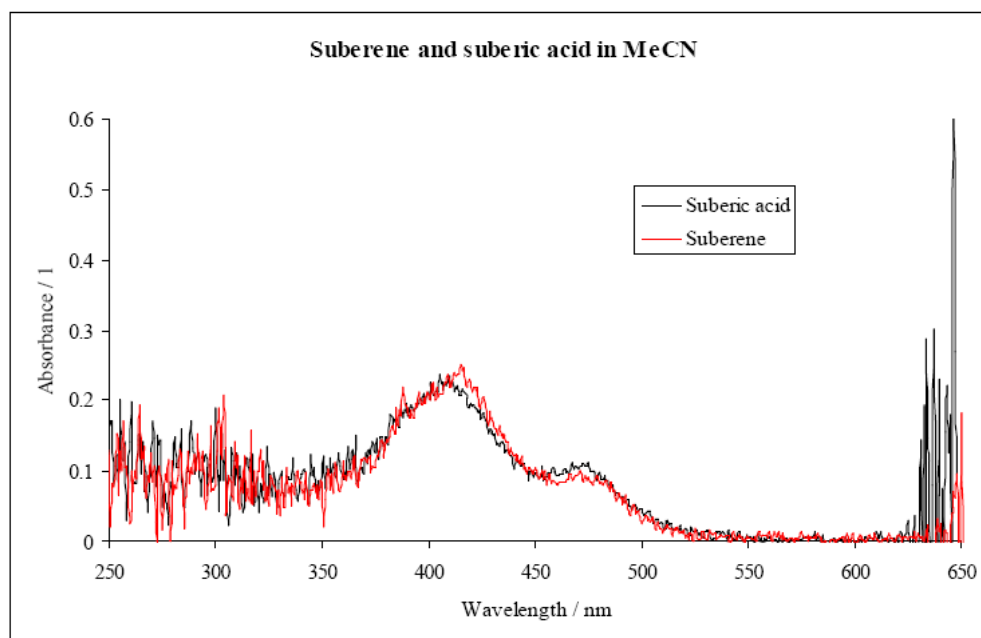
LFP experiments

Absorption spectra of the species originating from **1** and **3** upon irradiation are virtually identical (see **Fig. 7**). The two bands (one at 405 and the other at 475 nm) can be detected in O₂-saturated, as well in degassed solutions.

The two bands obviously do not belong to one transient, since the band at 405 nm (initially about 3 times more intense) decays about 10 times faster than the one at 475 nm (in aerated solutions).

Their mutual dependence is also questionable, since both of them appear immediately after the flash of the laser in air-saturated solutions. In degassed solutions, however, none of the bands is formed instantly and they grow within about 2 μ s before they start decaying again. Interestingly, none of the two species exhibits a nice monoexponential (pseudo-)1st-order decay.

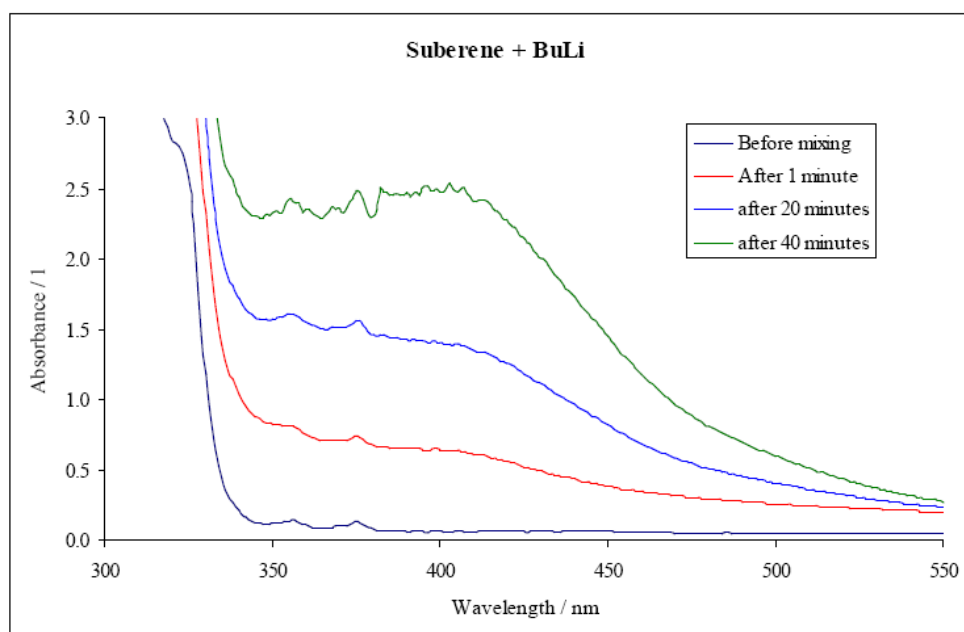
Fig. 7 Absorption spectra of **1** and **3** in non-degassed CH₃CN solutions right after the laser flash (248 nm).



Since the spectrum of suberenyl anion has not been published, I have tried to generate it by adding butyllithium to a THF-solution of suberene in the absence of oxygen (degassing cell). The generation of a suberenyl anion by adding butyllithium to a solution of **3** is the principle, based on which **1** is synthesized. The recorded spectra (**Fig. 8**) are thus very likely to be the spectra of the anion of interest. The first visible absorption band has a maximum of 405 nm, which corresponds to one of the bands observed in the previous LFP experiments (it is just maybe a bit broader than the one in **Fig. 7**). The other band (at 475 nm) was not observed at all.

When trying to assign the other band, a suberenyl radical (**7**) was also generated. **3** (5×10^{-3} M) was dissolved in a mixture of benzene and di-*tert*-butyl peroxide (3:1) and the solution was irradiated with a 351 nm-light (the absorption of **3** is negligible at this wavelength). The recorded spectrum of the suberenyl radical is shown in **Fig. 9**. The *t*-butoxyl radical, that is readily generated in such experiment, does not absorb in the given wavelength range and its spectrum therefore does not interfere with that of other species (radicals), that are formed as a result of H[•] abstraction by *t*-butoxyl radical itself.

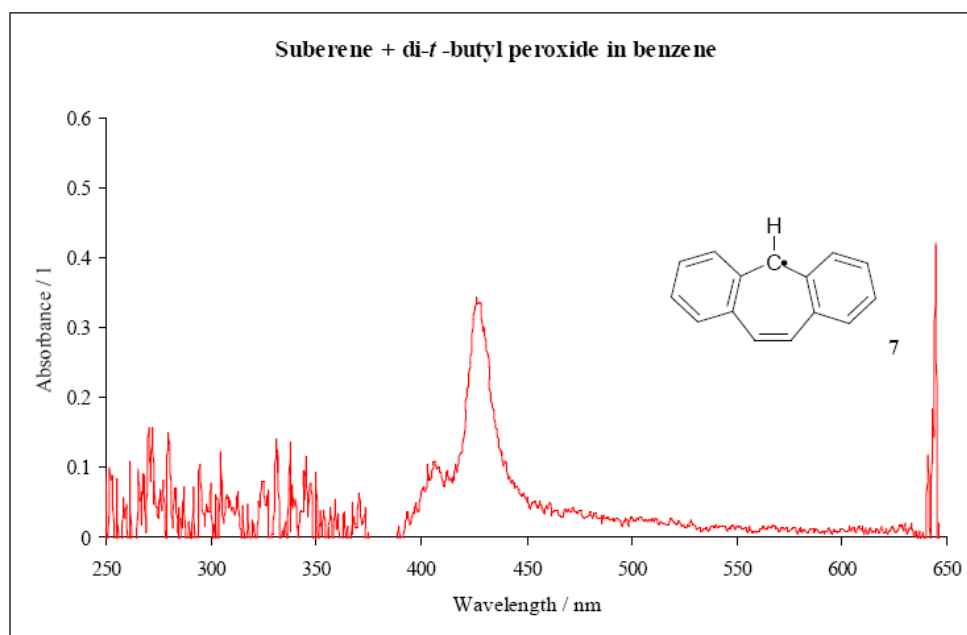
Fig. 8 UV-vis spectra of a mixture of **3** in dry THF and BuLi solution in hexane.



Apparently, the distinct absorption band of **7** at 430 nm cannot be identified with any of the species observed within the previous experiments.

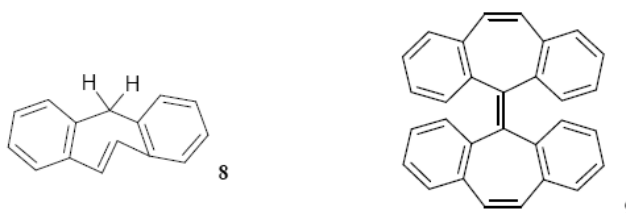
A photosensitization experiment has also been carried out. Benzophenone (BP, 1.5×10^{-3}) and suberene (0.5×10^{-3} M) in CH₃CN were irradiated at 351 nm and the absorption spectra of the short-lived species were recorded 50 and 300 ns after the laser flash. ³[BP]^{*} has an absorption maximum at 520 nm. After 50 ns, another strong band at ca 410 nm could be observed. 250 ns later, the ³[BP]^{*} absorption was already negligible but the band at 410 nm was still clearly visible. The rate constant of the ³[BP]^{*} decay in CH₃CN at room temperature is about $6.2 \times 10^6 \text{ s}^{-1}$. Under given conditions, the growth of the transient at 410 was characterized by a 2nd-order rate constant of $4.65 \times 10^7 \text{ M}^{-1}\text{s}^{-1}$ and its subsequent decay by a $k = 5.4 \times 10^6 \text{ s}^{-1}$.

Fig. 9 Suberene (5×10^{-3} M) in a mixture di-*tert*-butyl peroxide and benzene (1:3) irradiated at 351 nm.



At that point, there were already two possible “candidates” for the 405 nm transient but still none for the one at 475 nm. The bibliographic search on the UV-vis spectra of two other species that could theoretically be formed under given conditions, namely “trans”-suberene (**8**) and [5,5’]bi[dibenzo[a,d]cycloheptenyliidene (**9**), did not make things any clearer.

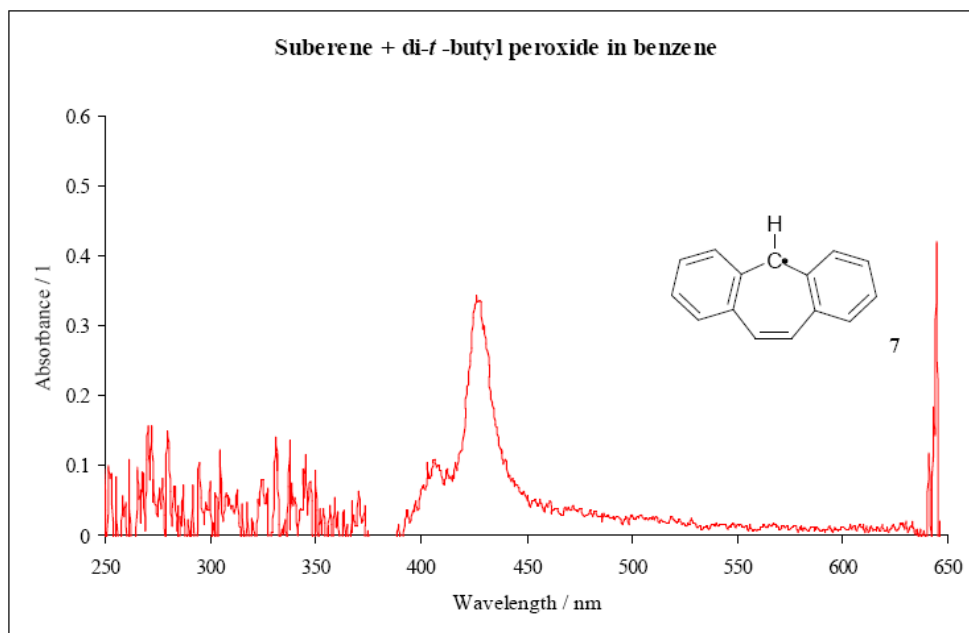
Trans-cycloheptatriene and its benzo- derivatives such as **8** are not known to be formed under any circumstances¹⁸, not even as intermediate reactive species. Such compounds are known to undergo a very efficient photorearrangement to bicycloheptadienes^{18, 19}. Not surprisingly, compound **9** absorbs at 280 nm²⁰.



Fluorescence experiments

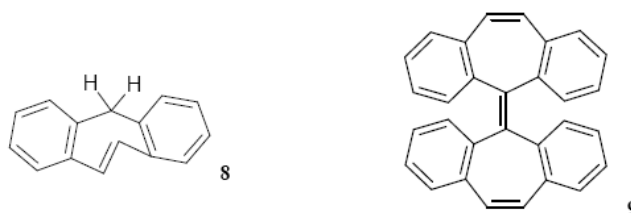
Both **1** and **3** fluoresce. The recorded fluorescence spectrum is shown in **Fig. 10**. The maximum is to be found at ca 430 nm. The lifetime of fluorescence is about 3 ns. The deviation from a Gaussian shape is most likely due to the absorption of the excited species at 410 and 470 nm (see also **Fig. 7**).

Fig. 9 Suberene (5×10^{-3} M) in a mixture di-*tert*-butyl peroxide and benzene (1:3) irradiated at 351 nm.



At that point, there were already two possible “candidates” for the 405 nm transient but still none for the one at 475 nm. The bibliographic search on the UV-vis spectra of two other species that could theoretically be formed under given conditions, namely “trans”-suberene (**8**) and [5,5']bi[dibenzo[a,d]cycloheptenylydene (**9**), did not make things any clearer.

Trans-cycloheptatriene and its benzo- derivatives such as **8** are not known to be formed under any circumstances¹⁸, not even as intermediate reactive species. Such compounds are known to undergo a very efficient photorearrangement to bicycloheptadienes^{18, 19}. Not surprisingly, compound **9** absorbs at 280 nm²⁰.



Fluorescence experiments

Both **1** and **3** fluoresce. The maximum is to be found at ca 430 nm. The lifetime of fluorescence is about 3 ns.

Conclusions

Photochemistry of **1** and **3** proved to be somewhat more complex than expected. It is not at all certain, that we are able to see the suberenyl anion predicted by P. Wan et al.⁴⁻¹¹ since none of the two bands observed in the LFP experiments could be assigned with certainty. The band at 405-410 nm could belong to the suberenyl anion, as well as to a T₁-state of **3**. The origin of the band at 475 nm remains entirely unknown. Whatever the two transients are, both of them seem to be quenched by oxygen, water and other acids.

Kinetics of both bands are complex (they do not obey (pseudo-)1st-order rate law) and seem to be mutually independent. Both species appear immediately after the flash of the laser in air-saturated solutions. In degassed solutions, however, none of the bands is formed instantly. The kinetics measurements are also complicated by a substantial fluorescence of both **1** and **3**, which causes a temporary oversaturation of the photomultiplier and thus its malfunction.

If the suberenyl anion is formed, it is likely to be highly reactive since it is anti-aromatic in its ground state. It is possible that it decays so fast, that we are not even able to register it on the given time scale. Carrying out faster pump-probe experiments might suggest more.

References

1. Gamby, J.; Hapiot, P.; Saveant, J. M., Dynamics of proton transfer at nonactivated carbons from laser flash electron photoinjection experiments. *Journal of the American Chemical Society* **2002**, 124, (30), 8798-8799.
2. Andrieux, C. P.; Gamby, J.; Hapiot, P.; Saveant, J. M., Evidence for inverted region behavior in proton transfer to carbanions. *Journal of the American Chemical Society* **2003**, 125, (33), 10119-10124.
3. Margerum, J. D.; Petrusis, C. T., Photodecarboxylation of Nitrophenylacetate Ions. *Journal of the American Chemical Society* **1969**, 91, (10), 2467-&.
4. McAuley, I.; Krogh, E.; Wan, P., Carbanion Intermediates in the Photodecarboxylation of Benzannelated Acetic-Acids in Aqueous-Solution. *Journal of the American Chemical Society* **1988**, 110, (2), 600-602.
5. Krogh, E.; Wan, P., Photodecarboxylation of Diarylacetic Acids in Aqueous-Solution - Enhanced Photogeneration of Cyclically Conjugated 8 Pi-Electron Carbanions. *Journal of the American Chemical Society* **1992**, 114, (2), 705-712.
6. Budac, D.; Wan, P., Excited-State Carbon Acids - Facile Benzylic C-H Bond Heterolysis of Suberene on Photolysis in Aqueous-Solution - a Photogenerated Cyclically Conjugated 8 Pi-Electron Carbanion. *Journal of Organic Chemistry* **1992**, 57, (3), 887-894.
7. Budac, D.; Wan, P., Excited state carbon acids. Photodeprotonation and photoreduction of suberenes by amines. *Journal of Photochemistry and Photobiology a-Chemistry* **1996**, 98, (1-2), 27-37.
8. Shukla, D.; Lukeman, M.; Shi, Y. J.; Wan, P., Excited state proton transfer to and from carbon: studies of enhanced excited state basicity of biphenyl derivatives and carbon acidity of dibenzosuberenes. *Journal of Photochemistry and Photobiology a-Chemistry* **2002**, 154, (1), 93-105.
9. Shukla, D.; Wan, P., Photogeneration of antiaromatic 8 pi xanthenide and thioxanthenide ('pi-excessive') carbanions via excited-state carbon acid deprotonation and photodecarboxylation. *Journal of Photochemistry and Photobiology a-Chemistry* **1998**, 113, (1), 53-64.
10. Wan, P.; Budac, D.; Earle, M.; Shukla, D., Excited-State Carbon Acids - Photochemical C-H Bond Heterolysis Vs Formal Di-Pi-Methane Rearrangement of

- 5h-Dibenzo[a,C]Cycloheptene and Related-Compounds. *Journal of the American Chemical Society* **1990**, 112, (22), 8048-8054.
11. Wan, P.; Krogh, E.; Chak, B., Enhanced Formation of 8- π (4n) Conjugated Cyclic Carbanions in the Excited-State - 1st Example of Photochemical C-H Bond Heterolysis in Photoexcited Suberene. *Journal of the American Chemical Society* **1988**, 110, (12), 4073-4074.
 12. Faria, J. L.; Steenken, S., Photoionization ($\lambda=248$ or 308 nm) of Triphenylmethyl Radical in Aqueous-Solution - Formation of Triphenylmethyl Carbocation. *Journal of the American Chemical Society* **1990**, 112, (3), 1277-1279.
 13. Grinter, R.; Mason, S. F., Symmetry-Determined Relationships in Electronic Spectra of Arylmethyl Ions. *Transactions of the Faraday Society* **1964**, 60, (4942), 264-&.
 14. Tseng, K. L.; Michl, J., Mcd Spectra of Diphenylmethyl Cation and Anion - Test of Pairing Theorem. *Journal of the American Chemical Society* **1976**, 98, (20), 6138-6141.
 15. Streitwieser, A.; Brauman, J. I., Spectra of Some Alkali Salts of Hydrocarbons. *Journal of the American Chemical Society* **1963**, 85, (17), 2633-&.
 16. Platzek, J.; Snatzke, G., Synthesis of Optically-Active 10,11-Dihydro-5h-Dibenzo[a,D]Cycloheptenes. *Tetrahedron* **1987**, 43, (21), 4947-4968.
 17. Horning, D. E.; Muchowski, Jm, Synthesis of 5h-Dibenzo[a,D]Cycloheptene-5-Carboxylic Acid and Related Compounds . 1,5-Hydride Transfer to Inductively Destabilized Carbonium Ions. *Canadian Journal of Chemistry* **1968**, 46, (23), 3665-&.
 18. Daino, Y.; Hagiwara, S.; Hakushi, T.; Inoue, Y.; Tai, A., Photochemistry of Cyclohepta-1,3-Diene and Cyclohepta-1,3,5-Triene - Photochemical Formation and Chemical-Reactivity of the Strained Trans-Isomer. *Journal of the Chemical Society-Perkin Transactions 2* **1989**, (3), 275-282.
 19. Steuhl, H. M.; Klessinger, M., Excited-State Carbon Acids - Theoretical-Studies of Suberene and Cycloheptatriene. *Angewandte Chemie-International Edition* **1995**, 33, (23-24), 2431-2433.
 20. Schonber, A; Sadtke, U.; Praefcke, K., Preparation Reactions and Stereochemistry of 2,3,6,7,2',3',6',7'-Tetrabenzoheptafulvalene. *Chemische Berichte-Recueil* **1969**, 102, (5), 1453-&.

9. Curriculum Vitae

Mgr. Pavel Müller
Spalenvorstadt 18
4051 Basel
Phone: 076 33 22 952
pavel.mueller@unibas.ch



12. 05. 1981 **Date of Birth**

Single **Marital Status**

Master's degree in chemistry **Education**

Czech **Nationality**

Education

- Ph.D. in chemistry 2004 – 2007
University of Basel, [Switzerland](#)
Research group of Prof. Jakob Wirz
- Master's degree program in organic chemistry 1999 – 2004
Masaryk University in Brno, [Czech Republic](#)
Research group of Assoc. Prof. Petr Klán Ph.D.
Mgr. title (MSc. equivalent)
- High school, [A-Level](#) 1992 – 1999
Gymnasium Taborska, Brno, [Czech Republic](#)

External Fellowships and Traineeships

- University of Missouri – Columbia, [USA](#) 2003 (2 months)
Research group of Prof. Kent Gates
[Synthesis](#) of 5-chloro- and 5-hydroxytirapazamines,
derivatives [of a prospective anti-cancer drug](#)
- Université Paris-Sud XI, [France](#) 2003 (3 months)
Research group of Prof. André Loupy
[Microwave photochemistry](#) in water under extreme
conditions (high pressure and temperatures).
- Institute of Macromolecular Chemistry 2002 (1 month)
Academy of Sciences of the [Czech Republic](#)
[Lab assistant](#)
Research group of Prof. Karel Ulbrich, DSc.
[Designing new drug-release/drug-delivery systems](#)

Language Skills and Certificates

| | |
|------------------------------|----------------|
| Mother tongue | Czech |
| Nearly as mother tongue (C2) | English |
| Fluent (C1/C2) | German |
| Good knowledge (B2) | French |
| Good knowledge (B1) | Russian |
| Nearly as mother tongue (C2) | Slovak |
| Good knowledge (B2) | Polish |
| Basic knowledge (A2) | Bulgarian |
| Basic knowledge (A2) | Serbo-Croatian |

Translations of scientific articles on geochemistry from Czech into English for the Czech Geological Survey in Brno, Czech Republic 2003 – 2007

Zentrale Mittelstufenprüfung, ZMP 2005
Very good: 108-120/120
Goethe Institut, Germany

Test of English as a Foreign Language, TOEFL 2004
627/677; Educational Testing Services, NJ, USA

General Graduate Record Examination, GRE 2004
Quantitative 780/800
Educational Testing Services, NJ, USA

Certificate in Advanced English, CAE 1999
University of Cambridge, UK

Analytical Techniques, Professional Skills

GC, GC/MS, HPLC, NMR
UV/Vis/IR spectroscopy
Laser flash photolysis, nanosecond spectroscopy

IT Skills

MS Windows, MS Office (Word, Excel, PowerPoint)
Adobe products, Corel Draw, ChemOffice
Maple (basic knowledge), SpecFit, Gaussian
SciFinder Scholar, CrossFire-Beilstein, etc.

Teaching Experience 2004 – 2006
(University of Basel)

Tutorials in kinetics and thermodynamics **Physical Chemistry**
(both in English and in German)
Lab courses (in German) **General Chemistry**

Awards

Dean's Award for an outstanding academic 2004
performance and research in the field
Masaryk University in Brno, Czech Republic

**Publications and Conference
Contributions/Participations**

Canonica S., Hellrung B., Müller P., Wirz J., *Environ.
Sci. Technol. (ACS)* **2006**, *40*, 6636-6641

Müller P., Loupy A., Klán P., *J. Photochem.
Photobiol. A: Chem.* **2005**, *172*, 146-150

Müller P., Klán P., Cirkva V., *J. Photochem.
Photobiol. A: Chem.* **2005**, *171*, 51-57

Müller P., Klán P., Cirkva V., *J. Photochem.
Photobiol. A: Chem.* **2003**, *158*, 1-5

Müller P., Wintner J., Wirz J., *A New* 2007
Photoremovable Protecting Group Absorbing Above
520 nm: (6-Hydroxy-3-oxo-3H-xanthen-9-yl)methyl
and its Derivatives (Poster); Frontiers in
Photochemistry, Villars sur Ollon, Switzerland

Müller P., Klán P., Literák J., Cirkva V. 2005
Application of Microwave-Assisted Photochemistry
(Poster); Solar Energy and Applied Photochemistry
[Solar'05], Luxor, Egypt, Book of Abstracts p. 92-93

Participation in the 4th and 5th *Swiss Snow Symposia* 2006, 2007
Swiss Young Chemists' Association
Grindelwald und Fiesch, Switzerland

Participation in the *Séminaire hors-ville du 3ème cycle en Chimie 2006 – Seminar on Computational Quantum Dynamics in Chemistry*, 2006
Lugano, Switzerland

Other Activities

Organization of the official Swiss Unihockey 2005 – 2006
tournaments
Basel Magic, Basel und Kaiseraugst, Switzerland

Personal Interests

Chemistry, Physics, Biology
Earth Sciences, Astronomy, IT
Traveling and foreign languages
Sports (squash, cycling, hiking, winter sports,
footballtennis, football, fitness)